Valuing Private Equity Investments Strip by Strip*

Arpit Gupta — NYU Stern

Stijn Van Nieuwerburgh — CBS, NBER, and CEPR

April 26, 2019

Abstract

We propose a new valuation method for private equity investments. First, we construct a cash-flow replicating portfolio for the private investment, using cash-flows on various listed equity and fixed income instruments. The second step values the replicating portfolio using a flexible asset pricing model that accurately prices the systematic risk in listed equity and fixed income instruments of different horizons. The method delivers a measure of the risk-adjusted profit earned on a PE investment, a time series for the expected return on PE fund categories, and a time series for the residual net asset value in a fund. We apply the method to real estate, infrastructure, buyout, and venture capital funds, and find modestly positive average risk-adjusted profits with substantial cross-sectional variation, and declining expected returns in the later part of the sample.

JEL codes: G24, G12

*Gupta: Department of Finance, Stern School of Business, New York University, 44 W. 4th Street, New York, NY 10012; agupta3@stern.nyu.edu; Tel: (212) 998-0305; http://arpitgupta.info. Van Nieuwerburgh: Department of Finance, Columbia Business School, Columbia 3022 Broadway, Uris Hall 809, New York, NY 10027; svnieuwe@gsb.columbia.edu; Tel: (212) 854-02289; https://www0.gsb.columbia.edu/faculty/svannieuwerburgh/. The authors would like to thank Arthur Korteweg and Stavros Panageas (discussants); as well as Ralph Koijen, Morten Sorensen, and Neng Wang, and seminar participants at the American Finance Association annual meetings, the 2018 UNC Real Estate Research Symposium, the Southern California Private Equity Conference, and NYU Stern. This work is supported by the NYU Stern Infrastructure Initiative.

1 Introduction

Private equity investments have risen in importance over the past twenty-five years, relative to public equity. Indeed, the number of publicly listed firms has been falling since 1997, especially among smaller firms. Private equity funds account for $4.7 trillion in assets under management, of which real estate funds comprise $800 billion (Preqin). Large institutional investors now allocate substantial fractions of their portfolios to such alternative investments. For example, the celebrated Yale University endowment has a portfolio weight of over 50% in alternative investments. Pension funds and sovereign wealth funds have also ramped up their allocations to alternatives. As the fraction of overall wealth that is held in the form of private investment grows, so does the importance of developing appropriate valuation methods. The non-traded nature of the assets and their irregular cash-flows makes this a challenging problem.

As with any investment, the value of a private equity (PE) investment equals the present discounted value of its cash-flows. The general partner (GP, fund manager) deploys the capital committed by the limited partners (LPs, investors) by investing in a portfolio of risky projects. The risky projects may pay some interim cash-flows that are distributed back to the LPs. The bulk of the cash flows arise when the GP sells the projects, and distributes the proceeds net of fees (carry, promote) to the LPs. The main challenge in evaluating a PE investment is how to adjust the profits the LP earns for the systematic risk inherent in the PE cash flows. Industry practice is to report the ratio of distributions to capital contributions (TVPI) and/or the internal rate of return (IRR). Neither metric takes into account the riskiness of the cash-flows.

We propose a novel two-step methodology that centers on the nature and the timing of cash-flow risk for PE investments. In a first step, we estimate the exposure of PE funds' cash-flows to the cash-flows of a set of publicly listed securities. The main analysis considers Treasury bonds, the aggregate stock market, a real estate stock index (REIT), an infrastructure stock index, small stocks, and growth stocks as the listed securities. The method considers a much richer cross-section of risks than the literature hitherto, and easily accommodates additional publicly-traded risk factors. Inspired by Lettau and Wachter (2011) and van Binsbergen, Brandt, and Koijen (2012), we "strip" the sequence of PE cash-flows horizon by horizon, and estimate factor exposures to the corresponding listed strip cash flows. Our identification assumes that the systematic cash-flow exposures depend on PE category, horizon, and the underlying market conditions at the time of fund origination, as proxied by the price-dividend ratio on the stock market. All PE funds within the same category and vintage have the same exposures to the asset strips. We estimate this exposure both using OLS as well as using a Lasso estimation which shrinks the cross-section and enforces only positive coefficients (corresponding to a long-only replicating portfolio).

In a second step, we use a rich, no-arbitrage asset pricing model that prices the asset strips. This is necessary since data on prices for dividend strips are not available for any asset besides the aggregate stock market, and even then only for a small fraction of the sample. Strips on REITs, infrastructure, or any other equity factor are unavailable. The model estimates the prices of risk by closely matching the history of bond yields of different maturities, as well as prices and expected returns on the five equity indices. It also matches the risk premium on short-maturity dividend futures from 2003-2014, calculated in the data by van Binsbergen, Hueskes, Koijen, and Vrugt (2013), and van Binsbergen and Koijen (2017), and the time series of the price-dividend ratio on 2-year cumulative dividend strips and the share of the overall stock market they represent from 1996-2009 as backed out from options data by van Binsbergen, Brandt, and Koijen (2012). With the market price of risk estimates in hand, we can price risky cash-flows at each date and at each horizon in the bond, aggregate stock, small stock, growth stock, REIT, and infrastructure markets. We use the shock price elasticities of Borovička and Hansen (2014) to understand how risk prices change with horizon in the model.

Combining the cash-flow replicating portfolio of strips obtained from the first step with the prices for these strips from the asset pricing model estimated in the second step, we obtain the fair price for the PE-replicating portfolio in each vintage and category. Each PE investment in the data is scaled to represent \$1 of capital committed. Therefore, the replicating portfolio of strips must deploy the same \$1 of capital. This budget feasibility constraint on the replicating portfolio directly affects PE fund performance evaluation. A time of high strip prices is a time when the replicating portfolio must buy fewer strips. PE funds started at that time (i.e., of that vintage) are more likely to have cash flows that exceed those on the replicating portfolio, all else equal. Of course, the assets that PE funds acquire may be more expensive as well, so that out-performance is an empirical question. The risk-adjusted profit (RAP) of an individual PE fund is the net present value of the excess cash flows, the difference between the realized cash flows on the PE fund and the realized cash flows on the replicating portfolio in that vintage-category. Under the joint null hypothesis of the correct asset pricing model and the absence of (asset selection or market timing) skill, the RAP is zero.

The asset pricing model is used also to compute the expected return on a PE investment, which reflects the systematic risk exposure of the PE fund. Our method breaks down the expected return into its various horizon components (strips), and, at each horizon, into its exposures to the various risk factors. Since the expected return on the listed strips varies with the state of the economy, so does the expected return on PE investments. Our method can also be used to ask what the expected return is on all outstanding PE investments, by aggregating across current vintages. The method can further be used to calculate the residual net asset value (NAV) of PE funds at each point during their life cycle, providing an alternative measure to the NAV reported by funds themselves. Finally, by providing the expected return on PE, and the covariances of PE funds with traded securities, our approach facilitates portfolio analysis with alternatives for which return time series are unavailable.

In the absence of a full menu of dividend strips (e.g., REIT strips or small growth stock strips are not currently available), our results imply that PE funds are a vehicle to provide an investor with exposure to short- and medium-horizon risk in real estate, infrastructure, or small growth markets. Access to such exposure is becoming increasingly important in light of the decline in the share of publicly listed investments, in particular in the small growth space, and in real estate and infrastructure markets.

We use data from Preqin on all PE funds with non-missing cash-flow information that were started between 1980 and 2017. Cash-flow data until December 2017 are used in the analysis. Our sample includes 4,223 funds in seven investment categories. The largest categories are Buyout, Real Estate, and Venture Capital. The main text reports results for these three categories as well as Infrastructure, and relegates the results for the other three to the appendix. The PE data from Preqin are subject to the usual selection bias concerns.[1]

Our key finding is that the risk-adjusted profit (RAP) to investors in PE funds exhibits strong cross-sectional variation. We find average RAP around 20-30 cents per $ invested in the Buyout category, and high RAP in the 1990s vintages of VC funds. While PE cashflows have significant exposures to several public market risk factors, the market prices of these exposures are high. PE funds therefore offer investors access to these exposures at a cost that is generally below that in public stock and bond markets. For the other categories, such as Real Estate and Infrastructure; and for more recent VC funds—we

[1] Preqin data are thought to understate performance. Some high-performing funds that are closed to outside investors to protect from FOIA requests are not in our data set. An alternative data set provided by Burgiss has superior coverage of these funds (Brown, Harris, Jenkinson, Kaplan, and Robinson, 2015). Preliminary results indicate that our main findings continue to hold in this data set.

find less evidence of outperformance.

Related Literature This paper contributes to a large empirical literature on performance evaluation in private equity funds, such as Kaplan and Schoar (2005), Cochrane (2005), Korteweg and Sorensen (2017), Harris, Jenkinson, and Kaplan (2014), Phalippou and Gottschalg (2009), Robinson and Sensoy (2011), among many others. Most of this literature focuses on Buyout and Venture Capital funds, though recent work in valuing privately-held real estate assets includes Peng (2016) and Sagi (2017). Ammar and Eling (2015) have studied infrastructure investments. This literature has found mixed results regarding PE fund outperformance and persistence thereof, depending on the data set and period in question. Our replicating portfolio approach results in a substantially positive estimate of risk-adjusted profits for PE funds, with large cross-sectional and time-series variation.

While performance evaluation in private equity is still often expressed as an internal rate of return or a ratio of distributions to capital committed, several important papers have incorporated risk into the analysis. The public market equivalent (PME) approach of Kaplan and Schoar (2005) compares the private equity investment to a public market benchmark (the aggregate stock market) with the same magnitude and timing of cash-flows. Sorensen and Jagannathan (2015) assess the PME approach from a SDF perspective. The closest antecedent to our paper is Korteweg and Nagel (2016), who propose a generalized PME approach (GPME) that relaxes the assumption that the beta of PE funds to the stock market is one. This is particularly important in their application to VC funds. Like ours, the PME and GPME approaches avoid making strong assumptions on the return-generating process of the PE fund, because they work directly with the cash-flows. Cochrane (2005) and Korteweg and Sorensen (2010) discuss this distinction. In contrast, much of the literature assumes linear beta-pricing relationships, e.g., Ljungqvist and Richardson (2003), Driessen, Lin, and Phalippou (2012).

The literature that estimates beta exposures of PE funds with respect to the stock market has generally estimated stock market exposures of Buyout funds above one and even higher estimates for VC funds. E.g., Gompers and Lerner (1997); Ewens, Jones, and Rhodes-Kropf (2013); Peng (2001); Woodward (2009); Korteweg and Nagel (2016). Our work contributes to this literature by allowing for a flexible estimation approach across horizon and vintage, for risk exposure estimates to differ by category, by considering a broader set of PE categories than typically examined, and especially by going beyond the aggregate stock market as the only source of aggregate risk. VC funds are found to load on small stock and growth stock risk. Results for VC funds have implications for the returns on entrepreneurial activity (Moskowitz and Vissing-Jorgensen, 2002). Finally, we connect the systematic risk exposures of funds to a rich asset pricing model, which allows us to estimate risk-adjusted profits and time-varying expected returns.

Like Korteweg and Nagel (2016), we estimate a stochastic discount factor (SDF) from public securities. Our SDF contains additional risk factors and richer price-of-risk dynamics. Those dynamics are important for generating realistic, time-varying risk premia on bond and stock strips, which are the building blocks of our PE valuation method. The SDF model extends earlier work by Lustig, Van Nieuwerburgh, and Verdelhan (2013) who value a claim to aggregate consumption to help guide the construction of consumption-based asset pricing models. The asset pricing model combines a vector auto-regression model for the state variables as in Campbell (1991, 1993, 1996) with a no-arbitrage model for the (SDF) as in Duffie and Kan (1996); Dai and Singleton (2000); Ang and Piazzesi (2003). The SDF model needs to encompass the sources of aggregate risk that the investor has access to in public securities markets and that PE funds are exposed to. The question of performance evaluation then becomes whether, at the margin, PE funds add value to a portfolio that already contains these traded assets.

In complementary work, Ang, Chen, Goetzmann, and Phalippou (2017) filter a time series of realized private equity returns using Bayesian methods. They then decompose that time series into a systematic component, which reflects compensation for factor risk exposure, and an idiosyncratic component (alpha). While our approach does not recover a time series of realized PE returns, it does recover a time series of *expected* PE returns. At each point in time, the asset pricing model can be used to revalue the replicating portfolio for the PE fund. Since it does not require a difficult Bayesian estimation step, our approach is more flexible in terms of number of factors as well as the factor risk premium dynamics. Other important methodological contributions to the valuation of private equity include Driessen, Lin, and Phalippou (2012), Sorensen, Wang, and Yang (2014), and Metrick and Yasuda (2010).

The rest of the paper is organized as follows. Section 2 describes our methodology. Section 3 sets up and solves the asset pricing model. Section 4 presents the main results on the risk-adjusted profits and expected returns of PE funds. Section 5 concludes. The appendix provides derivations and additional results.

2 Methodology

PE investments are finite-horizon strategies, typically around ten to fifteen years in duration. Upon inception of the fund, the investor (LP) commits capital to the fund manager (GP). The GP deploys that capital at his discretion, but typically within the first 2-4 years. Intermediate cash-flows may accrue from the operations of the assets, for example, net operating income from renting out an office building. Towards the end of the life of the fund (typically in years 5-10), the GP "harvests" the assets and distributes the proceeds to the investor after subtracting fees (including the carry or promote). These distribution cash-flows are risky, and understanding (and pricing) the nature of the risk in these cash-flows is the key question in this paper.

Denote the sequence of net-of-fee cash-flow distributions for fund i by $\{X^i_{t+h}\}^T_{h=0}$. Time t is the inception date of the fund, the vintage. The horizon h indicates the number of quarters since fund inception. We allocate all funds started in the same calendar year to the same vintage. The maximum horizon H is set to 60 quarters to allow for "zombie" funds that continue past their projected life span of approximately 10 years. All cash flows observed after quarter H are allocated to quarter H. Monthly fund cash-flows are aggregated to the quarterly frequency. All PE cash-flows in our data are reported for a \$1 investor commitment.

Once the capital is committed, the GP has discretion to call that capital. We take the perspective that the risk-adjusted profit (RAP) measure should credit the GP for the skillful timing of capital calls. Correspondingly, we assume that the replicating portfolio is fully invested at time zero. If strategic delay in capital deployment results in better investment performance, the RAP will reflect this. In sum, we purposely do not use the data on capital calls, only the distribution cash flow data.[2]

2.1 Two-Step Approach

In a first step, we use our asset pricing model, spelled out in the next section, to price the zero coupon bond and equity strips. Let the $HK \times 1$ vector $\boldsymbol{F}_{t,t+h}$ be the vector of cash flows on the securities in the replicating portfolio. The first H elements of $\boldsymbol{F}_{t,t+h}$ are constant equal to 1. They are the cash-flows on nominal zero-coupon U.S. Treasury bonds

[2] Note that under this assumption, the net present value of deployed capital may differ from \$1. Our methodology can handle capital calls, and we do robustness to this assumption in the appendix. The alternative assumption assumes that the replicating portfolio to mimic not only the distribution of cash flows but also the call cash flows. The calls are treated as negative bond strip positions.

that pay \$1 at time $t+h$. The other $H(K-1)$ elements of $\boldsymbol{F}_{t,t+h}$ denote risky cash-flow realizations at time $t+h$. They are the payoffs on "zero coupon equity" or "dividend strips" (Lettau and Wachter, 2011; van Binsbergen, Brandt, and Koijen, 2012). They pay one (risky) cash-flow at time $t+h$ and nothing at any other date. We scale the risky dividend at $t+h$ by the cash flow at fund inception time t. For example, a risky cash-flow of $F_{t,t+h}(k) = \frac{D_{t+h}(k)}{D_t(k)} = 1.05$ implies that there was a 5% realized cash-flow growth rate between periods t and $t+h$ on the k^{th} asset in the replicating portfolio. This scaling gives the strips a "face value" around 1, comparable to that of the zero coupon bond. It makes the bond and stock exposures comparable in magnitude to one another.

Denote the $HK \times 1$ price vector for strips by $\boldsymbol{P}_{t,h}$. The first $H \times 1$ elements of this price vector are the prices of nominal zero-coupon bonds of maturities $h = 1, \cdots, H$, which we denote by $\boldsymbol{P}_{t,h}(1) = \boldsymbol{P}^{\$}_{t,h}$. Let the one-period stochastic discount factor (SDF) be M_{t+1}, then the h-period SDF is:

$$M_{t,t+h} = \prod_{j=1}^{h} M_{t+j}.$$

The (vector of) strip prices satisfy the (system of) Euler equation:

$$\boldsymbol{P}_{t,h} = \mathbb{E}_t[M_{t,t+h}\boldsymbol{F}_{t,t+h}].$$

Strip prices reflect expectations of the SDF rather than realizations.

The second step of our approach is to obtain the cash-flow replicating portfolio of strips for the PE cash-flow distributions. Denote the cash flow on the replicating portfolio by $\boldsymbol{\beta}^i_{t,h}\boldsymbol{F}_{t,t+h}$, where the $1 \times HK$ vector $\boldsymbol{\beta}^i_{t,h}$ denotes the exposure of PE fund i to the HK assets in the replicating portfolio. We estimate the exposures from a projection of cash-flows realized at time $t+h$ of PE funds started at time t on the cash-flows of the risk-free and risky strips:

$$X^i_{t+h} = \boldsymbol{\beta}^i_{t,h}\boldsymbol{F}_{t,t+h} + e^i_{t+h}. \tag{1}$$

where e denotes the idiosyncratic cash-flow component, orthogonal to $F_{t,t+h}$. The vector $\beta^i_{t,h}$ describes how many units of each strip are in the replicating portfolio for the fund cash-flows. Equation (1) is estimated combining all funds in a given category, all vintages t, and all horizons h. We impose cross-equation restrictions on this estimation, as explained below.

Budget Feasibility We use the asset pricing model to ensure that the replicating portfolio of bond and stock strips for the PE fund is *budget feasible*. The portfolio of strips must cost exactly \$1, the same initial outlay as for the PE investment. The replicating portfolio, estimated from equation (1), does not automatically satisfy budget feasibility. We define a $1 \times HK$ vector of rescaled portfolio positions, $\boldsymbol{q}^i$, that costs exactly \$1 to buy:

$$\boldsymbol{q}^i_{t,h} = \frac{\boldsymbol{\beta}^i_{t,h}}{\sum_{h=1}^H \boldsymbol{\beta}^i_{t,h}\boldsymbol{P}_{t,h}} \quad \Rightarrow \quad \sum_{h=1}^H \boldsymbol{q}^i_{t,h}\boldsymbol{P}_{t,h} = 1.$$

The strip prices $\boldsymbol{P}_{t,h}$ are given by the asset pricing model. This is the first place we use the asset pricing model. Since the strip prices change over time, each vintage has its own rescaling. This induces time variation in addition to the time variation inherited from $\boldsymbol{\beta}^i_{t,h}$.

With the budget feasible replicating portfolio in hand, we redefine the idiosyncratic component of fund cash-flows as v^i:

$$v^i_{t+h} = X^i_{t+h} - \boldsymbol{q}^i_{t,h}\boldsymbol{F}_{t,t+h}.$$

Under the joint null hypothesis of the asset pricing model and no fund outperformance, the expected present discounted value of fund cash-flow distributions must equal the \$1 initially paid in by the investor:

$$\mathbb{E}_t\left[\sum_{h=1}^H M_{t,t+h}X^i_{t+h}\right] = \mathbb{E}_t\left[\sum_{h=1}^H M_{t,t+h}\boldsymbol{q}^i_{t,h}\boldsymbol{F}_{t,t+h}\right] = \sum_{h=1}^H \boldsymbol{q}^i_{t,h}\boldsymbol{P}_{t,h} = 1, \tag{2}$$

where the first equality follows from the fact that the idiosyncratic cash-flow component v^i is uncorrelated with the SDF since all priced cash-flow shocks are included in the vector F under the null hypothesis.

Expected Returns The second place where we use the asset pricing model is to calculate the expected return on the PE investment over the life of the investment. It equals the expected return on the replicating portfolio of strips:

$$\mathbb{E}_t\left[R^i\right] = \sum_{h=1}^H \sum_{k=1}^K \boldsymbol{w}^i_{t,h}(k)\mathbb{E}_t\left[\boldsymbol{R}_{t+h}(k)\right] \tag{3}$$

where $\boldsymbol{w}^i$ is a $1 \times HK$ vector of replicating portfolio weights with generic element $w^i_{t,h}(k) = q^i_{t,h}(k)P_{t,h}(k)$. The $HK \times 1$ vector $\mathbb{E}_t[\boldsymbol{R}]$ denotes the expected returns on the K traded asset strips at each horizon h. The asset pricing model provides the expected returns on these strips. Equation (3) decomposes the risk premium into compensation for exposure to the various risk factors, horizon by horizon. The expected return is measured over the life of the fund (not annualized). It can be annualized by taking into account the maturity of the fund. Akin to a MacCauley duration, we define the maturity of the fund, expressed in years (rather than quarters), as:

$$\delta_t^i = \frac{1}{4} \sum_{h=1}^{H} \sum_{k=1}^{K} \boldsymbol{w}_{t,h}^i(k) h \tag{4}$$

The annualized expected fund return is then:

$$\mathbb{E}_t \left[R_{ann}^i \right] = \left(1 + \mathbb{E}_t \left[R^i \right] \right)^{1/\delta_t^i} - 1 \tag{5}$$

Risk-Adjusted Profit Performance evaluation of PE funds requires quantifying the LP's profit on a particular PE investment, after taking into account its riskiness. This ex-post realized, risk-adjusted profit is the second main object of interest. Under the maintained assumption that all the relevant sources of systematic risk are captured by the replicating portfolio, the PE cash-flows consist of one component that reflects compensation for risk and a risk-adjusted profit (RAP) equal to the discounted value of the idiosyncratic cash-flow component. The latter component for fund i in vintage t equals:

$$RAP_t^i \quad = \quad \sum_{h=1}^{H} P_{t,h}^{\$} v_{t+h}^i \tag{6}$$

Since the idiosyncratic cash-flow components are orthogonal to the priced cash-flow shocks, they are simply discounted at the risk-free interest rate. Since the term structure of risk-free bond prices $P_{t,h}^{\$}$ is known at time t, there is no measurement error involved in the discounting. The null hypothesis of no outperformance on average across funds is that $\mathbb{E}[RAP_t^i] = 0$.

A fund with strong asset selection skills, which picks investment projects with payoffs superior to the payoffs on the traded assets, will have a positive RAP. Additionally, a fund with market timing skills, which invests at the right time (within the investment period) and sells at the right time (within the harvesting period) will have positive risk-adjusted profit.[3] Alternatively, if capital lock-up in the PE fund structure enables managers to earn

[3]The fund's horizon is endogenous because it is correlated with the success of the fund. As noted by

an illiquidity premium, we would also expect this to be reflected in a positive RAP on average. When calculating our RAP measure, we exclude vintages after 2010 for which we are still missing a substantial fraction of the cash-flows.

To assess the performance of PE funds, we report both the distribution of risk-adjusted profits across all funds in the sample, as well as the equal-weighted average RAP by vintage. This approach quantifies whether the estimated replicating portfolios deliver returns across horizons to the LP that are similar to the realized returns based on investing in a broad basket of PE funds directly. Similarity in returns between PE funds and our replicating portfolio does not follow immediately from our estimating approach due to the additional role of strip prices. We require that replicating portfolios fit the cash flows of PE funds, and that they be budget feasible given our estimated strip prices. Our approach, therefore, credits PE funds with over-performance to the extent they are able to deliver factor exposure at an (after-fee) expense lower than that of existing publicly traded assets as estimated by our model.

Appendix **??** discusses the relationship between our approach and the PME approach of Kaplan and Schoar (2005) and the GPME approach of Korteweg and Nagel (2016). The rest of this section discusses implementation issues related to estimating equation (1).

2.2 Identifying and Estimating Cash-Flow Betas

The replicating portfolio must be rich enough that it spans all priced (aggregate) sources of risk, yet it must be parsimonious enough that its exposures can be estimated with sufficient precision. Allowing every fund in every category and vintage to have its own unrestricted cash-flow beta profile for each risk factor leads to parameter proliferation and lack of identification. We impose cross-equation restrictions to aid identification.

One-factor Model To fix ideas, we start with a simple model in which all private equity cash-flows are assumed to only have interest rate risk. We refer to this as the one-factor model. The empirical model assumes that the cash-flows X of all funds i in the same category c (category superscripts are omitted for ease of notation) have the same bond betas at each horizon h. To simplify the time dimension, we categorize different vintages t according to the tercile of the price-dividend ratio on the aggregate stock market in that

Korteweg and Nagel (2016), this endogeneity does not pose a problem as long as cash-flows are observed. They write: “Even if there is an endogenous state-dependence among cash-flows, the appropriate valuation of a payoff in a certain state is still the product of the state’s probability and the SDF in that state.”

year. Terciles are defined over the same 1974-2017 sample for which we estimate our asset pricing model. Allowing risk exposures to scale up and down with the current value of the pd^m ratio allows the cash-flow model to capture dependence on the overall investment climate at the time of PE fund origination. The pd_t^m ratio is one of the key state variables in the asset pricing model of Section 3. The restricted cash-flow model can be expressed as:

$$X_{t+h}^{i\in c} = \beta_{t,h}^{b} + e_{t+h}^{i} = q_{t,h}^{b} + v_{t+h}^{i} = a_{pd_t^m} + b_h + v_{t+h}^{i}. \tag{7}$$

We estimate the first equation in (7) using either OLS or a Lasso model. We obtain budget-feasible bond exposures as explained above. We impose that the rescaled bond positions q_{t+h}^{b} are the sum of a *vintage effect* a_{pd_t} and a *horizon effect* b_h. With 3 pd_t^m terciles and H horizons, we estimate $H+3$ parameters using $N_f \times T \times H$ observations, where T reflects the number of different vintages. Identification is achieved both from the cross-section (N_f funds in category c per vintage) and from the time series (T). Specifically, the vintage effects (the "a's") are only allowed to shift the horizon effects (the "b"-profiles) up and down in parallel fashion. The vintage effects are normalized to be zero on average across terciles, and the horizon effects correspondingly rescaled. We include all available vintages that have at least eight quarters of cash flows because the extra information from recent vintages may be useful to better identify the first few elements of b_h.

Three-factor Model Our main model is a three-factor model in which we allow for three separate capital market factors to proxy for PE fund cash flows. We price this cross-section of assets in the model of Section 3. The precise assets we pick vary by category based on an empirical assessment of which are the most relevant risk factors for each category. In our benchmark estimation (for the categories: Buyout, Fund of Funds, Restructuring, and Debt Funds), we include: bond, stock, and small stock factors (defined as those stocks in the bottom quintile of size). In the real estate category, we include a bond, stock, and REIT factor. Similarly, in infrastructure funds, we include a relevant traded factor, an index of infrastructure stocks, in addition to the bond and stock factors. Among Venture Capital funds, we find that aggregate stocks are an imperfect fit for cash flows. Instead, we use a small stock and a growth stock factor in addition to the bond factor. Size and growth are proxies for the sort of rapidly expanding early-stage companies that are in the portfolios of VC funds. While our model can be extended to an arbitrary number of $K > 3$ risk factors; we opt in our benchmark estimation to focus on the set of factors with the best apparent fit with our data while avoiding in-sample over-fitting.

The key identifying assumption is that the cash-flows of all PE funds in the same category and whose vintage belongs to the same pd^m tercile have the same $1 \times KH$ cash-flow beta horizon profile. The beta horizon profiles on the $K = 3$ different factors are allowed to be different from one another, and to shift in different ways across vintages. But each pd^m tercile is only allowed to shift the corresponding horizon profile up and down in parallel fashion, rather than allowing for arbitrary shifting. Here, we illustrate the estimation for Buyout funds, but the basic approach is similar across PE fund categories with a different subset of chosen factors:

$$\begin{aligned} X_{t+h}^{i\in c} &= q_{t,h}^{b} + q_{t,h}^{m} F_{t,t+h}^{m} + q_{t,h}^{small} F_{t,t+h}^{small} + v_{t+h}^{i} \\ &= a_t^1 + b_h^1 + \left(a_t^2 + b_h^2\right) F_{t,t+h}^{m} + \left(a_t^3 + b_h^3\right) F_{t,t+h}^{small} + v_{t+h}^{i}. \end{aligned} \tag{8}$$

With $K = 3$ factors and $H = 60$ horizons , we estimate $3K = 9$ vintage-tercile effects $\{a_t^1, a_t^2, a_t^3\}_{t=1}^{3}$ and $KH = 180$ horizon profiles $\{b_h^1, b_h^2, b_h^3\}_{h=1}^{H}$ for a total of 189 coefficients.

We use two estimation techniques. The first is a standard OLS model. The second is a Lasso approach that constrains all penalized coefficients to be non-negative. This second approach follows a recent literature on Machine Learning in asset pricing, such as Gu, Kelly, and Xiu (2018) and Kozak, Nagel, and Santosh (2017). It aims to reduce the potential set of factors in our replicating portfolio. This estimation offers two key economic advantages: it constrains the replicating portfolio to long positions only, which avoids costs and difficulties of short positions. Additionally, this model will set to zero many possible factor and horizon terms in the replicating portfolio. This simplifies the resulting replicating positions considerably and avoids over-fitting due to extreme long-short positions. The Lasso estimation of equation (1) can be written as:

$$\hat{\beta}_{lasso} = \arg \min_{\beta \in \mathbf{R}^{KH}} \| X_{t+h}^{i} - \beta_{t,h}^{i} \boldsymbol{F}_{t,t+h} \|_2^2 + \lambda \mathbf{1}\{\beta > 0\} \tag{9}$$

We set the hyper-parameter $\lambda = \infty$, which ensures only positive coefficients.

3 Asset Pricing Model

The second main challenge is to price the replicating portfolio. If the only sources of risk were the risks inherent in the term structure of interest rates, this step would be straightforward. After all, on each date t, we can infer the prices of zero-coupon bonds of all maturities j from the observed yield curve. However, interest rate risk is not the only and (arguably) not even the main source of risk in the cash-flows of private equity funds. If stock market risk were the only other source of aggregate risk, then we could in principle use price information from dividend strips. Those prices can either be inferred from options and stock markets (van Binsbergen, Brandt, and Koijen, 2012) or observed directly from dividend strip futures markets (van Binsbergen, Hueskes, Koijen, and Vrugt, 2013). However, the available time series is too short for our purposes. Moreover, these strips are not available in one-quarter horizon increments. Third, the only dividend strip data are for the aggregate stock market, not for publicly listed real estate or infrastructure assets, a small stock index, or a growth stock index, additional traded factors we wish to include in our analysis. Fourth, we do not observe expected returns on those strips, only realized excess returns over relatively short time series. For all those reasons, we need an asset pricing model to obtain the time series of strip prices, $\boldsymbol{P}_{t,h}$, and the corresponding expected returns. We impose that this asset pricing model is consistent with the available dividend strip evidence, in addition to the standard asset pricing moments.

We propose a reduced-form asset pricing model rather than a structural model that starts from preferences, since it is more important for our purposes to price the replicating portfolio of publicly traded assets correctly than to understand the fundamental sources of risk that underly the pricing of stocks and bonds. Our approach builds on Lustig, Van Nieuwerburgh, and Verdelhan (2013), who price a claim to aggregate consumption and study the properties of the price-dividend ratio of this claim, the wealth-consumption ratio. A virtue of the reduced-form model is that is fairly flexible and can accommodate a substantial number of aggregate risk factors. We argue that it is important to go beyond the aggregate stock market and bonds to capture the risk embedded in PE fund cashflows.

As emphasized by Korteweg and Nagel (2016), the objective is not to test the asset pricing model, but rather to investigate whether a potential PE investment adds value to an investor who already has access to securities whose sources of risk are captured by the SDF.

3.1 Setup

3.1.1 State Variable Dynamics

Time is denoted in quarters. We assume that the $N \times 1$ vector of state variables follows a Gaussian first-order VAR:

$$z_t = \mathbf{\Psi} z_{t-1} + \mathbf{\Sigma}^{\frac{1}{2}} \boldsymbol{\varepsilon}_t, \tag{10}$$

with shocks $\boldsymbol{\varepsilon}_t \sim i.i.d. \mathcal{N}(0, I)$ whose variance is the identity matrix. The companion matrix Ψ is a $N \times N$ matrix. The vector z is demeaned. The covariance matrix of the innovations to the state variables is Σ; the model is homoscedastic. We use a Cholesky decomposition of the covariance matrix, $\Sigma = \Sigma^{\frac{1}{2}} \Sigma^{\frac{1}{2}\prime}$, which has non-zero elements only on and below the diagonal. The Cholesky decomposition of the residual covariance matrix allows us to interpret the shock to each state variable as the shock that is orthogonal to the shocks of all state variables that precede it in the VAR. We discuss the elements of the state vector and their ordering below. For now, we note that the (demeaned) one-month bond nominal yield is one of the elements of the state vector: $y^{\$}_{t,1} = y^{\$}_{0,1} + e'_{yn} z_t$, where $y^{\$}_{0,1}$ is the unconditional average 1-quarter nominal bond yield and e_{yn} is a vector that selects the element of the state vector corresponding to the one-quarter yield. Similarly, the (demeaned) inflation rate is part of the state vector: $\pi_t = \pi_0 + e'_\pi z_t$ is the (log) inflation rate between $t-1$ and t. Lowercase letters denote logs.

3.1.2 SDF

We specify an exponentially affine stochastic discount factor (SDF), similar in spirit to the no-arbitrage term structure literature (Ang and Piazzesi, 2003). The nominal SDF $M^{\$}_{t+1} = \exp(m^{\$}_{t+1})$ is conditionally log-normal:

$$m^{\$}_{t+1} \quad = \quad -y^{\$}_{t,1} - \frac{1}{2} \mathbf{\Lambda}'_t \mathbf{\Lambda}_t - \mathbf{\Lambda}'_t \boldsymbol{\varepsilon}_{t+1}. \tag{11}$$

Note that $y^{\$}_{t,1} = \mathbb{E}_t[-m^{\$}_{t+1}]$. The real SDF is $M_{t+1} = \exp(m_{t+1}) = \exp(m^{\$}_{t+1} + \pi_{t+1})$; it is also conditionally Gaussian. The innovations in the vector ε_{t+1} are associated with a $N \times 1$ market price of risk vector $\mathbf{\Lambda}_t$ of the affine form:

$$\mathbf{\Lambda}_t = \mathbf{\Lambda}_0 + \mathbf{\Lambda}_1 z_t.$$

The $N \times 1$ vector $\mathbf{\Lambda}_0$ collects the average prices of risk while the $N \times N$ matrix $\mathbf{\Lambda}_1$ governs the time variation in risk premia. Asset pricing in this model amounts to estimating the market prices of risk $(\mathbf{\Lambda}_0, \mathbf{\Lambda}_1)$. We specify the restrictions on the market price of risk vector below.

3.1.3 Bond Pricing

Proposition 1 in Appendix A shows that nominal bond yields of maturity τ are affine in the state variables:

$$y^{\$}_{t,\tau} = -\frac{1}{\tau} A^{\$}_{\tau} - \frac{1}{\tau} B^{\$\prime}_{\tau} z_t.$$

The scalar $A^{\$}(\tau)$ and the vector $B^{\$}_{\tau}$ follow ordinary difference equations that depend on the properties of the state vector and on the market prices of risk. The appendix also calculates the real term structure of interest rates, the real bond risk premium, and the inflation risk premium on bonds of various maturities. We will price a large cross-section of nominal bonds that differ by maturity, paying special attention to the one- and twenty-quarter bond yields since those are part of the state vector.

3.1.4 Equity Pricing

The present-value relationship says that the price of a stock equals the present-discounted value of its future cash-flows. By value-additivity, the price of the stock, P^m_t, is the sum of the prices to each of its future cash-flows. These future cash-flow claims are the so-called dividend strips or zero-coupon equity (Wachter, 2005). Dividing by the current dividend D^m_t:

$$\frac{P^m_t}{D^m_t} = \sum_{\tau=1}^{\infty} P^d_{t,\tau} \tag{12}$$

$$\exp\left(\overline{pd} + e'_{pd^m} z_t\right) = \sum_{\tau=0}^{\infty} \exp\left(A^m_\tau + B^{m\prime}_\tau z_t\right), \tag{13}$$

where $P^d_{t,\tau}$ denotes the price of a τ-period dividend strip divided by the current dividend. Proposition 2 in Appendix A shows that the log price-dividend ratio on each dividend strip is affine in the state vector and provides recursions for the coefficients $(A^m_\tau, \boldsymbol{B}^m_\tau)$. Since the log price-dividend ratio on the stock market is an element of the state vector, it is affine in the state vector by assumption. Equation (13) restates the present-value relationship from equation (12). It articulates a non-linear restriction on the coefficients

$\{A_\tau^m, B_\tau^m\}_{\tau=1}^{\infty}$ at each date (for each state z_t), which we impose in the estimation. Analogous present value restrictions are imposed for the other traded equity factors, whose price-dividend ratios and dividend growth rates are also included in the state vector.

If dividend growth were unpredictable and its innovations carried a zero risk price, then dividend strips would be priced like real zero-coupon bonds. The strips' dividend-price ratios would equal yields on real bonds with the coupon adjusted for deterministic dividend growth. All variation in the price-dividend ratio would reflect variation in the real yield curve. In reality, the dynamics of real bond yields only account for a small fraction of the variation in the price-dividend ratio, implying large prices of risk associated with shocks to dividend growth that are orthogonal to shocks to bond yields.

3.1.5 Dividend Futures

The model readily implied the price of a futures contract that received the single realized nominal dividend at some future date, $D_{t+k}^{\$}$. That futures price, $F_{t,\tau}^d$, scaled by the current nominal dividend $D_t^{\$}$, is:

$$\frac{F_{t,\tau}^d}{D_t^{\$}} = P_{t,\tau}^d \exp\left(\tau y_{t,\tau}^{\$}\right),$$

The one-period realized return on this futures contract for $k > 1$ is:

$$R_{t+1,\tau}^{fut,d} = \frac{F_{t+1,\tau-1}^d}{F_{t,\tau}^d} - 1.$$

The appendix shows that $\log(1 + R_{t+1,\tau}^{fut,d})$ is affine in the state vector z_t and in the shocks ε_{t+1}. It is straightforward to compute average realized returns over any subsample, and for any portfolio of futures contracts. Appendix A provides the expressions and details.

3.2 Estimation

3.2.1 State Vector Elements

The state vector contains the following demeaned variables, in order of appearance: (1) GDP price inflation, (2) real per capita GDP growth, (3) the nominal short rate (3-month nominal Treasury bill rate), (4) the spread between the yield on a five-year Treasury note and a three-month Treasury bill,[4] (5) the log price-dividend ratio on the CRSP value-

[4] All yields we use are the average of daily Constant Maturity Treasury yields within the quarter.

weighted stock market, (6) the log real dividend growth rate on the CRSP stock market, (7) the log price-dividend ratio on the NAREIT All Equity REIT index of publicly listed real estate companies, (8) the corresponding log real dividend growth rate on REITs, (9) the log price-dividend ratio on a listed infrastructure index, and (10) the corresponding log real dividend growth rate, (11) the log price-dividend ratio on the first size quintile of stocks, (12) the corresponding log real dividend growth rate, (13) the log-price dividend ratio on the first book-to-market quintile of stocks, and (14) the corresponding log real dividend growth rate:

$$z_t = [\pi_t, x_t, y^{\$}_{t,1}, y^{\$}_{t,20} - y^{\$}_{t,1}, pd^m_t, \Delta d^m_t, pd^{reit}_t, \Delta d^{reit}_t, pd^{infra}_t, \Delta d^{infra}_t, pd^{small}_t, \Delta d^{small}_t, pd^{growth}_t, \Delta d^{growth}_t]'.$$

This state vector is observed at quarterly frequency from 1974.Q1 until 2017.Q4 (176 observations). This is the longest available time series for which all variables are available.[5] Our PE cash flow data starts shortly thereafter in the early 1980s. While most of our PE fund data are after 1990, we deem it advantageous to use the longest possible sample to more reliably estimate the VAR dynamics and especially the market prices of risk.

The VAR is estimated by OLS in the first stage of the estimation. We recursively zero out all elements of the companion matrix Ψ whose t-statistic is below 1.96. Appendix **??** contains the resulting point estimates for Ψ and $\Sigma^{\frac{1}{2}}$.

3.2.2 Market Prices of Risk

The state vector contains both priced sources of risk as well as predictors of bond and stock returns. We estimated 8 parameters in the constant market price of risk vector Λ_0 and 40 elements of the matrix Λ_1 which governs the dynamics of the risk prices. The point estimates are listed in Appendix **??**. We use the following target moments to estimate the market price of risk parameters.

First, we match the time-series of nominal bond yields for maturities of one quarter, one year, two years, five years, ten years, twenty years, and thirty years. They constitute about $7 \times T$ moments, where $T = 176$ quarters.[6]

Second, we impose restrictions that we exactly match the average five-year bond yield

[5]The first observation for REIT dividend growth is in 1974.Q1. We seasonally adjust dividends, which means we lose the first 8 quarters of data in 1972 and 1973. The seasonal adjustment is the same for the overall stock market and the infrastructure stock index.

[6]The 20-year bond yield is missing prior to 1993.Q4 while the 30-year bond yield data is missing from 2002.Q1-2005.Q4. In total 107 observations are missing, so that we have 1232-107=1125 bond yields to match.

and its dynamics. This delivers 15 additional restrictions:

$$-A^{\$}_{20}/20 = y^{\$}_{0,20} \quad \text{and} \qquad - B^{\$}_{20}/20 = [0,0,1,1,0,0,0,0,0,0,0,0,0,0,0]$$

Because the five-year bond yield is the sum of the third and fourth element in the state vector, the market prices of risk must be such that $-B^{\$}_{20}/20$ has a one in the third and fourth place and zeroes everywhere else.

Third, we match the time-series of log price-dividend ratios on the stock market, real estate stocks, infrastructure stocks, small stocks, and growth stocks. The model-implied price-dividend ratios are built up from 3,500 quarterly dividend strips according to equation (12). We impose these present-value relationships in each quarter, delivering $5 \times T$ moments.

Fourth, we impose that the time series of risk premia for the five stock indices in the model match those given in the data, i.e., as implied by the VAR. As usual, the expected excess return in logs (including a Jensen adjustment) must equal minus the conditional covariance between the log SDF and the log return. For example, for the overall stock market:

$$\begin{aligned}
E_t\left[r^{m,\$}_{t+1}\right] - y^{\$}_{t,1} + \frac{1}{2}V_t\left[r^{m,\$}_{t+1}\right] &= -Cov_t\left[m^{\$}_{t+1}, r^{m,\$}_{t+1}\right] \\
r^m_0 + \pi_0 - y^{\$}_0(1) + \left[(e_{divm} + \kappa^m_1 e_{pd} + e_\pi)'\Psi - e'_{pd} - e'_{yn}\right] z_t & \\
+\frac{1}{2}\left(e_{divm} + \kappa^m_1 e_{pd} + e_\pi\right)' \Sigma \left(e_{divm} + \kappa^m_1 e_{pd} + e_\pi\right) &= \left(e_{divm} + \kappa^m_1 e_{pd} + e_\pi\right)' \Sigma^{\frac{1}{2}} \Lambda_t
\end{aligned}$$

The left-hand side is given by the VAR (data), while the right-hand side is determined by the market prices of risk Λ_0 and Λ_1 (model). Similar restrictions apply for real estate, infrastructure, small , and growth stocks. This provides 57 additional restrictions. These moments dictate the 6th, 8th, 10th, 12th, and 14th elements of Λ_0 and rows of Λ_1.

Fifth, we price a claim that pays the next eight quarters of realized nominal dividends on the aggregate stock market. The value of this claim is the sum of the prices to the nearest eight dividend strips. Data for the price-dividend ratio on this claim and the share it represents in the overall stock market (S&P500) are obtained from van Binsbergen, Brandt, and Koijen (2012) for the period 1996.Q1-2009.Q3 (55 quarters). This delivers 2×55 moments. We also want to make sure our model is consistent with the high average realized returns on short-horizon dividend futures, first documented by van Binsbergen, Hueskes, Koijen, and Vrugt (2013). Table 1 in van Binsbergen and Koijen (2017) reports the observed average monthly return on one- through seven-year U.S. SPX dividend futures over the period Nov 2002 - Jul 2014 . That average portfolio return is 0.726% per month or 8.71% per year. We construct an average return for the same short maturity futures portfolio (paying dividends 2 to 29 quarters from now) in the model:

$$R_{t+1}^{fut,portf} = \frac{1}{28} \sum_{\tau=2}^{29} R_{t+1,\tau}^{fut,d}$$

We average the realized return on this dividend futures portfolio between 2003.Q1 and 2014.Q2, and annualize it. We target 8.71% for this return. This results in one additional restriction. We free up the market price of risk associated with the market price-dividend ratio (fifth element of Λ_0 and first six elements of the fifth row of Λ_1) to help match the dividend strip evidence.

Sixth, we impose a good deal bound on the standard deviation of the log SDF, the maximum Sharpe ratio, in the spirit of Cochrane and Saa-Requejo (2000).

Seventh, we impose regularity conditions on bond yields. We impose that very long-term real bond yields have average yields that weakly exceed average long-run real growth, which is 1.65% per year in our sample. Long-run nominal yields must exceed long-run real yields by 2%, an estimate of long-run average inflation. These regularity conditions are satisfied at the final solution.

Not counting the regularity conditions, we have 2, 296 moments to estimate 76 market price of risk parameters. Thus, the estimation is massively over-identified.

3.2.3 Model Fit

Figure 1 plots the bond yields on bonds of maturities 3 months, 1 year, 5 years, and 10 years. Those are the most relevant horizons for the private equity cash-flows. The model matches the time series of bond yields in the data closely for the horizons that matter for PE funds (below 15 years). It matches nearly perfectly the one-quarter and 5-year bond yield which are part of the state space.

The top panels of Figure 2 show the model's implications for the average nominal (left panel) and real (right panel) yield curves at longer maturities. These long-term yields are well behaved. The bottom left panel shows that the model generates the right compensation for interest rate risk through time. It matches the dynamics of the nominal bond risk premium, defined as the expected excess return on five-year nominal bonds. The bottom right panel shows a decomposition of the nominal bond yield on a five-year bond into the

Figure 1: Dynamics of the Nominal Term Structure of Interest Rates

The figure plots the observed and model-implied 1-, 4-, 20-, 40-quarter nominal bond yields.

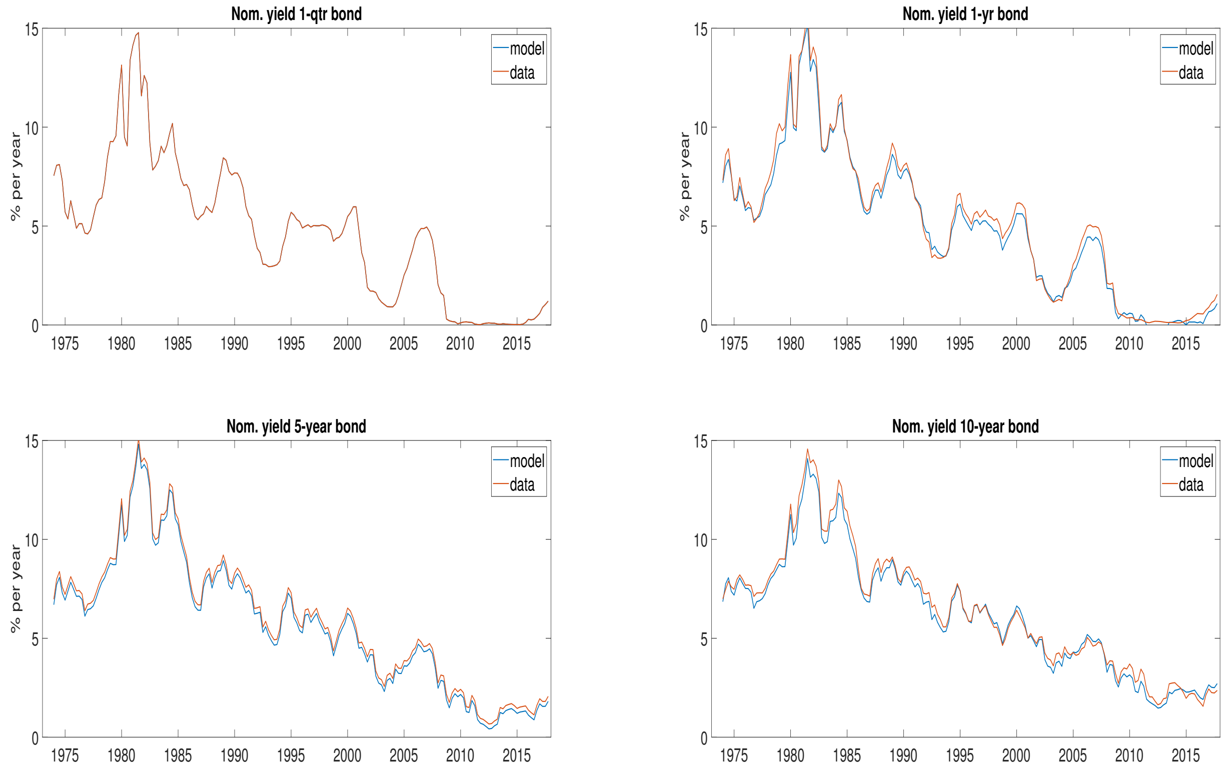

five-year real bond yield, annual expected inflation inflation over the next five years, and the five-year inflation risk premium. On average, the 5.7% five-year nominal bond yield is comprised of a 1.7% real yield, a 3.3% expected inflation rate, and a 0.8% inflation risk premium. The importance of these components fluctuates over time.

Figure 3 shows the equity risk premium, the expected excess return, in the left panels and the price-dividend ratio in the right panels. The top row is for the overall stock market, the second row for REITs, the third row for infrastructure stocks, fourth row for small stocks, and last row for growth stocks. The dynamics of the risk premia in the data are dictated by the VAR. The model chooses the market prices of risk to fit these risk premium dynamics as closely as possible.[7] The price-dividend ratios in the model are formed from the price-dividend ratios on the strips of maturities ranging from 1 to 3500 quarters, as explained above. The figure shows a good fit for price-dividend levels and

[7]The quarterly risk premia are annualized by multiplying them by 4 for presentational purposes only. We note that the VAR does not restrict risk premia to remain positive. The VAR-implied market equity risk premium is negative in 21% of the quarters. For REITs this is 10% and for infrastructure only 5% of quarters. The most negative value of the risk premium on the market is -8% quarterly. For REITs the most negative value for the risk premium is -2.9% quarterly, while it is -1.2% for infrastructure.

Figure 2: Long-term Yields and Bond Risk Premia

The top panels plot the average bond yield on nominal (left panel) and real (right panel) bonds for maturities ranging from 1 quarter to 200 quarters. The bottom left panel plots the nominal bond risk premium in model and data. The bottom right panel decomposes the model's five-year nominal bond yield into the five-year real bond yield, the five-year inflation risk premium and the five-year real risk premium.

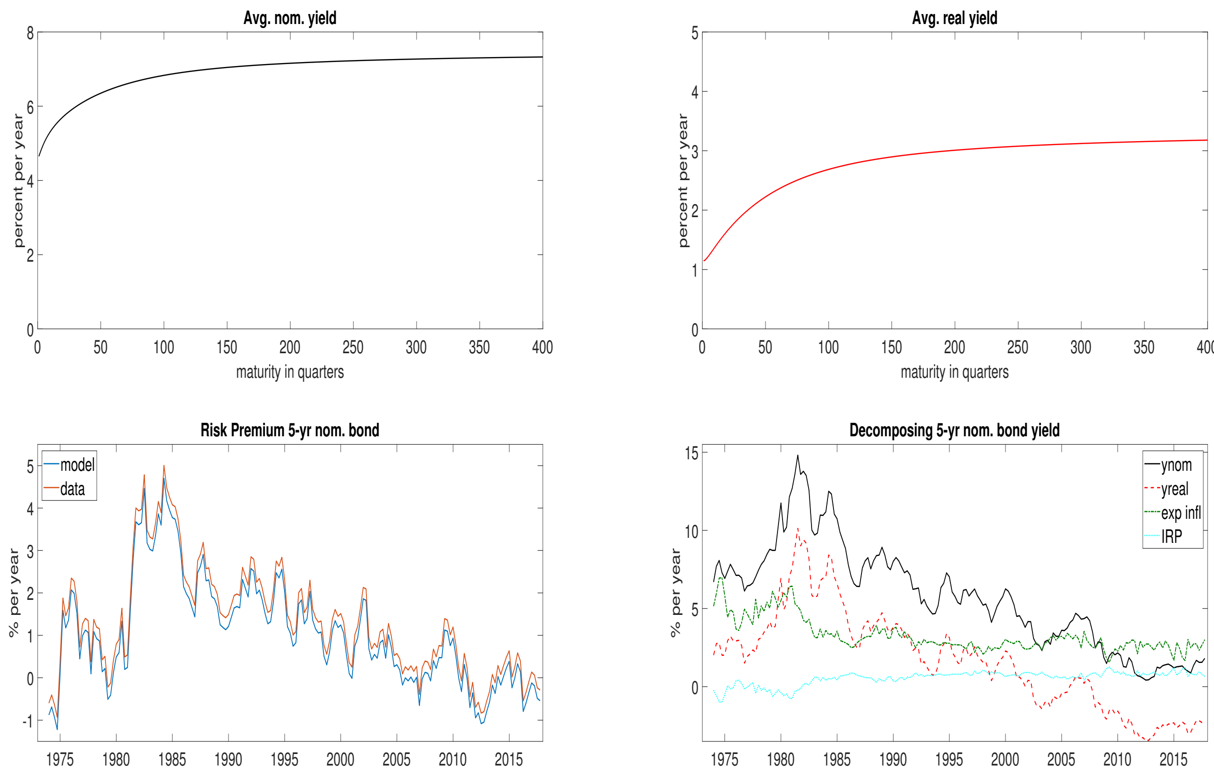

for risk premium dynamics. Some of the VAR-implied risk premia have outliers which the model does not fully capture. This is in part because the good deal bounds restrict the SDF from becoming too volatile and extreme.

3.3 Temporal Pricing of Risk

Zero-Coupon Bond and Zero-Coupon Equity Prices The key inputs from the model into the private equity valuation exercises in equation (3) are the prices of nominal zero-coupon bonds and the various dividend strips with maturities ranging from one to 60 quarters. The price of the dividend strips are scaled by the current quarter dividend. Figure 4 plots these strip prices. For readability, we plot only three maturities: one-month, five-years, and ten-years. The model implies substantial variation in strip prices over time as well as across risky assets. If the replicating portfolio for VC funds originated in the year 2000 loads heavily on growth strips, when growth strips are expensive, then all

Figure 3: Equity Risk Premia and Price-Dividend Ratios

The figure plots the observed and model-implied equity risk premium on the overall stock market, REIT market, and infrastructure sector, in the left panels, as well as the price-dividend ratio in the right panels.

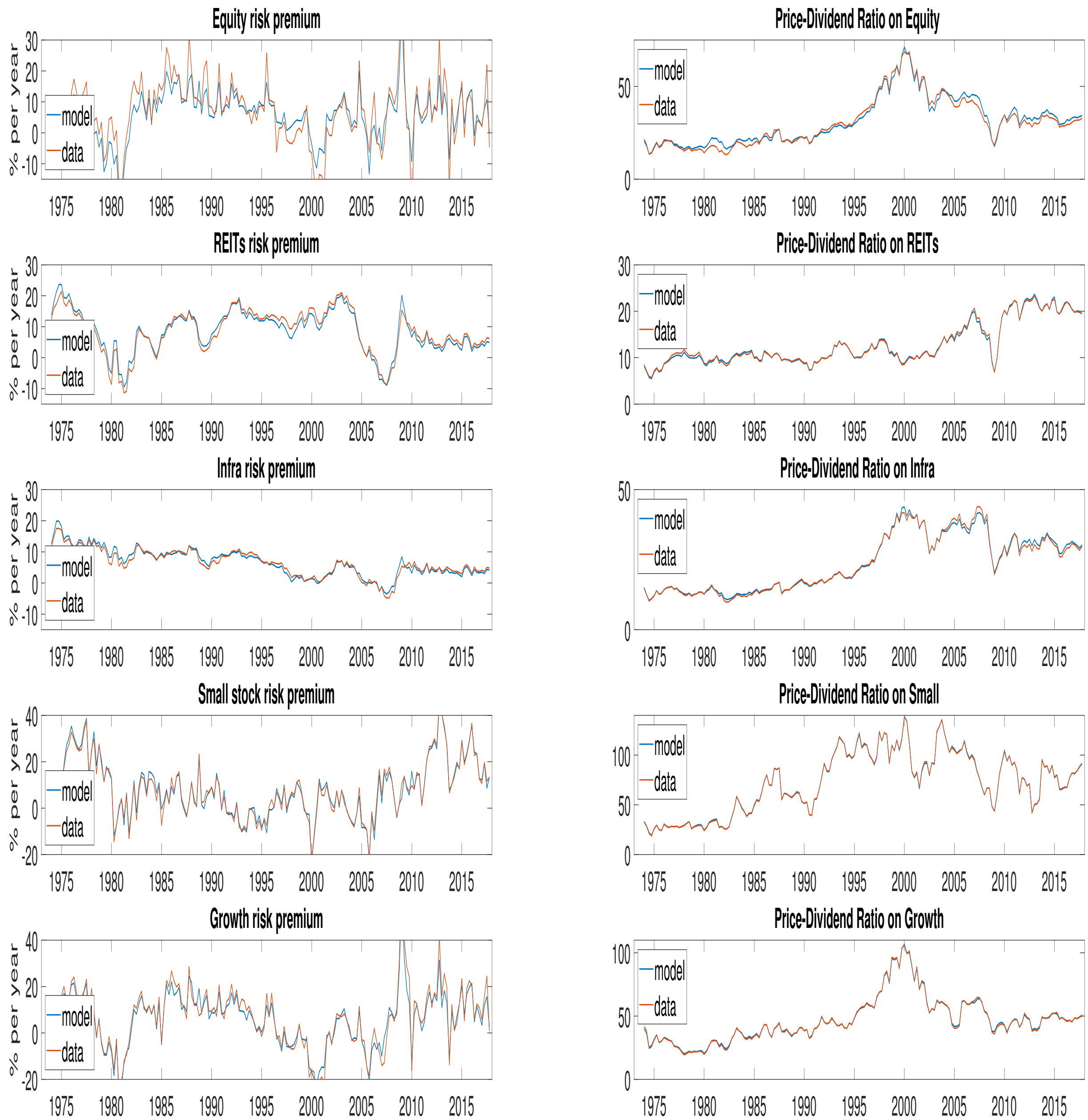

strip positions need to be scaled down in order to make the replicating portfolio budget feasible. This increases the risk-adjusted performance of vintage-2000 VC funds, all else equal.

As part of the estimation, the model fits several features of traded dividend strips on the aggregate stock market. Figure 5 shows the observed time series of the price-

Figure 4: Zero Coupon Bond Prices and Dividend Strip Prices

The figure plots the model-implied prices on zero-coupon Treasury bonds in the first panel, and price-dividend ratios for dividend strips on the overall stock market, REIT market, infrastructure stocks, small stocks, and growth stocks in the next five panels, for maturities of 4, 20, and 40 quarters. The prices/price-dividend ratios are expressed in levels and each claim pays out a single cash flow.

dividend ratio on a claim to the first 8 quarters of dividends (red line, left panel), as well as the share of the total stock market value that these first eight quarters of dividends represent (red line, right panel). The blue line is the model. The model generates the right level for the price-dividend ratio for the short-horizon claim. For the same 55 quarters for which the data are available, the average is 7.75 in the model and 7.65 in the data. The first 8 quarters of dividends represent 3.4% of the overall stock market value in the data and 4.5% in the model, over the period in which there are data. The model mimics the observed dynamics of the short-horizon value share quite well, including the sharp decline in 2000.Q4-2001.Q1 when the short-term strip value falls by more than the overall stock market. This reflects the market's perception that the recession would be short-lived. In contrast, the share of short-term strips increases in the Great Recession, both in the data and in the model, in recognition of the persistent nature of the crisis.

Figure 5: Short-run Cumulative Dividend Strips

The left panel plots the model-implied price-dividend ratio on a claim that pays the next eight quarters of dividends on the aggregate stock market. The right panel plots the share that this claim represents in the overall value of the stock market. The data are from van Binsbergen, Brandt, and Koijen (2012) and available from 1996.Q1-2009.Q3.

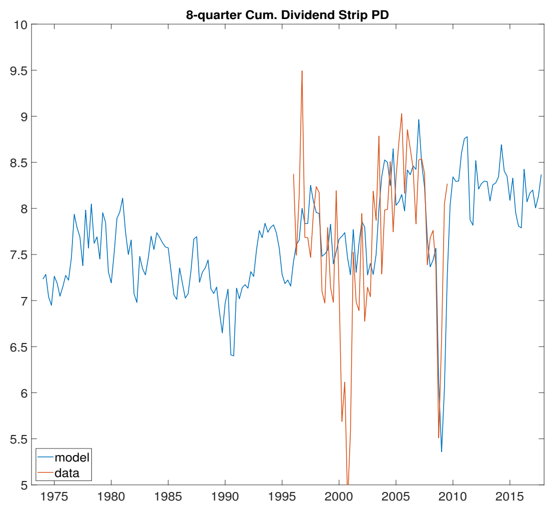

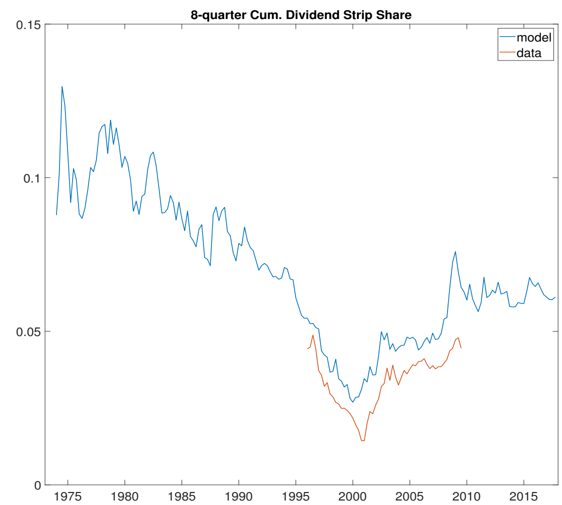

A second key input in the private equity valuation exercise derived from the model is the expected excess return on the bond and stock strips of horizons of 1-60 quarters. After all, the expected return of the PE-replicating portfolio is a linear combination of these expected returns. Figure 6 plots the average risk premium on nominal zero coupon bond yields (top left panel) and on dividend strips (other five panels). Risk premia on nominal bonds are increasing with maturity from 0 to 3.5%. The second panel shows the risk premia on dividend strips on the overall stock market (solid blue line). It also plots the dividend futures risk premium. The difference between the dividend spot and futures risk premium is approximately equal to the nominal bond risk premium. The unconditional dividend futures risk premium (red line) is downward sloping in maturity at the short end of the curve, and then flattens out. The graph also plots the model-implied dividend futures risk premium, averaged over the period 2003.Q1-2014.Q2 (yellow line). It is substantially more downward sloping at the short end than the risk premium averaged over the entire 1974-2017 sample. Indeed, the model matches the *realized* portfolio return on dividend futures of maturities 1-7 years over the period 2003.Q1-2014.Q2, which is 8.7% in the data and 8.7% in the model.[8]

[8] As an aside, the conditional risk premium, which is the *expected* return on the dividend futures portfolio over the 2003.Q1-2014.Q2 period is 6.0% per year in the model. The unconditional risk premium on the dividend futures portfolio (over the full sample) is 5.2%.

Figure 6: Zero Coupon Bond Prices and Dividend Strip Prices

The figure plots the model-implied average risk premia on nominal zero-coupon Treasury bonds in the first panel, and on dividend strips on the overall stock market, REIT market, and infrastructure sector in the next three panels, for maturities ranging from 1 to 180 months.

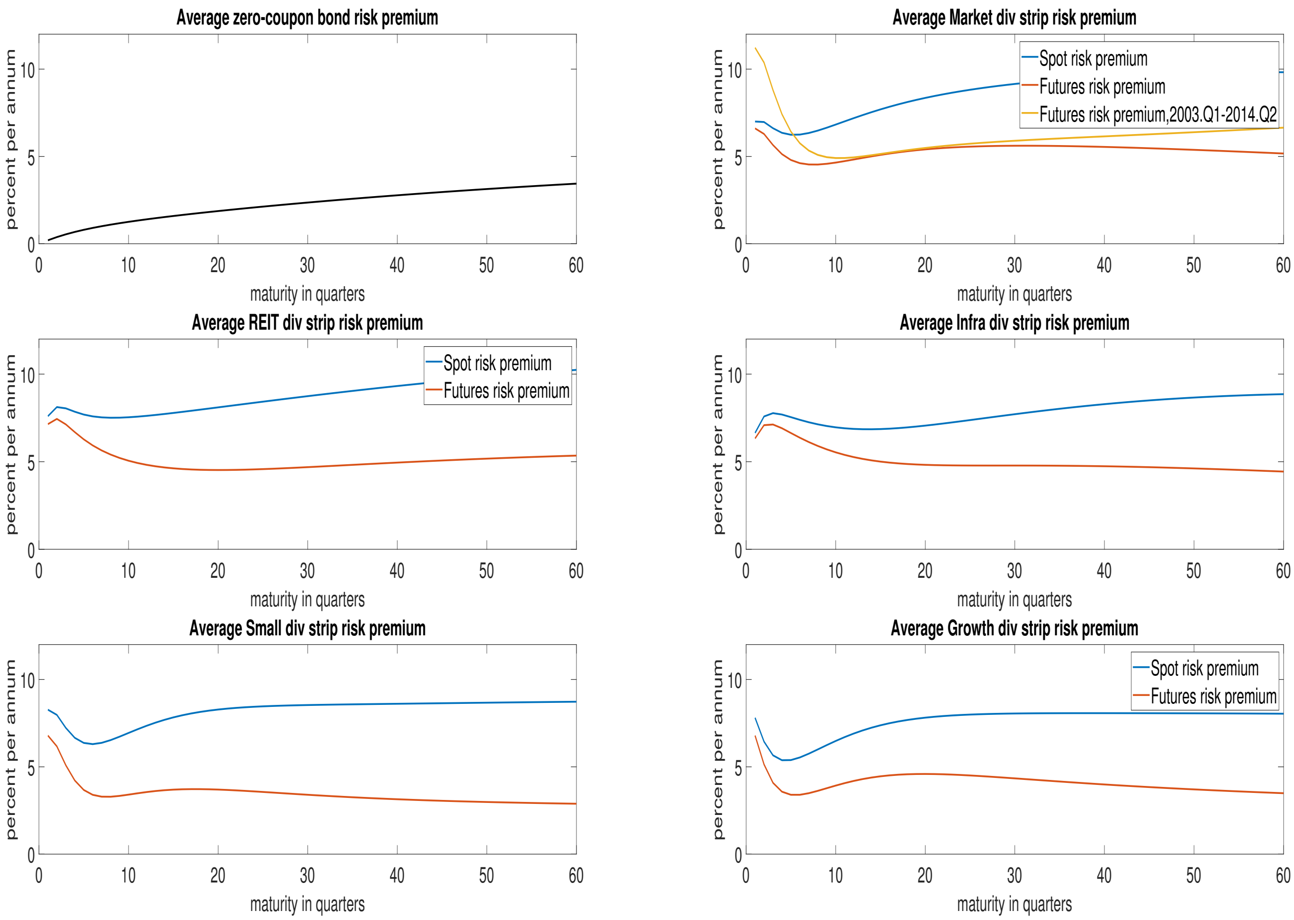

The remaining four panels of Figure 6 show the dividend strip risk spot and future premia for real estate, infrastructure, small, and growth stocks. They differ in shape and level of risk premia, with future risk premia generally declining in maturity. The upward slope in the spot risk premia is inherited from the nominal bond risk premia. Heterogeneity in risk premia by horizon and by asset class will give rise to heterogeneity in the risk premia on the PE-replicating portfolios.

Appendix **??** provides further insight into how the model prices risk at each horizon using the shock exposure and shock price elasticity tools developed by Hansen and Scheinkman (2009) and Borovička and Hansen (2014).

4 Expected Returns and Risk-adjusted Profits in PE Funds

In this section, we combine the cash-flow exposures from section 2 with the asset prices from section 3 to obtain risk-adjusted profits on private equity funds.

4.1 Summary Statistics

Our fund data cover the period January 1981 until December 2017. The data source is Preqin. We group private equity funds into seven categories: Buyout (LBO), Venture Capital (VC), Real Estate (RE), Infrastructure (IN), Fund of Funds (FF), Debt Funds (DF), and Restructuring (RS). Our FF category contains the Preqin categories Fund of Funds, Hybrid Equity, and Secondaries. The Buyout category is commonly referred to as Private Equity, whereas we use the PE label to refer to the combination of all investment categories.[9]

We include all funds with non-missing cash-flow information. We group funds also by their vintage, the quarter in which they make their first capital call. The last vintage we consider in the analysis is the 2017.Q4 vintage. Table 1 reports the number of funds and the aggregate AUM in each vintage-category pair. In total, we have 4,223 funds in our analysis and an aggregate of $4.1 trillion in assets under management. There is clear business cycle variation in when funds funds get started as well as in their size (AUM). Buyouts are the largest category by AUM, followed by Real Estate, and then Venture Capital. The last column of the table shows the tercile of the price/dividend ratio on the aggregate market, which we use as a conditioning variable, averaged over the quarters (vintages) within each year.

Figure 7 shows the average cash-flow profile in each category for distribution events, pooling all funds and vintages together and equally weighting them. We combine all monthly cash-flows into one quarterly cash-flow for each fund. Quarter zero is the first quarter of the fund's vintage. The last bar is for the last quarter 15 years after fund formation (quarter 60). For the purposes of making this figure and in the cash-flow beta estimation, we include all observed cash-flows until 2017.Q4. Thus, the 2010 vintage funds have at most 32 quarters of cash-flows. Cash-flows arriving after quarter 60 are included in the last quarter under a separately highlighted color (green), and we similarly collapse all post-15 year cash flows to the last quarter in our estimation. These terminal cash-flows are generally a substantial portion of the total cash received by LPs. The distribution cash-

[9] One may be able to further enrich the analysis by defining categories more granularly. For example, real estate strategies are often subdivided into opportunistic, value-add, core plus, and core funds. Infrastructure could be divided into greenfield and brownfield, etc.

Table 1: Summary Statistics

Panel A: Fund Count

Vintage	Buyout	Debt Fund	Fund of Funds	Infrastructure	Real Estate	Restructuring	Venture Capital	Total	P/D Ratio
1981	0	0	0	0	0	0	1	1	1
1982	0	0	0	0	0	0	3	3	1
1983	0	0	1	0	0	0	1	2	1
1984	0	0	0	0	0	0	3	3	1
1985	4	0	0	0	0	0	6	10	1
1986	2	0	3	0	0	0	7	12	1.3
1987	5	0	0	0	0	0	5	10	1.7
1988	7	0	1	0	0	0	4	12	1
1989	3	0	0	1	0	0	5	9	1.8
1990	7	0	2	0	0	1	8	18	1.4
1991	2	0	1	0	0	2	4	9	2
1992	9	0	0	1	1	2	12	25	2
1993	9	0	2	1	0	0	11	23	2
1994	15	0	1	2	1	1	12	32	2
1995	14	0	5	1	2	0	17	39	2
1996	20	0	1	3	3	3	21	51	2.8
1997	23	0	4	2	6	2	26	63	3
1998	40	0	11	4	3	1	32	91	3
1999	31	1	9	1	2	3	47	94	3
2000	33	2	17	0	6	3	84	145	3
2001	21	0	19	1	2	5	55	103	3
2002	24	1	13	3	3	3	29	76	3
2003	18	1	12	2	7	4	20	64	3
2004	27	1	19	6	11	2	33	99	3
2005	55	2	33	5	19	6	49	169	3
2006	71	1	51	8	32	11	59	233	3.0
2007	72	1	48	13	35	13	72	254	2.9
2008	65	5	61	11	31	11	62	246	2.0
2009	27	2	30	9	12	8	26	114	1.4
2010	39	4	38	18	28	8	39	174	2.6
2011	53	2	64	22	46	12	49	248	2.5
2012	63	3	54	19	36	12	44	231	2.3
2013	63	15	66	19	59	20	53	295	2.3
2014	68	12	67	26	46	16	67	302	2.9
2015	72	16	72	21	73	18	76	348	2
2016	91	13	78	32	59	10	72	355	2
2017	47	20	39	22	61	7	60	256	2

Panel B: Fund AUM ($m)

Vintage	Buyout	Debt Fund	Fund of Funds	Infrastructure	Real Estate	Restructuring	Venture Capital	Total
1981	0	0	0	0	0	0	0	0
1982	0	0	0	0	0	0	55	55
1983	0	0	75	0	0	0	0	75
1984	0	0	0	0	0	0	189	189
1985	1,580	0	0	0	0	0	74	1,654
1986	59	0	1,510	0	0	0	293	1,862
1987	1,608	0	0	0	0	0	1,061	2,669
1988	2,789	0	0	0	0	0	463	3,252
1989	761	0	0	160	0	0	305	1,226
1990	2,457	0	1,906	0	0	153	1,125	5,641
1991	242	0	0	0	0	329	431	1,002
1992	1,150	0	0	184	0	59	1,320	2,713
1993	3,192	0	597	54	0	0	1,438	5,281
1994	6,882	0	140	1,519	488	93	1,413	10,535
1995	9,169	0	1,172	205	523	0	2,645	13,714
1996	7,435	0	242	1,114	1,851	1,600	3,820	16,062
1997	23,633	0	1,337	480	3,642	1,700	6,308	37,100
1998	38,956	0	10,879	3,933	3,461	52	8,441	65,722
1999	34,297	109	9,248	42	2,293	3,133	17,093	66,215
2000	56,299	730	13,570	0	6,757	3,320	37,802	118,478
2001	23,856	0	11,942	1,375	3,225	7,461	23,852	71,711
2002	23,705	100	10,043	1,795	5,507	1,844	7,391	50,385
2003	31,264	366	8,767	884	3,435	5,105	6,670	56,491
2004	32,855	215	5,808	5,446	6,269	2,580	8,419	61,592
2005	102,231	412	23,252	6,353	25,523	5,830	16,280	179,881
2006	215,875	778	41,728	9,726	42,442	22,928	37,285	370,762
2007	176,849	400	45,660	21,568	44,657	40,486	24,198	353,818
2008	165,982	4,697	39,493	27,228	37,789	26,158	31,839	333,186
2009	38,738	195	11,544	12,108	9,451	11,170	8,880	92,086
2010	30,612	1,684	20,662	19,891	20,125	11,855	21,457	126,286
2011	97,669	1,720	26,915	21,581	48,951	19,237	23,747	239,820
2012	94,732	733	40,384	34,467	23,417	23,943	29,566	247,242
2013	88,022	16,333	20,013	32,762	65,703	25,660	26,026	274,519
2014	126,182	5,638	37,191	50,504	32,206	21,792	35,863	309,376
2015	115,376	12,421	52,430	33,903	75,627	34,845	31,294	355,896
2016	165,779	10,721	47,705	53,388	45,416	11,368	36,433	370,810
2017	112,820	15,942	18,539	20,385	52,750	9,609	25,659	255,704

flows follow a hump-shaped pattern. While a majority of distribution cash-flows occur between years 5 and 10, there meaningful cash-flow distributions before year 5 and after year 10. This is especially true for IN and VC funds.

Figure 7: Distribution Cash-flow Profiles

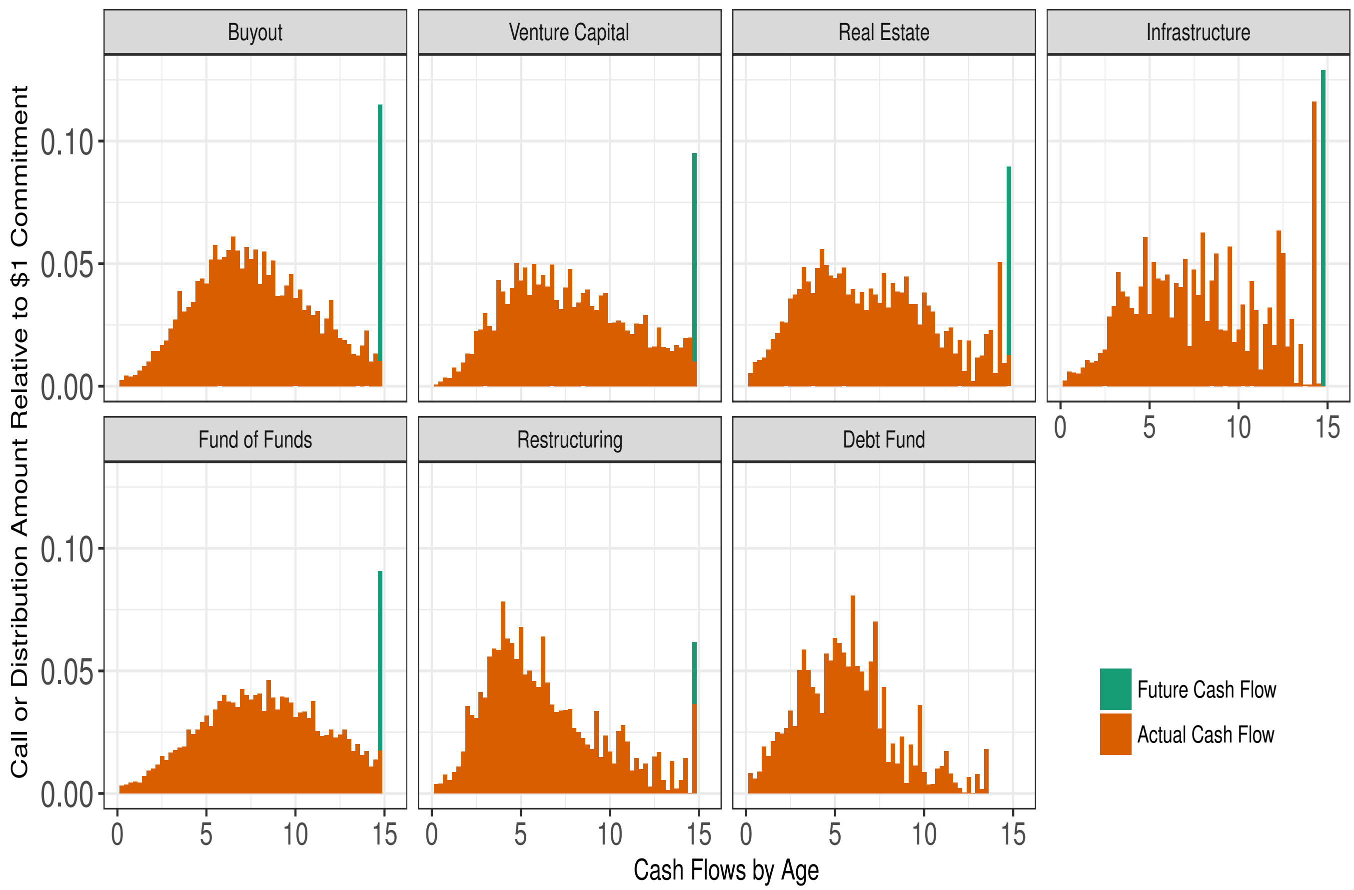

Figure 8 zooms in on the four investment categories of most interest to us: LBO, VC, RE, and IN. The figure shows the average cash-flow profile for each vintage. Since there are few LBO and VC funds prior to 1990 and few RE and IN funds prior to 2000, we start the former two panels with vintage year 1990 and the latter two panels with vintage year 2000. The figure shows that there is substantial variation in cash-flows across vintages, even within the same investment category. This variation will allow us to identify vintage effects. Appendix Figures **??** shows cash-flow profiles for the remaining categories.

The figure also highlights that there is a lot of variation in cash-flows across calendar years. VC funds started in the mid- to late-1990s vintages realized very high average cash-flows around calendar year 2000 and a sharp drop thereafter. Since the stock market also had very high cash-flow realizations in the year 2000 and a sharp drop thereafter, this type of variation will help the model identify a high stock market beta for VC funds. This is an important distinction with other methods, such as the PME, which assume constant risk exposure and so would attribute high cash flow distributions in this period to excess returns.

Figure 8: Cash-flows by Vintage

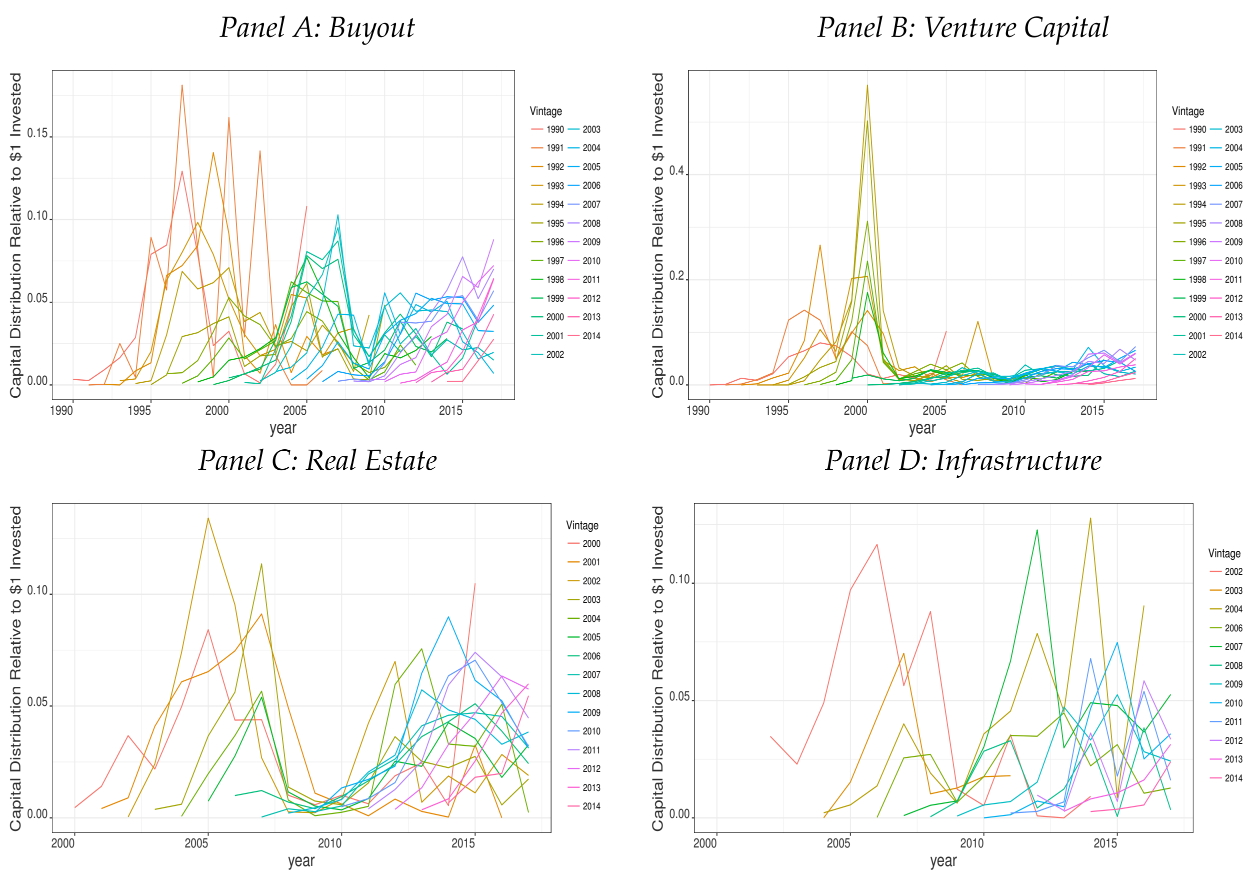

4.2 Three-Factor OLS Model

We start with a discussion of our benchmark three-factor model estimated through an OLS model. This estimation is run separately for each fund category, and we choose three factors for each category to correspond to the fundamental economic risks taken on by managers specific to that domain.

Figure 9: OLS 3-Factor Model

Panel A: Buyout

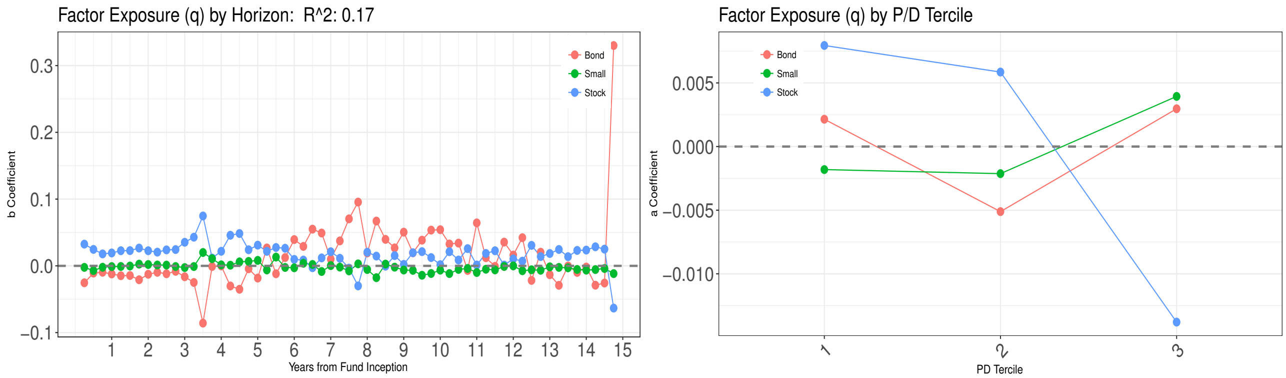

Panel B: Venture Capital

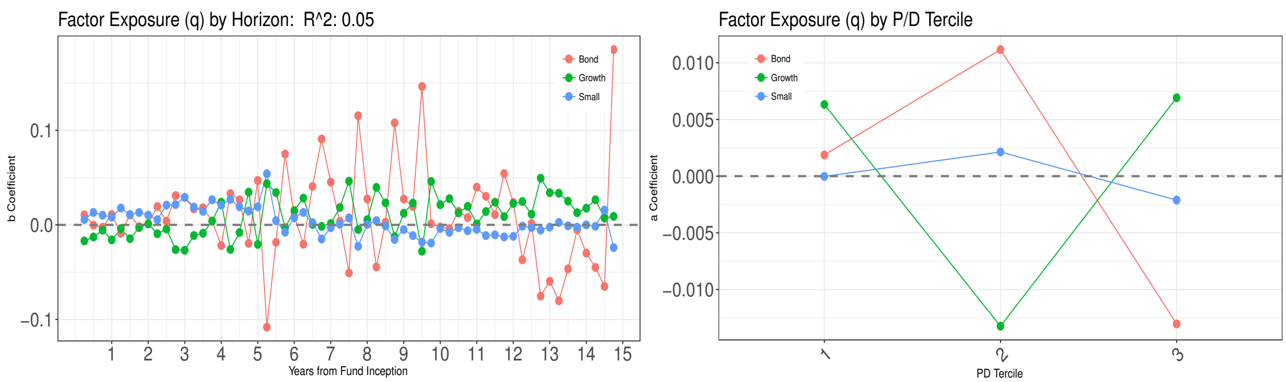

Panel C: Real Estate

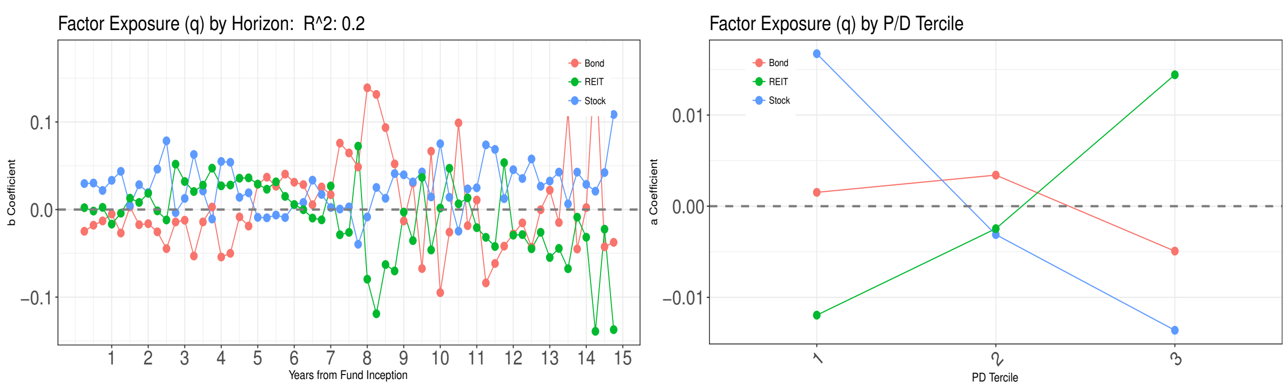

Panel D: Infrastructure

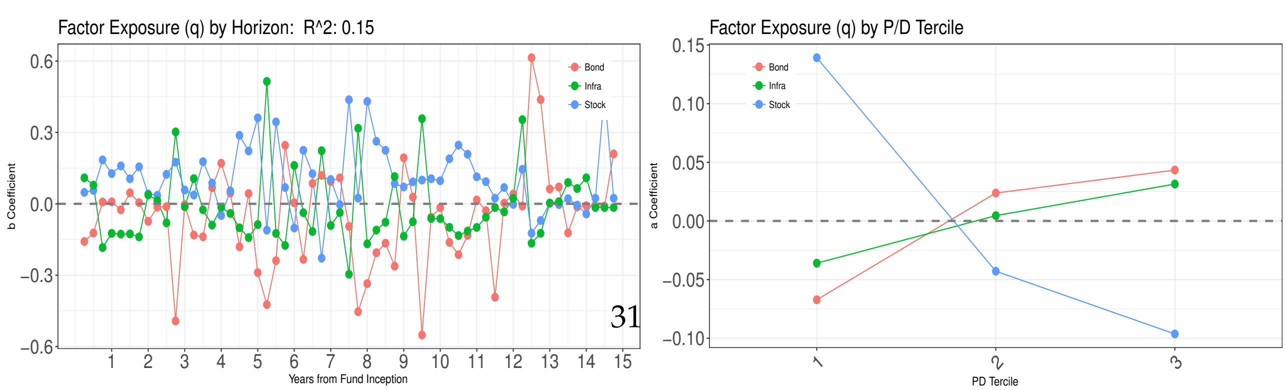

The key parameters from the model are the factor exposures across each horizon, corresponding to the replicating portfolio exposure in a zero-coupon bond or equity strip payoff in that same horizon. We additionally allow these factor exposures to vary depending on the price/dividend tercile in the originating vintage to account for general market conditions at the time of fund formation.

Finally, we scale the resulting positions in the zero coupon bonds and equity dividend strips of various maturities based on the model prices to ensure budget feasibility. The high cash flows of a particular PE category may not be achievable/replicable with a budget-feasible bond portfolio, but only with a budget infeasible one. This will result in high "errors" v and high average risk-adjusted profits across the funds in that vintage-category.

Figure 9 show the estimated horizon effects $\widehat{b}_h$ in the left panels and the PD-tercile effects $\widehat{a}_t$ in the right panels. Appendix Figure **??** contains the same figure for other fund categories. Each row is for one of our four main investment categories. The plotted coefficients on the left are the positions that the replicating portfolio holds in bond strips (zero-coupon bonds) of the various horizons, as well as in the equity strips.

The precise equity strips chosen vary by category. For the Buyout category, we choose the aggregate stock index as well as small stocks, corresponding to two salient forms of equity risk taken on by PE managers in this category, who are generally operating and managing companies smaller the typical listed firm. Our index of "small" firms corresponds to those in the bottom quintile of size in the market. In our estimation of this model, we find we are able to fit cash flows with an R^2 of around 17% at the fund-level. In terms of the factor loadings, we observe a meaningful difference around the 6th or 7th year of fund life, which corresponds to roughly the peak distribution years of fund life. Prior to this period, PE cash flows take on the strongest loading to the equity factor, with smaller loadings small stock factors; and negative loadings on the bond factor. After the 6th year of fund life, estimated loadings rise substantially for the bond factor, while they drop for the equity component. The terminal cash flow (around age 15) exhibits a higher bond factor exposure, which accounts for the agglomeration of all future cash flows beyond age 15 to this year. These late in fund age cash flows likely reflect "zombie" funds which have continued well past the expected lifespan.

This suggests that the PE cash flow distributions exhibit different risk characteristics over the fund's life cycle. Early fund cash flow risk looks more equity-like; while later cash flow risk is closer to the levered exposure we would expect based on a scaled bond factor. Small stock and bond loadings are higher in period of greater price-to-dividend valuation ratios, while equity loadings are lower. The rich dynamics in the estimated factor exposures across fund life and in the time-series suggest that the analysis of risk and return in PE should take into account a richer factor structure than has traditionally been explored.

In Panel B of this figure, we examine the VC category, which has also been a focus of research. We use small stocks as a factor, since VC funds also invest in companies in early stages of development. However, we find that the stock equity factor does not meaningfully assist in the estimation.[10] Instead, we replace this factor with a "growth" equity factor for listed firms in the bottom quintile of the book-to-market distribution. Again, these firms should correspond to the category of early-stage and rapidly expanding entrepreneurial companies invested in by VC funds. We find that VC funds do indeed have considerable exposure to the small stock, growth stock, and bond factors over their life. We find that the size of the exposure to the small stock factor decreases after year 6-7. Exposure to the bond factor remains elevated in our estimation until about year 10 or so, at which point VC funds on average continue to be distributing substantial amounts of cash to LPs. We find that VC funds retain substantial exposure to the growth factor across their life. Still, despite the fact that our replicating portfolio takes on meaningful exposure to economically related factors, the model fit ($R^2 = 5\%$) is not as high as with the Buyout category. This suggests a greater role for idiosyncratic risk, and in turn, a greater possibility for out-performance among funds in this category, which we will examine further below.

In the next two panels, we turn to real estate and infrastructure funds; and for these categories include stock, bond, and a sector specific factor (REITs for RE, and an listed infrastructure index for IN funds). We estimate an R^2 of 0.20 in the real estate category, and 0.15 in the infrastructure category. In the real estate category, we find a substantial role for the REIT factor, which rises and falls in a hump-shape across fund age, in close parallel with the bond factor. This REIT exposure is greatest for funds originated in the riskier PD-tercile. By contrast, we see less of a role for the stock market aggregate factor; suggesting that the risk and returns for RE funds are better proxied by real estate-linked assets which dominate their portfolios.

We see a slightly different pattern for infrastructure funds. There, the sector-specific

[10] We confirm this in a separate analysis using our Lasso estimator in which allow for our generic stock factor, the small factor, as well as the growth to enter in separately. We find that the best fit replicating portfolio generally does not invest in the stock factor.

factor—infrastructure—has some explanatory power throughout the fund's life cycle.

These rich dynamics across horizon, vintage, and choice of factors have important asset pricing implications. A key takeaway is that the risk loadings on private equity funds broadly cannot be assumed to be static either in the time-series or across the maturity of fund age. Additionally, they exhibit important sector-specific variation. A generic finding is that the sector-specific factors frequently offer better predictive fit for each of the categories (small stocks for PE and VC; growth for VC; REIT for real estate; and listed infrastructure stocks for infrastructure funds). We provide the first systematic analysis of the asset pricing properties of these some of these alternative fund categories, and find that they carry this sector-specific asset exposure. These exposures are generally not constant across fund life; but are frequently concentrated in the first half of the fund cash flows.

As a consequence, the analysis of risk and return for these sorts of funds must take into account a more accurate assessment of the relevant factor risk for the different categories. Our dividend-strip estimation approach allows us to translate these complex risk dynamics into the expected return for different fund categories and to revisit the question of performance evaluation.

OLS Model: Expected Return With the replicating portfolio of zero-coupon bonds and dividend strips in hand (details in Appendix A), we can calculate the expected return on PE funds in each investment category as in equation (3). The left panels of Figure 10 plot the total expected return over the life of the investment, broken down into the different horizon components and various factors, and averaged across all vintages. Since most of the cash-flows come later and later cash flows are riskier (higher bond beta), the risk premium is "backloaded." The right panels plot the time-series of the expected return; by aggregating all of the different horizon effects; and annualizing the resulting expected return as in equation (5).

Our estimation delivers rich dynamics in terms of the variation in expected returns; in the cross-section across different categories; across different maturities depending on the precise factor loadings; and in the time-series. The nature of expected returns depends on the fund category. Across Buyout, VC, and Infrastructure funds, a sizable fraction of the expected return is dominated by the expected returns to stocks; while expected returns primarily reflect compensation for REIT exposure among real estate funds.

In Buyout funds, we additionally observe interesting variation across fund age. Earlier on in fund age, the expected return is largely aggregate stock-based, and to a lesser extent associated with size; while there is a greater component associated with bond risk in the middle of fund life. All three factors are important drivers of the expected return by the end of the fund life. These life-cycle dynamics of expected return correspond, economically, to the different stages of PE activity. Early in fund life, the focus is primarily on acquiring target companies; and resulting cash flows are generally produced by distributing cash from company operations. Our results suggest that this produces an expected risk exposure which is more associated with that of small companies and of equities overall. The bulk of cash flow distributions happen in a wind-down stage of fund operations as portfolio companies are re-sold. This produces more bond-like risk exposures from the perspective of the cash flows. Finally, the "zombie" cash flows (fund life is traditionally thought to end after 10 years) reflect a mix of all three risk exposures.

Aside from the life-cycle, we also observe interesting patterns in the time-series of expected returns; shown in the right panels. Time variation in the exposure, through dependence on the pd-tercile of the vintage, but especially through the state variables of the VAR drive variation in the expected return of the replicating portfolio of the PE fund. Our results suggest that the annualized expected returns that investors can anticipate in their PE investments has seen large variation over time, with a declining pattern at low frequencies. In our estimation, this is because the risk exposure offered by PE funds generally carries lower expected returns in the post 2000-sample. In turn, this implies that PE investors should expect to see lower returns in the later periods. The level of expected returns varies dramatically across fund categories. Buyout and VC fund expected returns reached a maximum of about 20% per year in the 1980s and declined to about 5% per year in the recent period. Real estate funds had similarly high expected returns in the 1980s and have stabilized just below 10% in the last several years.

Performance Evaluation Next, we turn to performance evaluation in the context of our three-factor OLS model. We do so in two ways. The left panels of Figure 11 plots the histogram of risk-adjusted profits (RAP), pooling all vintages. The right panels plot the average risk-adjusted profit for each vintage. Appendix Figure **??** reports on the remaining investment categories. While our model estimation attempts to fit fund cash flow using a number of bond and stock dividend strips; the resulting replicating portfolio's cash flows need not resemble the underlying PE funds' because the former additionally satisfy a budget constraint. To the extent that PE funds are able to offer a comparable risk exposure to our replicating portfolio, but do so more cheaply than the replicating basket of bond and stock assets, they will be credited with positive risk-adjusted profits.[11]

Our measures of fund performance show substantial dispersion both across and within categories. The strongest evidence of out-performance can be found in the VC category. We estimate average profits of 8% above that of the replicating portfolio on average, and 31% of funds generating more than 10% in RAP. However, these risk-adjusted profits are much higher for the 1990s vintages reaching a maximum of two dollars returned to investors in risk-adjusted present value for each dollar invested. Average profit is also quite high in the Infrastructure category, at 25%, though this category features many fewer observations. Our estimates of relative out-performance in the Buyout category are also sizable; suggesting that the typical fund delivers 26% additional in risk-adjusted out-performance and that 63% of funds delivered more than 10 cent in risk-adjusted profits per dollar invested. Average RAP among real estate funds is 8.9%, and 48% of REPE funds deliver more than 10% RAPs.

The evidence suggests that PE funds are able to deliver excess cash flows relative to publicly-traded assets, for a comparable factor exposure, or equivalently, that they deliver this exposure more cheaply. This out-performance can be interpreted as superior performance relative to a benchmark, investment skill, with the caveat that some or all of this out-performance may reflect compensation for illiquidity risk taken on by PE fund investors.

In Figure 12 we plot an alternate measure of model fit, contrasting the IRR of an investment in our replicating portfolio with an equal-weighted IRR average of all PE funds originated in that vintage. This approach offers a natural comparison of the returns experienced by investors in PE funds compared with our replicating approach. Consistent with the evidence of positive average risk-adjusted profit, the IRR of the average fund's cash-flows is above the IRR on the replicating portfolio.[12]

[11] Appendix Figure **??** also compares with the TVPI measure.
[12] Appendix Figure **??** plots these estimates for other categories.

Figure 10: OLS Model — Expected Return

Panel A: Buyout

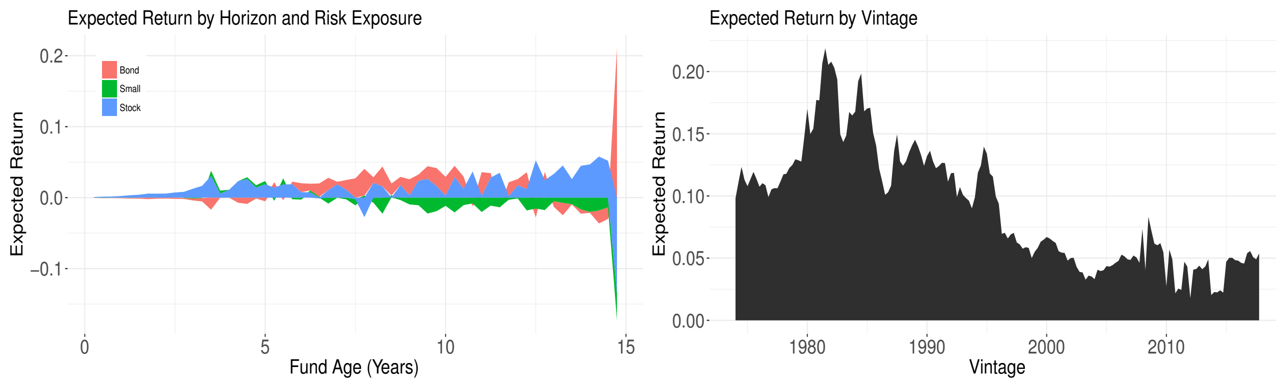

Panel B: Venture Capital

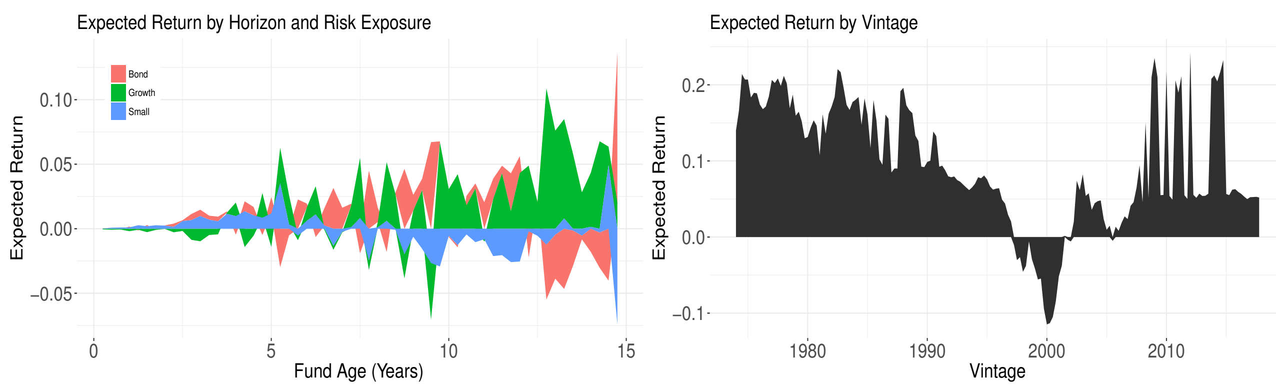

Panel C: Real Estate

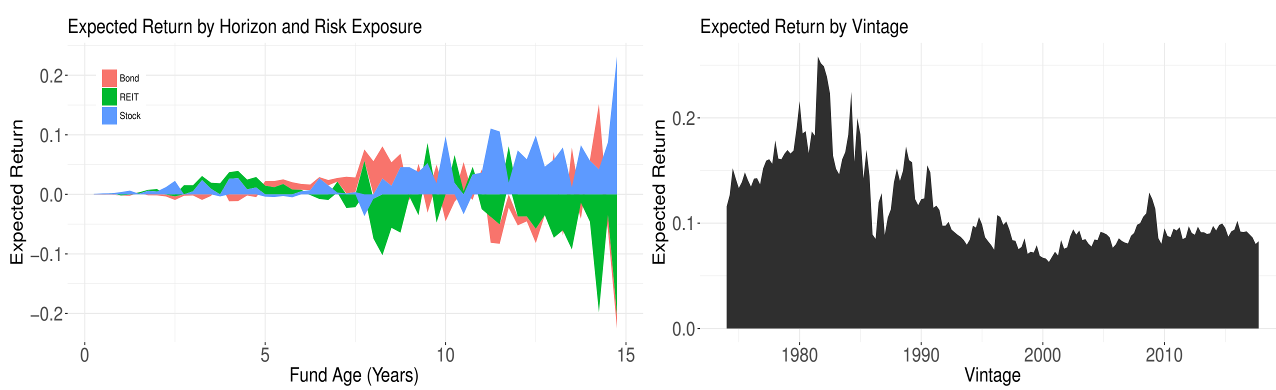

Panel D: Infrastructure

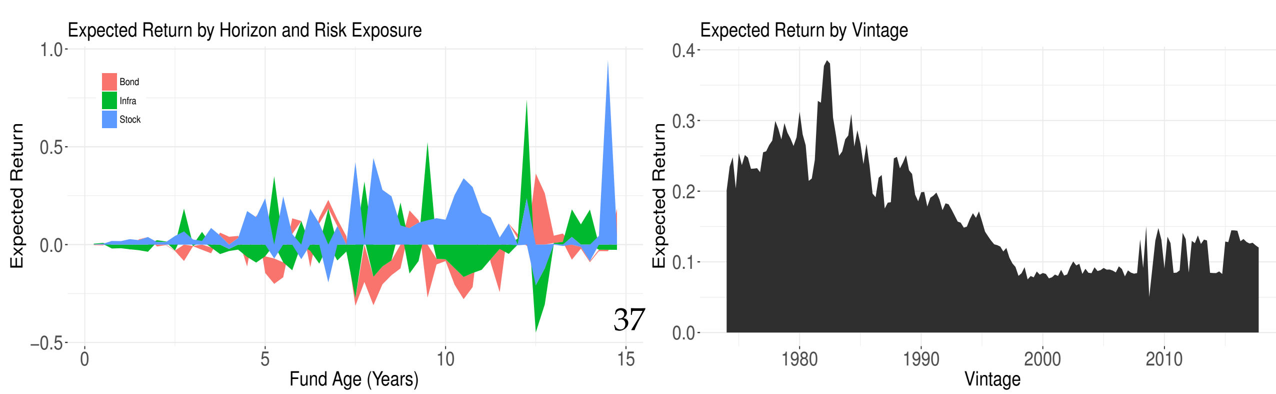

Figure 11: OLS 3-Factor Model, Model Comparison

Panel A: Buyout

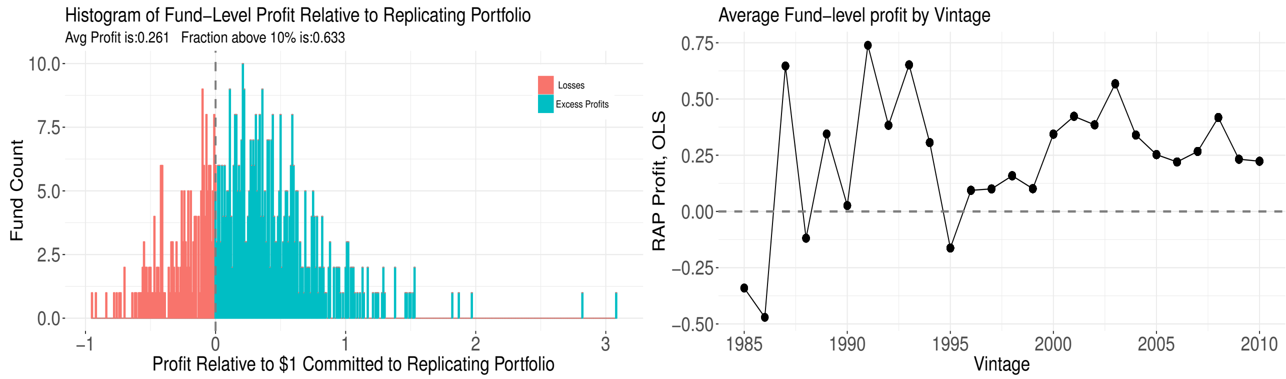

Panel B: Venture Capital

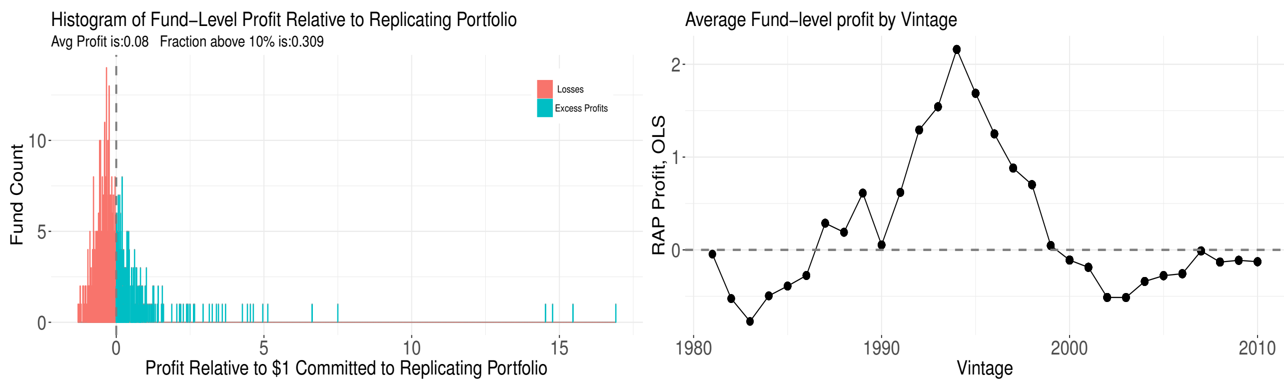

Panel C: Real Estate

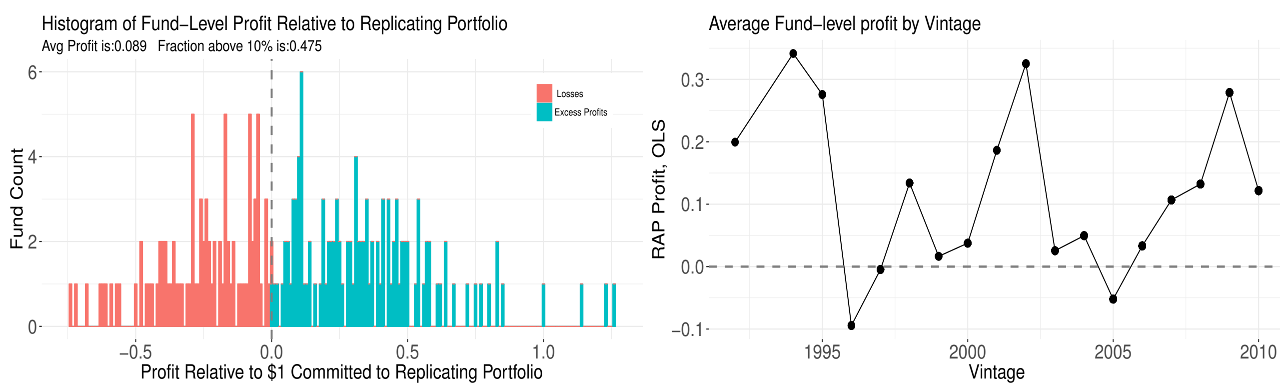

Panel D: Infrastructure

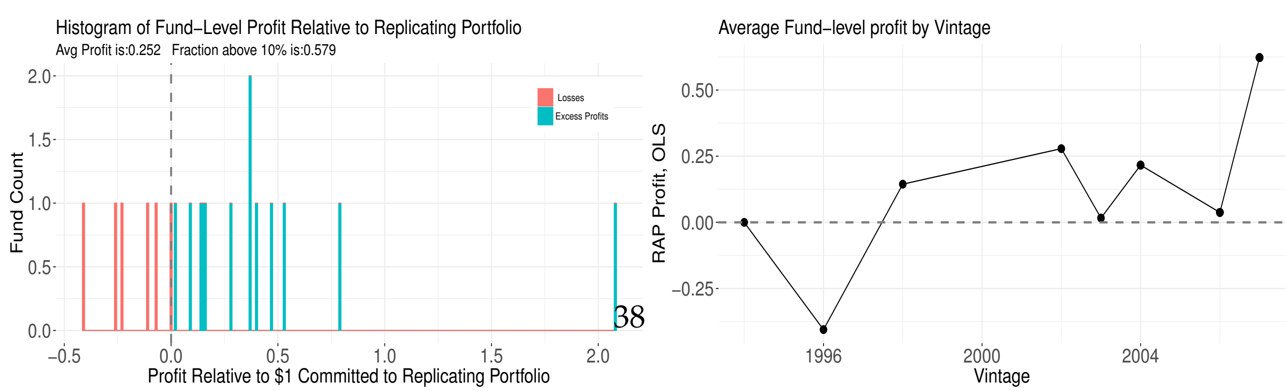

Figure 12: OLS 3-Factor Model, Comparison

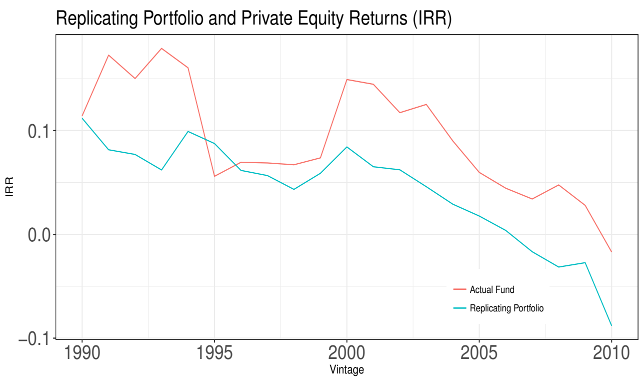

Panel A: Buyout

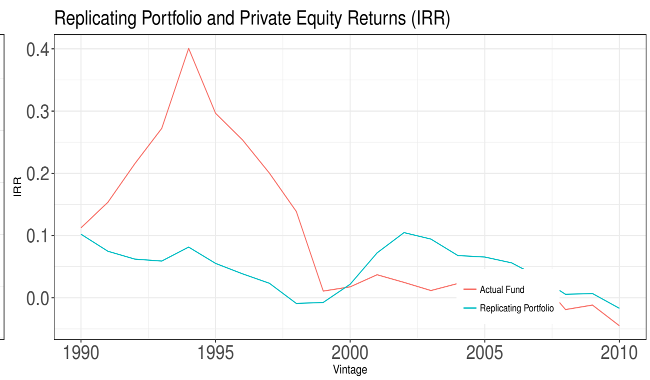

Panel B: Venture Capital

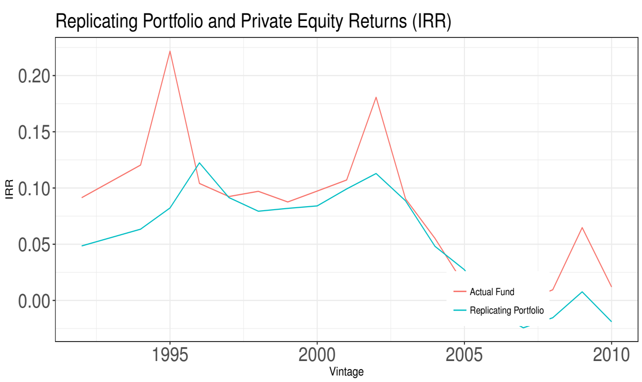

Panel C: Real Estate

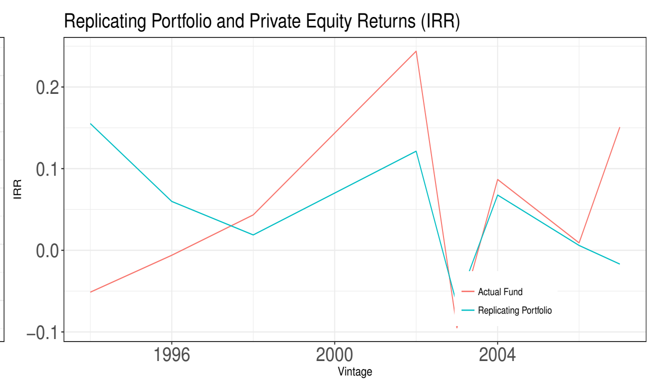

Panel D: Infrastructure

4.3 Positive Coefficient Lasso Model

Next, we turn to our positive exposure model, which constrains all $\beta_{t,h}$ coefficient estimates to be positive. The resulting replicating portfolio consist of long-only exposures. We implement this requirement using a Machine Learning Lasso estimation, which imposes a penalty on any negative coefficient estimates, and "shrinks" such negative coefficients to be precisely zero. This approach has the additional benefit that it results in substantial dimension reduction of our estimation problem, which is attempting to estimate a large number of parameters across a variety of horizons, factors, and underlying vintage states. Applying a penalized term to this estimation results in a more parsimonious replicating portfolio.

Figure 13 show the estimated horizon effects $\widehat{b}_h$ in the left panels, and the vintage effects $\widehat{a}_t$ based on the tercile of the PD-index in the vintage quarter of fund origination in the right panels. The appendix contains the same plot for the three remaining categories. Our model illustrates a rich pattern of factor risk exposures. There are several key takeaways from this approach in estimation.

The first is that the different categories have substantial loading on non-standard, but plausible proxies for sector-specific risk. The Real Estate category, for instance, places substantial weight on the REIT factor; while in the VC and PE categories we observe a strong role for the small stock factor. This is not as true for the Infrastructure category, in which infrastructure loadings are substantial for many horizons, but are shrunk closer to zero for many others. In that category, the bond and stock loadings tend to be more persistently included in the final factor exposure calculation.

The second key takeaway is that we also generally observe different risk exposures across fund-life. Fund cash flow exposure generally looks more equity-like in the early years of fund life (small stocks and aggregate equity for the Buyout category; small stocks in the VC category; REIT in the RE category and aggregate stocks and some infra in the Infra category). However, between years 6–10, when fund assets are most commonly being liquidated, cash flow exposure beings to look much more bond-like; especially for the Buyout and VC categories. This echoes the OLS results.

We also observe some variation in these risk exposures across the PD measure, but with varying impacts across categories. We sometimes observe higher equity factor exposures, particularly in Real Estate, but in other categories these estimates are instead shrunk to zero, indicating relatively little time-varying factor exposure associated with funds originated in vintages with different PD-terciles.

Relative to the OLS model, went tend to observe lower model fits as measured by R^2. This is because the Lasso estimation restricts short-positions, and so avoids the long-short combinations present in the OLS model. In addition, the more sparse representation of coefficients results in a higher estimate of Mean-Square Error. This shrinkage estimation effectively trades off bias in parameter estimates in favor of lowering the variance.

Expected Return Figure 14 plots the expected returns by horizon and factor (the left panels) as well as the annualized expected return for each vintage (the right panels). Appendix Figure **??** plots these for the remaining categories. Overall, the aggregate expected return in the Lasso model is quite similar to that in the OLS model. However, the composition of the expected returns across horizons and factors is somewhat different. The positive coefficient approach sets many factor exposures to zero, resulting greater sparsity, as many exposures only turn on for limited durations.

The categories which see the largest changes across the specification approaches are VC and IN, as these were the categories with the largest role for negative exposures in the OLS model. For VC, we eliminate the negative exposures to growth stocks. As a result, we see expected returns across fund life follow a three-part pattern. Early in fund life, expected returns are dominated by the small stock factor; in the middle of fund life they are mostly bond related; and in the end of fund life they are largely due to growth funds. In the Infrastructure category, we see a expected return exposure which is largely stock related prior to age 9; but now we observe a greater role for infrastructure itself across a number of horizons; especially later in fund life.

In the time series, expected returns follow the same pattern as in OLS. One difference is that expected returns are higher for the 2009 vintage across categories. The higher expected returns in turn lead to a finding of smaller RAPs for this vintage than in the OLS approach. The appendix extends the analysis for the remaining three fund categories.

Performance Evaluation Figure 15 plots the histogram of risk-adjusted profits for the Lasso model, pooling all vintages, in the left panels. The right panels plot the average risk-adjusted profit for each vintage. We generally observe lower levels of average outperformance of PE funds. Buyout funds outperform the most in our estimation, resulting in an additional 21 cents in risk-adjusted profits to investors per $1 committed. The VC category sees its average RAP drop to 3.9%, a drop from 8.9% in the OLS. Real estate remains similar at 8% while IN frops from 25% to 15%. The largest difference in the time series of RAP is that the Lasso model for real estate implies a modest RAP for the

2009 vintage, compared to a spectacular RAP under the OLS, because the Lasso model estimates higher risk exposure and therefore higher expected return for that vintage.

Figure 16 plots the IRRs of a portfolio of aggregate PE funds, against our replicating portfolio. As in the OLS model, the IRR of the replicating portfolio implied by Lasso tracks the time-series of the observed fund IRR, while being slightly above it. This is consistent with superior performance in certain categories—most saliently, Buyout and VC in the 1990s.

4.4 Comparison of Alternative Approaches

To benchmark our results against other commonly used PE fund performance metrics, Figure 17 plots fund-level IRR against our RAP measure (based on the OLS model) in the left panels. The right panels plot a comparison of the Kaplan and Schoar (2005) PME measure against our measure of RAP (based on OLS). Appendix Figure **??** repeats this comparison for the positive coefficient Lasso model. Plots showing PME draw a horizontal line at 1, above which funds deliver additional returns above a portfolio invested in the S&P 500 index (which respects the cash flow timing of the PE cash flows).

The key takeaway from a comparison of various approaches is the broad similarity of performance evaluation. Our measure of RAP generally correlates between 0.6–0.8 with the IRR and PME approaches. The correlation is generally slightly higher in comparison with the K-S PME as opposed to the IRR in the Buyout and VC categories for which we have the most data. This is reasonable as the PME approach also incorporates a role for public market assets. This similarity indicates that our measure of RAP generally agrees with the other commonly accepted measures of PE performance, lending some credibility to our approach. The measures are not identical, however, so that there will be funds which conventional measures assess to be high-performing but our estimates suggest only offer fair (or too little) compensation for factor risk.

Additionally, the key ways in which our approach differs from conventional measures lies in its ability to evaluate factor loadings and expected returns across different fund categories and different horizons. These results here indicate that our approach is able to considerably deepen our analysis of the asset pricing characteristics of privately listed funds, while refining the broad conclusions about performance in prior literature.

Figure 13: Positive Coefficient 3-Factor Model

Panel A: Buyout

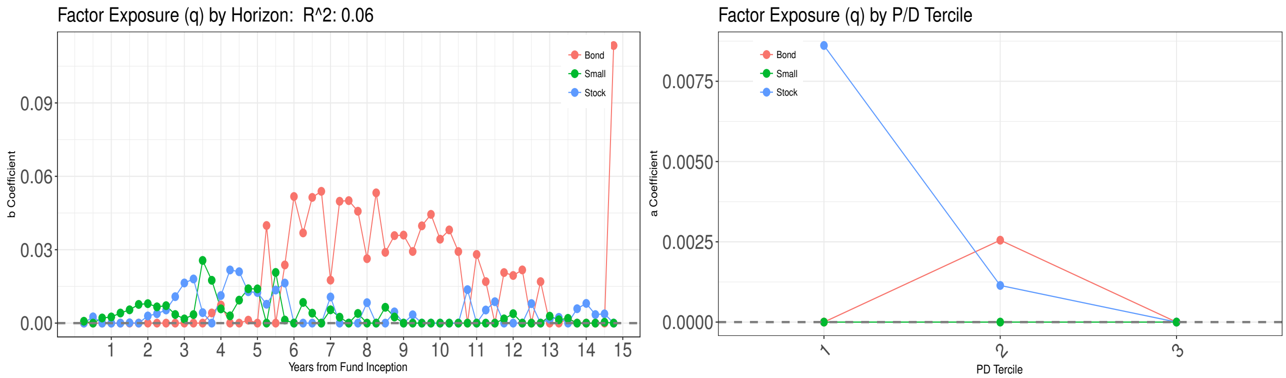

Panel B: Venture Capital

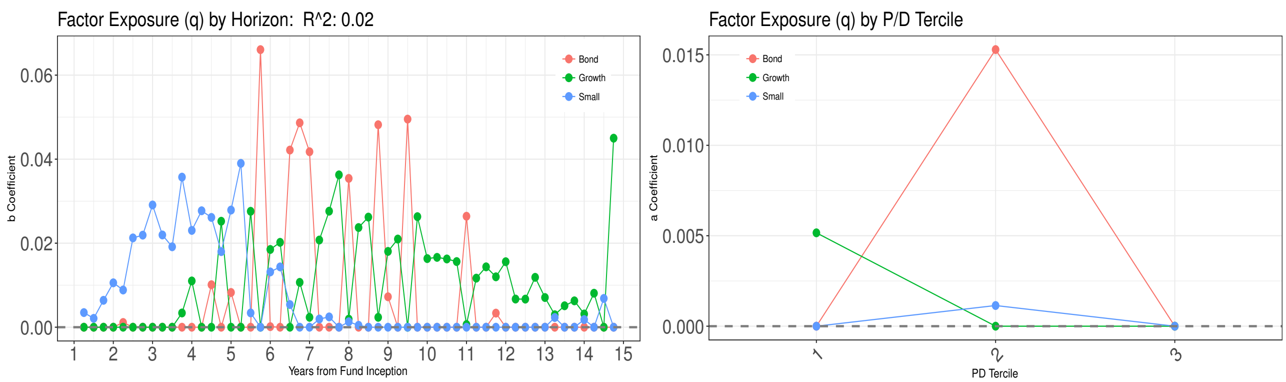

Panel C: Real Estate

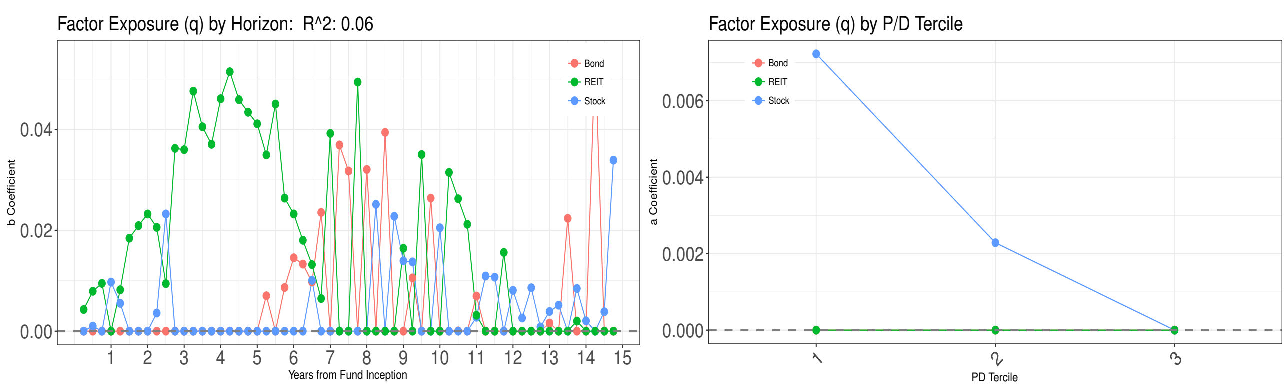

Panel D: Infrastructure

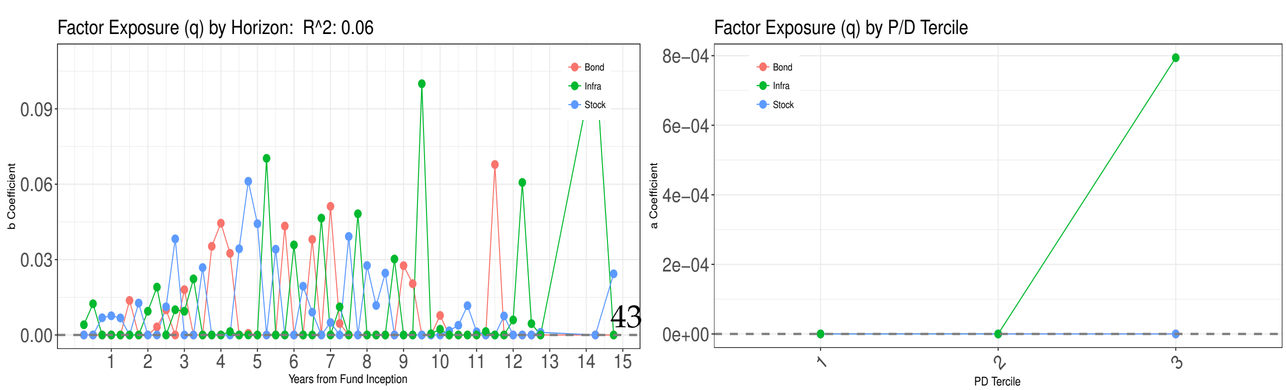

Figure 14: Positive Coefficient Model — Expected Return

Panel A: Buyout

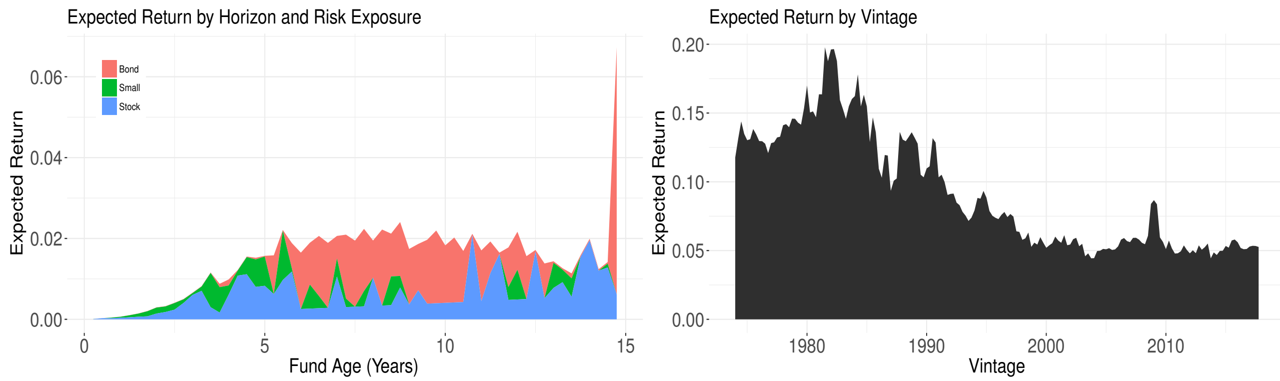

Panel B: Venture Capital

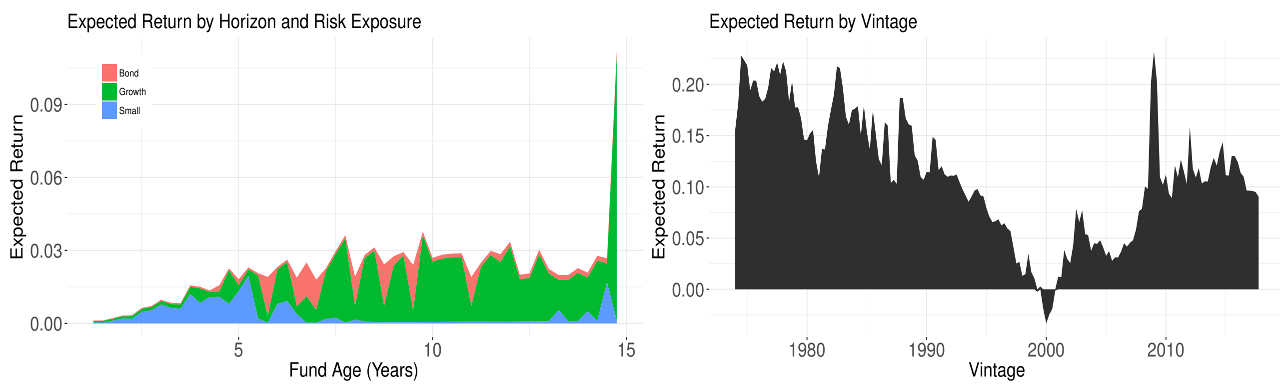

Panel C: Real Estate

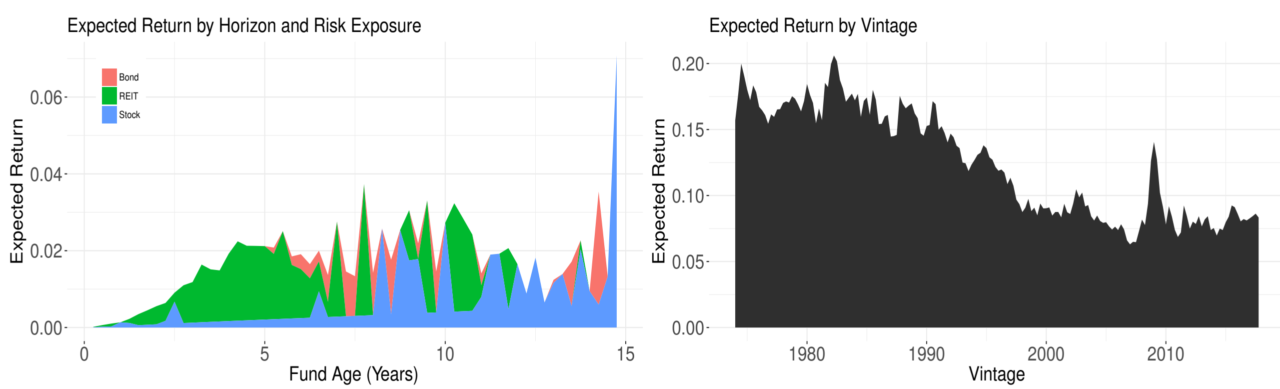

Panel D: Infrastructure

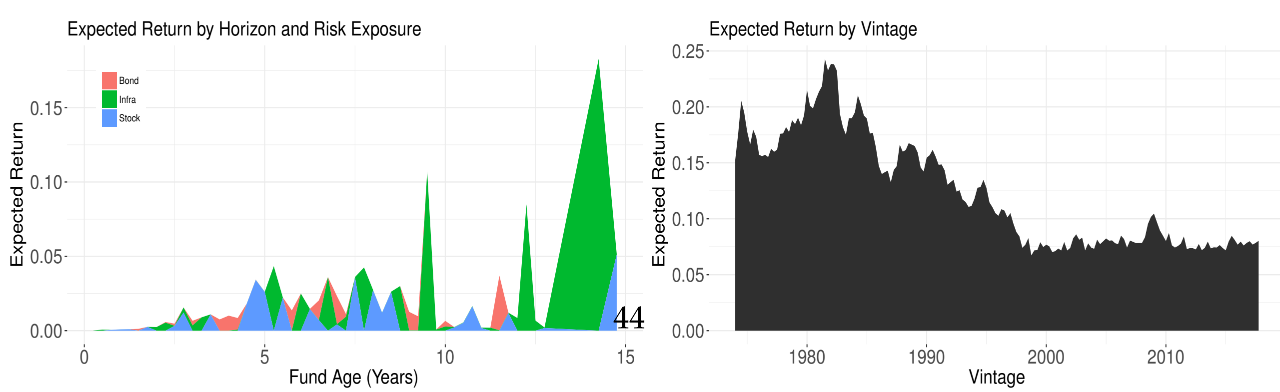

Figure 15: Positive Coefficients 3-Factor Model, Profits

Panel A: Buyout

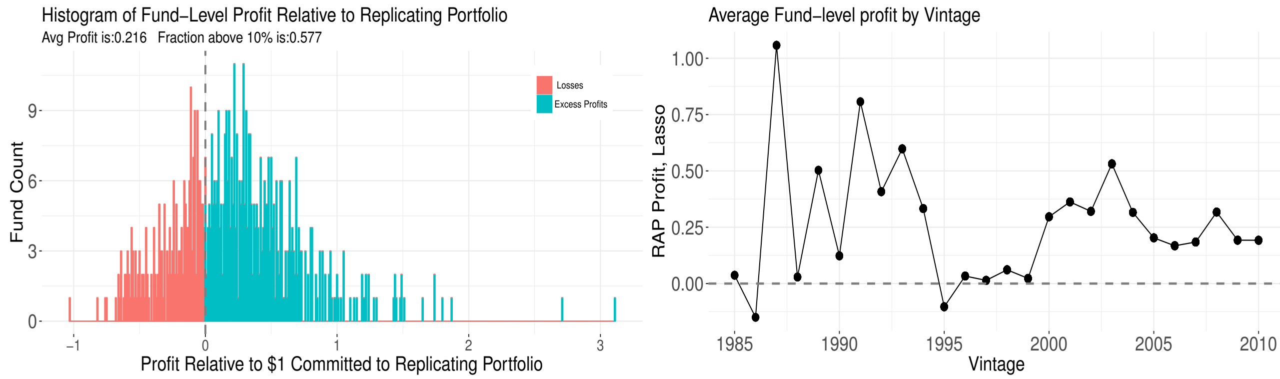

Panel B: Venture Capital

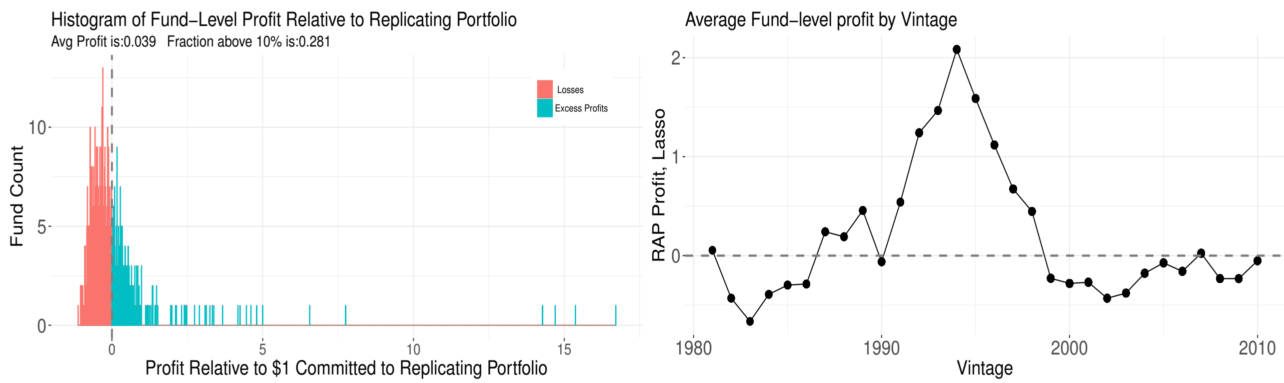

Panel C: Real Estate

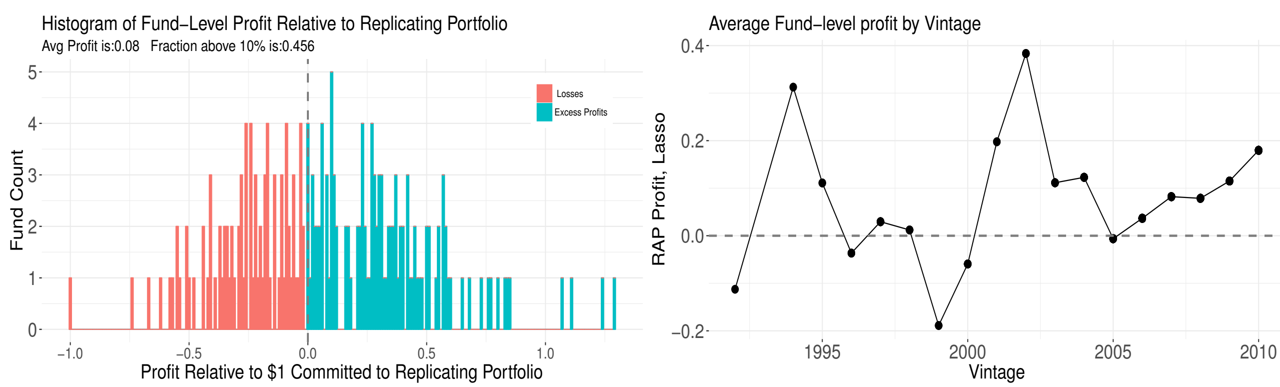

Panel D: Infrastructure

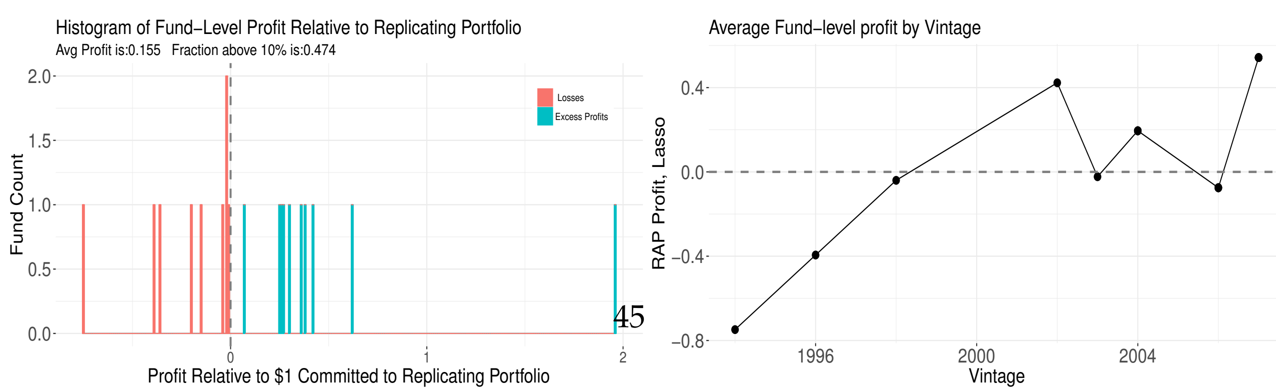

Figure 16: Lasso 3-Factor Model, Comparison

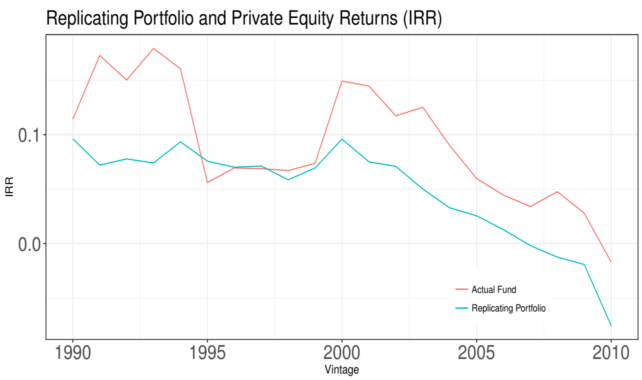

Panel A: Buyout

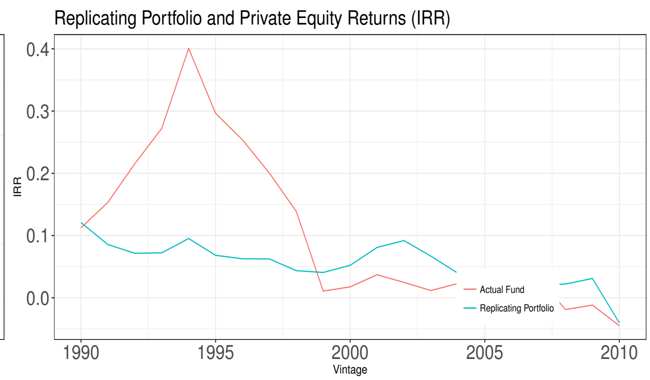

Panel B: Venture Capital

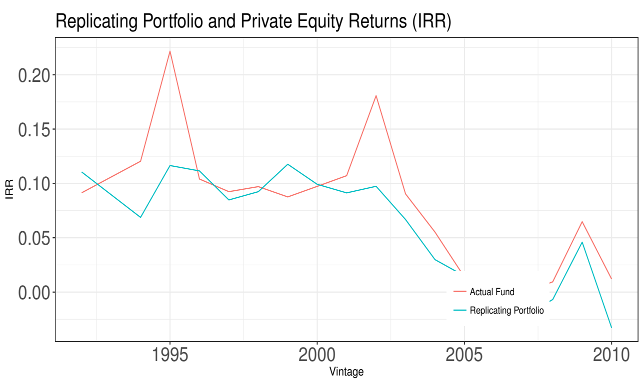

Panel C: Real Estate

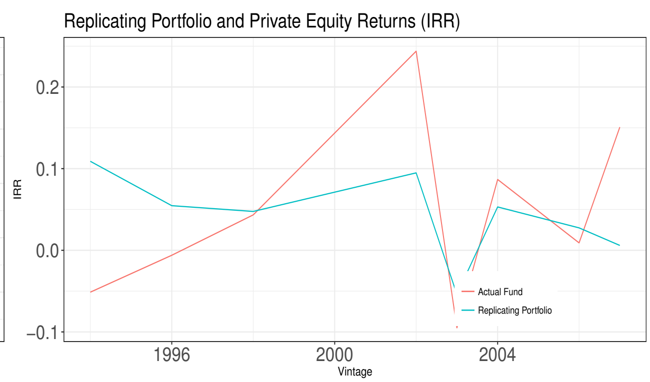

Panel D: Infrastructure

Figure 17: OLS Model Alternative Approach Comparison

Panel A: Buyout

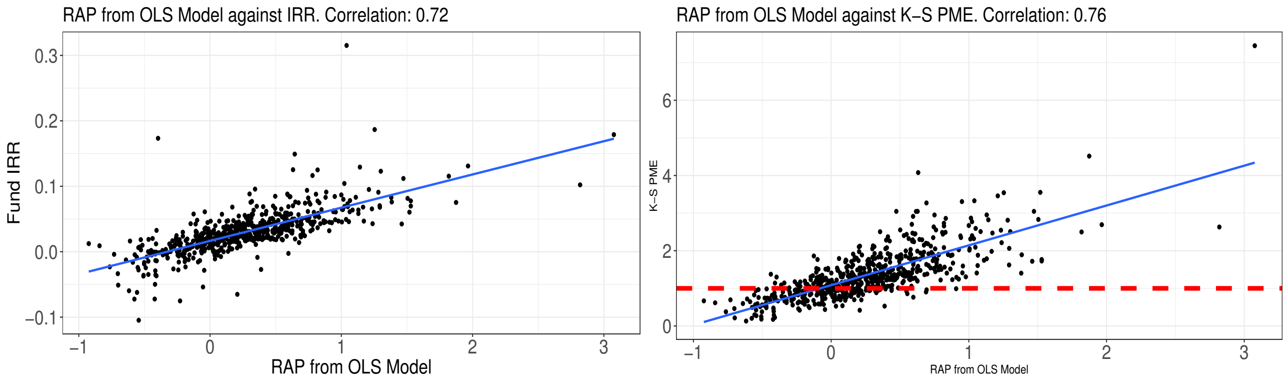

Panel B: Venture Capital

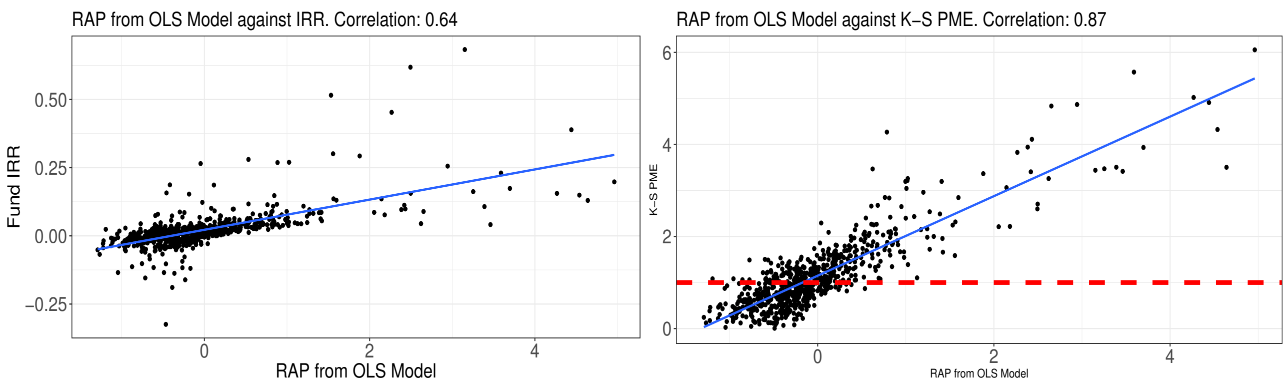

Panel C: Real Estate

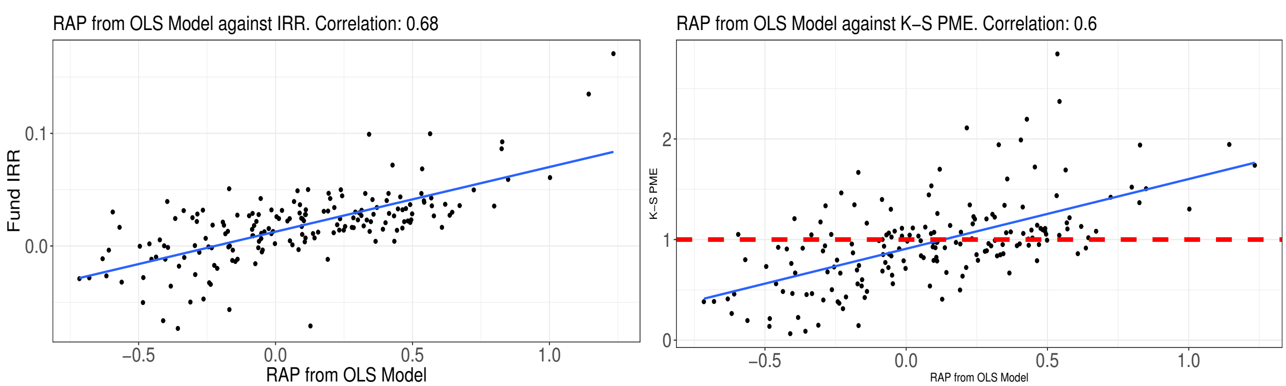

Panel D: Infrastructure

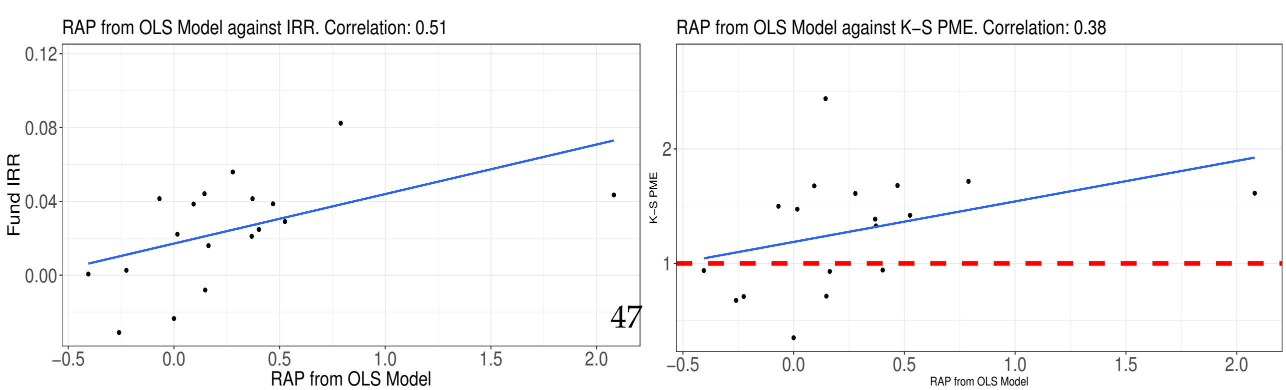

5 Conclusion

We provide a novel valuation method for private equity cash-flows that decomposes the cash-flow at each horizon into a systematic component that reflects exposure to various sources of aggregate risk, priced in listed securities markets, and an idiosyncratic component which reflects the risk-adjusted profit to the PE investor. The systematic component represents a portfolio of stock and bond strips paying safe or risky cash flows at horizons over which PE funds make cash flow distributions. A state-of-the-art no-arbitrage asset pricing model estimates prices and expected returns for these strips, fitting the time series of bond yields and stock prices, including dividend strips.

Using both OLS and Lasso approaches, we estimate rich heterogeneity in PE fund risk exposures across horizons, in the cross-section, and in the time-series. PE fund risk exposure is best modeled not only using bonds and stocks; but is improved with the addition of sector-specific factor exposures. Generally, younger funds have risk exposures which look more like equity in the relevant category (i.e., small stocks for VC); while later cash flows look more like bond exposures. In the time series, expected returns on PE investments have been declining substantially between the 1980s and 2010s.

On average, PE funds considerably outperform their replicating portfolio benchmark, suggesting that they can offer investors access to these various risk factors at a cheaper price than public markets. The risk adjusted performance fluctuates substantially by vintage and across funds within the same vintage and category.

Our analysis highlights the value of a methodological advance in the assessment of risk and return for unlisted assets, which are an increasing component of the total investable universe for many institutional investors. While Private Equity is an especially important application of our approach, given the size of this category, our method can be applied more broadly to study the asset pricing characteristics of project finance and any other cash-flowing asset that is not listed on the capital markets.

References

Ammar, S. B., and M. Eling, 2015, “Common risk factors of infrastructure investments,” *Energy Economics*.

Ang, A., B. Chen, W. N. Goetzmann, and L. Phalippou, 2017, “Estimating Private Equity Returns from Limited Partner Cash Flows,” *Netspar Discussion Paper No. 06/2014-021; Sad Business School WP 2014-8*.

Ang, A., and M. Piazzesi, 2003, “A No-Arbitrage Vector Autoregression of Term Structure Dynamics with Macroeconomic and Latent Variables,” *Journal of Monetary Economics*, 50, 745–787.

Borovička, J., and L. P. Hansen, 2014, “Examining Macroeconomic Models through the Lens of Asset Pricing,” *Journal of Econometrics*, 183(1), 67–90.

Brown, G., R. Harris, T. Jenkinson, S. N. Kaplan, and D. Robinson, 2015, “What Do Different Commercial Data Sets tell Us About Private Equity Performance?,” Working Paper University of North Carolina Kenan Institute.

Campbell, J. Y., 1991, “A Variance Decomposition for Stock Returns,” *Economic Journal*, 101, 157–179.

——— , 1993, “Intertemporal Asset Pricing Without Consumption Data,” *American Economic Review*, 83(3), 487–511.

——— , 1996, “Understanding Risk and Return,” *The Journal of Political Economy*, 104(2), 298–345.

Campbell, J. Y., and R. J. Shiller, 1991, “Yield Spreads and Interest Rate Movements: A Bird’s Eye View,” *Review of Economic Studies*, 58, 495–514.

Cochrane, J. H., 2005, “The risk and return of venture capital,” *Journal of Financial Economics*, 75, 3–52.

Cochrane, J. H., and M. Piazzesi, 2006, “Decomposing the Yield Curve,” Working Paper, University of Chicago.

Cochrane, J. H., and J. Saa-Requejo, 2000, “Beyond Arbitrage: ’Good deal’ asset price bounds in incomplete markets,” *Journal of Political Economy*, 108, 79–119.

Cox, J., J. Ingersoll, and S. Ross, 1985, "An Intertemporal General Equilibrium Model of Asset Pricing," *Econometrica*, 53, 363–384.

Dai, Q., and K. J. Singleton, 2000, "Specification Analysis of Affine Term Structure Models," *Journal of Finance*, 55, 1943–1978.

Driessen, J., T.-C. Lin, and L. Phalippou, 2012, "A new method to estimate risk and return of nontraded assets from cash flows: The case of private equity funds," *Journal of Financial and Quantitative Analysis*, 47(3), 511–535.

Duffie, D., and R. Kan, 1996, "A Yield Factor Model of Interest Rates," *Mathematical Finance*, 6, 379–406.

Ewens, M., C. M. Jones, and M. Rhodes-Kropf, 2013, "The Price of Diversifiable Risk in Venture Capital and Private Equity," *Review of Financial Studies*, 26, 1854–1889.

Gompers, P. A., and J. Lerner, 1997, "Risk and Reward in Private Equity Investments: The Challenge of Performance Assessment," *Journal of Private Equity*, 1, 5–12.

Gu, S., B. Kelly, and D. Xiu, 2018, "Empirical Asset pricing via Machine Learning," *National Bureau of Economic Research Working Paper No. 25398*.

Hansen, L. P., and J. Scheinkman, 2009, "Long-Term Risk: An Operator Approach," *Econometrica*, 77 (1), 177–234.

Harris, R. S., T. Jenkinson, and S. N. Kaplan, 2014, "Private Equity Performance: What Do We Know?," *Journal of Finance*, 69(5).

Kaplan, S. N., and A. Schoar, 2005, "Private equity performance: Returns, persistence, and capital flows," *Journal of Finance*, 60(4), 1791–1823.

Koijen, R. S. J., H. Lustig, and S. Van Nieuwerburgh, 2017, "The Cross-Section and Time-Series of Stock and Bond Returns," *Journal of Monetary Economics*, 88, 50–69.

Korteweg, A., and S. Nagel, 2016, "Risk-Adjusting the Returns to Venture Capital," *Journal of Finance*, 71(3), 1437–1470.

Korteweg, A., and M. Sorensen, 2010, "Risk and return characteristics of venture capital-backed entrepreneurial companies," *Review of Financial Studies*, 23(10), 3738–3772.

——— , 2017, "Skill and Luck in Private Equity Performance," *Journal of Financial Economics*, 0.

Kozak, S., S. Nagel, and S. Santosh, 2017, "Shrinking the Cross Section," *National Bureau of Economic Research Working Paper No. 24070*.

Lettau, M., and J. Wachter, 2011, "The Term Structures of Equity and Interest Rates," *Journal of Financial Economics*, 101 (1), 90–113.

Ljungqvist, A., and M. Richardson, 2003, "The cash flow, return and risk characteristics of private equity," *Working Paper, NYU Stern*.

Lustig, H., S. Van Nieuwerburgh, and A. Verdelhan, 2013, "The Wealth-Consumption Ratio," *Review of Asset Pricing Studies*, 3(1), 38–94., Review of Asset Pricing Studies.

Metrick, A., and A. Yasuda, 2010, "The economics of private equity funds," *Review of Financial Studies*, 23(6), 2303–2341.

Moskowitz, T. J., and A. Vissing-Jorgensen, 2002, "The returns to entrepreneurial investment: A private equity premium puzzle?," *American Economic Review*, 92, 745–778.

Peng, L., 2001, "Building a Venture Capital Index," *Working Paper*.

——— , 2016, "The risk and return of commercial real estate: A property level analysis," *Real Estate Economics*, 44(3), 555–583.

Phalippou, L., and O. Gottschalg, 2009, "The performance of private equity funds," *Review of Financial Studies*, 22(4), 1747–1776.

Robinson, D. T., and B. A. Sensoy, 2011, "Cyclicality, Performance Measurement, and Cash Flow Liquidity in Private Equity," *Working Paper*.

Sagi, J. S., 2017, "Asset-level risk and return in real estate investments," *Working Paper, UNC Kenan-Flagler Business School*.

Sorensen, M., and R. Jagannathan, 2015, "The Public Market Equivalent and Private Equity Performance," *Financial Analysts Journal*, 71(4), 43–50.

Sorensen, M., N. Wang, and J. Yang, 2014, "Valuing private equity," *Review of Financial Studies*, 27(7), 1977–2021.

van Binsbergen, J., M. Brandt, and R. Koijen, 2012, "On the Timing and Pricing of Dividends," *American Economic Review*, 102(4), 1596–1618.

van Binsbergen, J. H., W. H. Hueskes, R. S. J. Koijen, and E. B. Vrugt, 2013, "Equity Yields," *Journal of Financial Economics*, 110(3), 503–519.

van Binsbergen, J. H., and R. S. J. Koijen, 2017, "The Term Structure of Returns: Facts and Theory," *Journal of Financial Economics*, 124(1), 1.

Van Nieuwerburgh, S., 2019, "Why Are REITs Currently So Expensive?," *Real Estate Economics*, 47(1), 18–65.

Wachter, J., 2005, "Solving Models with External Habit," *Finance Research Letters*, 2, 210–226.

Woodward, S., 2009, "Measuring Risk for Venture Capital and Private Equity Portfolios," *Working Paper*.

A Appendix: Asset Pricing Model

A.1 Risk-free rate

The real short yield $y_{t,1}$, or risk-free rate, satisfies $E_t[\exp\{m_{t+1} + y_{t,1}\}] = 1$. Solving out this Euler equation, we get:

$$\begin{aligned} y_{t,1} &= y^{\$}_{t,1} - E_t[\pi_{t+1}] - \frac{1}{2} e'_\pi \Sigma e_\pi + e'_\pi \Sigma^{\frac{1}{2}} \Lambda_t \\ &= y_0(1) + \left[e'_{yn} - e'_\pi \Psi + e'_\pi \Sigma^{\frac{1}{2}} \Lambda_1 \right] z_t. \qquad \text{(A.1)} \\ y_0(1) &\equiv y^{\$}_{0,1} - \pi_0 - \frac{1}{2} e'_\pi \Sigma e_\pi + e'_\pi \Sigma^{\frac{1}{2}} \Lambda_0. \qquad \text{(A.2)} \end{aligned}$$

where we used the expression for the real SDF

$$\begin{aligned} m_{t+1} &= m^{\$}_{t+1} + \pi_{t+1} \\ &= -y^{\$}_{t,1} - \frac{1}{2} \Lambda'_t \Lambda_t - \Lambda'_t \varepsilon_{t+1} + \pi_0 + e'_\pi \Psi z_t + e'_\pi \Sigma^{\frac{1}{2}} \varepsilon_{t+1} \\ &= -y_{t,1} - \frac{1}{2} e'_\pi \Sigma e_\pi + e'_\pi \Sigma^{\frac{1}{2}} \Lambda_t - \frac{1}{2} \Lambda'_t \Lambda_t - \left(\Lambda'_t - e'_\pi \Sigma^{\frac{1}{2}} \right) \varepsilon_{t+1} \end{aligned}$$

The real short yield is the nominal short yield minus expected inflation minus a Jensen adjustment minus the inflation risk premium.

A.2 Nominal and real term structure

Proposition 1. Nominal bond yields are affine in the state vector:

$$y^{\$}_t(\tau) = -\frac{A^{\$}_\tau}{\tau} - \frac{B^{\$\prime}_\tau}{\tau} z_t,$$

where the coefficients $A^{\$}_\tau$ and $B^{\$}_\tau$ satisfy the following recursions:

$$\begin{aligned} A^{\$}_{\tau+1} &= -y^{\$}_{0,1} + A^{\$}_\tau + \frac{1}{2} \left(B^{\$}_\tau \right)' \Sigma \left(B^{\$}_\tau \right) - \left(B^{\$}_\tau \right)' \Sigma^{\frac{1}{2}} \Lambda_0, \qquad \text{(A.3)} \\ \left(B^{\$}_{\tau+1} \right)' &= \left(B^{\$}_\tau \right)' \Psi - e'_{yn} - \left(B^{\$}_\tau \right)' \Sigma^{\frac{1}{2}} \Lambda_1, \qquad \text{(A.4)} \end{aligned}$$

initialized at $A^{\$}_0 = 0$ and $B^{\$}_0 = 0$.

Proof. We conjecture that the $t+1$-price of a τ-period bond is exponentially affine in the state:

$$\log(P^{\$}_{t+1,\tau}) = A^{\$}_{\tau} + \left(B^{\$}_{\tau}\right)' z_{t+1}$$

and solve for the coefficients $A^{\$}_{\tau+1}$ and $B^{\$}_{\tau+1}$ in the process of verifying this conjecture using the Euler equation:

$$\begin{aligned}
P^{\$}_{t,\tau+1} &= E_t[\exp\{m^{\$}_{t+1} + \log\left(P^{\$}_{t+1,\tau}\right)\}] \\
&= E_t[\exp\{-y^{\$}_{t,1} - \frac{1}{2}\Lambda_t'\Lambda_t - \Lambda_t'\varepsilon_{t+1} + A^{\$}_{\tau} + \left(B^{\$}_{\tau}\right)' z_{t+1}\}] \\
&= \exp\{-y^{\$}_{0,1} - e_{yn}' z_t - \frac{1}{2}\Lambda_t'\Lambda_t + A^{\$}_{\tau} + \left(B^{\$}_{\tau}\right)' \Psi z_t\} \times \\
&\quad E_t\left[\exp\{-\Lambda_t'\varepsilon_{t+1} + \left(B^{\$}_{\tau}\right)' \Sigma^{\frac{1}{2}}\varepsilon_{t+1}\}\right].
\end{aligned}$$

We use the log-normality of ε_{t+1} and substitute for the affine expression for Λ_t to get:

$$\begin{aligned}
P^{\$}_{t,\tau+1} &= \exp\left\{-y^{\$}_{0,1} - e_{yn}' z_t + A^{\$}_{\tau} + \left(B^{\$}_{\tau}\right)' \Psi z_t + \frac{1}{2}\left(B^{\$}_{\tau}\right)' \Sigma \left(B^{\$}_{\tau}\right)\right. \\
&\quad \left. - \left(B^{\$}_{\tau}\right)' \Sigma^{\frac{1}{2}}(\Lambda_0 + \Lambda_1 z_t)\right\}.
\end{aligned}$$

Taking logs and collecting terms, we obtain a linear equation for $\log(p_t(\tau+1))$:

$$\log\left(P^{\$}_{t,\tau+1}\right) = A^{\$}_{\tau+1} + \left(B^{\$}_{\tau+1}\right)' z_t,$$

where $A^{\$}_{\tau+1}$ satisfies (A.3) and $B^{\$}_{\tau+1}$ satisfies (A.4). The relationship between log bond prices and bond yields is given by $-\log\left(P^{\$}_{t,\tau}\right)/\tau = y^{\$}_{t,\tau}$. □

Define the one-period return on a nominal zero-coupon bond as:

$$r^{b,\$}_{t+1,\tau} = \log\left(P^{\$}_{t+1,\tau}\right) - \log\left(P^{\$}_{t,\tau+1}\right)$$

The nominal bond risk premium on a bond of maturity τ is the expected excess return corrected for a Jensen term, and equals negative the conditional covariance between that bond return and the nominal SDF:

$$\begin{aligned}
E_t\left[r^{b,\$}_{t+1,\tau}\right] - y^{\$}_{t,1} + \frac{1}{2}V_t\left[r^{b,\$}_{t+1,\tau}\right] &= -Cov_t\left[m^{\$}_{t+1}, r^{b,\$}_{t+1,\tau}\right] \\
&= \left(B^{\$}_{\tau}\right)' \Sigma^{\frac{1}{2}}\Lambda_t
\end{aligned}$$

Real bond yields, $y_{t,\tau}$, denoted without the \$ superscript, are affine as well with coefficients that follow similar recursions:

$$A_{\tau+1} = -y_{0,1} + A_\tau + \frac{1}{2}B'_\tau \Sigma B_\tau - B'_\tau \Sigma^{\frac{1}{2}} \left(\Lambda_0 - \Sigma^{\frac{1}{2}\prime} e_\pi\right), \tag{A.5}$$

$$B'_{\tau+1} = -e'_{yn} + (e_\pi + B_\tau)' \left(\Psi - \Sigma^{\frac{1}{2}} \Lambda_1\right). \tag{A.6}$$

For $\tau = 1$, we recover the expression for the risk-free rate in (A.1)-(A.2).

A.3 Stock Market

We define the real return on equity as $R^m_{t+1} = \frac{P^m_{t+1} + D^m_{t+1}}{P^m_t}$, where P^m_t is the end-of-period price on the equity market. A log-linearization delivers:

$$r^m_{t+1} = \kappa^m_0 + \Delta d^m_{t+1} + \kappa^m_1 pd^m_{t+1} - pd^m_t. \tag{A.7}$$

The unconditional mean log real stock return is $r^m_0 = E[r^m_t]$, the unconditional mean dividend growth rate is $\mu^m = E[\Delta d^m_{t+1}]$, and $\overline{pd^m} = E[pd^m_t]$ is the unconditional average log price-dividend ratio on equity. The linearization constants κ^m_0 and κ^m_1 are defined as:

$$\kappa^m_1 = \frac{e^{\overline{pd^m}}}{e^{\overline{pd^m}} + 1} < 1 \text{ and } \kappa^m_0 = \log\left(e^{\overline{pd^m}} + 1\right) - \frac{e^{\overline{pd^m}}}{e^{\overline{pd^m}} + 1}\overline{pd^m}. \tag{A.8}$$

Our state vector z contains the (demeaned) log real dividend growth rate on the stock market, $\Delta d^m_{t+1} - \mu^m$, and the (demeaned) log price-dividend ratio $pd^m - \overline{pd^m}$.

$$\begin{aligned} pd^m_t(\tau) &= \overline{pd^m} + e'_{pd} z_t, \\ \Delta d^m_t &= \mu^m + e'_{divm} z_t, \end{aligned}$$

where e'_{pd} (e_{divm}) is a selector vector that has a one in the fifth (sixth) entry, since the log pd ratio (log dividend growth rate) is the fifth (sixth) element of the VAR.

We *define* the log return on the stock market so that the return equation holds exactly, given the time series for $\{\Delta d^m_t, pd^m_t\}$. Rewriting (A.7):

$$\begin{aligned} r^m_{t+1} - r^m_0 &= \left[(e_{divm} + \kappa^m_1 e_{pd})'\Psi - e'_{pd}\right] z_t + \left(e_{divm} + \kappa^m_1 e_{pd}\right)' \Sigma^{\frac{1}{2}} \varepsilon_{t+1}. \\ r^m_0 &= \mu^m + \kappa^m_0 - \overline{pd^m}(1 - \kappa^m_1). \end{aligned}$$

The equity risk premium is the expected excess return on the stock market corrected for a Jensen term. By the Euler equation, it equals minus the conditional covariance between the log SDF and the log return:

$$\begin{aligned}
1 &= E_t\left[M_{t+1}\frac{P^m_{t+1}+D^m_{t+1}}{P^m_t}\right] = E_t\left[\exp\{m^{\$}_{t+1}+\pi_{t+1}+r^m_{t+1}\}\right] \\
&= E_t\left[\exp\left\{-y^{\$}_{t,1}-\frac{1}{2}\Lambda_t'\Lambda_t-\Lambda_t'\varepsilon_{t+1}+\pi_0+e_\pi' z_{t+1}+r^m_0+(e_{divm}+\kappa^m_1 e_{pd})'z_{t+1}-e_{pd}'z_t\right\}\right] \\
&= \exp\left\{-y^{\$}_0(1)-\frac{1}{2}\Lambda_t'\Lambda_t+\pi_0+r^m_0+\left[(e_{divm}+\kappa^m_1 e_{pd}+e_\pi)'\Psi-e_{pd}'-e_{yn}'\right]z_t\right\} \\
&\quad \times E_t\left[\exp\{-\Lambda_t'\varepsilon_{t+1}+\left(e_{divm}+\kappa^m_1 e_{pd}+e_\pi\right)'\Sigma^{\frac{1}{2}}\varepsilon_{t+1}\right] \\
&= \exp\left\{r^m_0+\pi_0-y^{\$}_0(1)+\left[(e_{divm}+\kappa^m_1 e_{pd}+e_\pi)'\Psi-e_{pd}'-e_{yn}'\right]z_t\right\} \\
&\quad \times \exp\left\{\frac{1}{2}\left(e_{divm}+\kappa^m_1 e_{pd}+e_\pi\right)'\Sigma\left(e_{divm}+\kappa^m_1 e_{pd}+e_\pi\right)-\left(e_{divm}+\kappa^m_1 e_{pd}+e_\pi\right)'\Sigma^{\frac{1}{2}}\Lambda_t\right\}
\end{aligned}$$

Taking logs on both sides delivers:

$$\begin{aligned}
r^m_0+\pi_0-y^{\$}_0(1)+\left[(e_{divm}+\kappa^m_1 e_{pd}+e_\pi)'\Psi-e_{pd}'-e_{yn}'\right]z_t & \\
+\frac{1}{2}\left(e_{divm}+\kappa^m_1 e_{pd}+e_\pi\right)'\Sigma\left(e_{divm}+\kappa^m_1 e_{pd}+e_\pi\right) &= \left(e_{divm}+\kappa^m_1 e_{pd}+e_\pi\right)'\Sigma^{\frac{1}{2}}\Lambda_t \\
E_t\left[r^{m,\$}_{t+1}\right]-y^{\$}_{t,1}+\frac{1}{2}V_t\left[r^{m,\$}_{t+1}\right] &= -Cov_t\left[m^{\$}_{t+1,}r^{m,\$}_{t+1}\right]
\end{aligned} \tag{A.9}$$

The left-hand side is the expected excess return on the stock market, corrected for a Jensen term, while the right-hand side is the negative of the conditional covariance between the (nominal) log stock return and the nominal log SDF. We refer to the left-hand side as the equity risk premium in the data, since it is implied directly by the VAR. We refer to the right-hand side as the equity risk premium in the model, since it requires knowledge of the market prices of risk.

Note that we can obtain the same expression using the log real SDF and log real stock return:

$$\begin{aligned}
E_t\left[r^m_{t+1}\right]-y_{t,1}+\frac{1}{2}V_t\left[r^m_{t+1}\right] &= -Cov_t\left[m_{t+1,}r^m_{t+1}\right] \\
r^m_0-y_0(1) &+ \left[(e_{divm}+\kappa^m_1 e_{pd}+e_\pi)'\Psi-e_{pd}'-e_{yn}'-e_\pi'\Sigma^{1/2}\Lambda_1\right]z_t \\
+\frac{1}{2}(e_{divm}+\kappa^m_1 e_{pd})'\Sigma(e_{divm}+\kappa^m_1 e_{pd}) &= \left(e_{divm}+\kappa^m_1 e_{pd}\right)'\Sigma^{1/2}(\Lambda_t-\left(\Sigma^{1/2}\right)'e_\pi)
\end{aligned}$$

We combine the terms in Λ_0 and Λ_1 on the right-hand side and plug in for $y_0(1)$ from (A.2) to get:

$$\begin{aligned} r_0^m + \pi_0 - y_{0,1}^{\$} + \frac{1}{2} e_\pi' \Sigma e_\pi & \qquad + \frac{1}{2}(e_{divm} + \kappa_1^m e_{pd})' \Sigma (e_{divm} + \kappa_1^m e_{pd}) + e_\pi' \Sigma \left(e_{divm} + \kappa_1^m e_{pd} \right. \\ + \left[(e_{divm} + \kappa_1^m e_{pd} + e_\pi)' \Psi - e_{pd}' - e_{yn}' \right] z_t & = \left(e_{divm} + \kappa_1^m e_{pd}\right)' \Sigma^{1/2} \Lambda_t + e_\pi' \Sigma^{\frac{1}{2}} \Lambda_0 + e_\pi' \Sigma^{1/2} \Lambda_1 z_t \end{aligned}$$

This recovers equation (A.9).

A.4 Dividend Strips

A.4.1 Affine Structure for Price-Dividend Ratio on Equity Strip

Proposition 2. Log price-dividend ratios on dividend strips are affine in the state vector:

$$p_{t,\tau}^d = \log\left(P_{t,\tau}^d\right) = A_\tau^m + B_\tau^{m\prime} z_t,$$

where the coefficients A_τ^m and B_τ^m follow recursions:

$$\begin{aligned} A_{\tau+1}^m &= A_\tau^m + \mu_m - y_0(1) + \frac{1}{2}\left(e_{divm} + B_\tau^m\right)' \Sigma \left(e_{divm} + B_\tau^m\right) \\ &\quad - \left(e_{divm} + B_\tau^m\right)' \Sigma^{\frac{1}{2}} \left(\Lambda_0 - \Sigma^{\frac{1}{2}\prime} e_\pi\right), \qquad \text{(A.10)} \\ B_{\tau+1}^{m\prime} &= \left(e_{divm} + e_\pi + B_\tau^m\right)' \Psi - e_{yn}' - \left(e_{divm} + e_\pi + B_\tau^m\right)' \Sigma^{\frac{1}{2}} \Lambda_1, \qquad \text{(A.11)} \end{aligned}$$

initialized at $A_0^m = 0$ and $B_0^m = 0$.

Proof. We conjecture the affine structure and solve for the coefficients $A_{\tau+1}^m$ and $B_{\tau+1}^m$ in the process of verifying this conjecture using the Euler equation:

$$\begin{aligned} P_{t,\tau+1}^d &= \mathbb{E}_t\left[M_{t+1} P_{t+1,\tau}^d \frac{D_{t+1}^m}{D_t^m}\right] = E_t\left[\exp\{m_{t+1}^{\$} + \pi_{t+1} + \Delta d_{t+1}^m + p_{t+1}^d(\tau)\}\right] \\ &= \mathbb{E}_t\left[\exp\{-y_{t,1}^{\$} - \frac{1}{2}\Lambda_t'\Lambda_t - \Lambda_t'\varepsilon_{t+1} + \pi_0 + e_\pi' z_{t+1} + \mu^m + e_{divm}' z_{t+1} + A_\tau^m + B_\tau^{m\prime} z_{t+1}\}\right] \\ &= \exp\{-y_0^{\$}(1) - e_{yn}' z_t - \frac{1}{2}\Lambda_t'\Lambda_t + \pi_0 + e_\pi' \Psi z_t + \mu_m + e_{divm}' \Psi z_t + A_\tau^m + B_\tau^{m\prime} \Psi z_t\} \\ &\quad \times \mathbb{E}_t\left[\exp\{-\Lambda_t'\varepsilon_{t+1} + \left(e_{divm} + e_\pi + B_\tau^m\right)' \Sigma^{\frac{1}{2}} \varepsilon_{t+1}\right]. \end{aligned}$$

We use the log-normality of ε_{t+1} and substitute for the affine expression for Λ_t to get:

$$
\begin{aligned}
P^d_{t,\tau+1} &= \exp\{-y^{\$}_0(1) + \pi_0 + \mu_m + A^m_\tau + \left[(e_{divm} + e_\pi + B^m_\tau)'\,\Psi - e'_{yn}\right] z_t \\
&\quad + \frac{1}{2}\,(e_{divm} + e_\pi + B^m_\tau)'\,\Sigma\,(e_{divm} + e_\pi + B^m_\tau) \\
&\quad - (e_{divm} + e_\pi + B^m_\tau)'\,\Sigma^{\frac{1}{2}}(\Lambda_0 + \Lambda_1 z_t)\}
\end{aligned}
$$

Taking logs and collecting terms, we obtain a log-linear expression for $p^d_t(\tau+1)$:

$$
p^d_{t,\tau+1} = A^m_{\tau+1} + B^{m\prime}_{\tau+1} z_t,
$$

where:

$$
\begin{aligned}
A^m_{\tau+1} &= A^m_\tau + \mu_m - y^{\$}_0(1) + \pi_0 + \frac{1}{2}\,(e_{divm} + e_\pi + B^m_\tau)'\,\Sigma\,(e_{divm} + e_\pi + B^m_\tau) \\
&\quad - (e_{divm} + e_\pi + B^m_\tau)'\,\Sigma^{\frac{1}{2}}\Lambda_0, \\
B^{m\prime}_{\tau+1} &= (e_{divm} + e_\pi + B^m_\tau)'\,\Psi - e'_{yn} - (e_{divm} + e_\pi + B^m_\tau)'\,\Sigma^{\frac{1}{2}}\Lambda_1.
\end{aligned}
$$

We recover the recursions in (**??**) and (**??**) after using equation (A.2). □

Like we did for the stock market as a whole, we define the strip risk premium as:

$$
\begin{aligned}
\mathbb{E}_t\left[r^{d,\$}_{t+1,\tau}\right] - y^{\$}_{t,1} + \frac{1}{2} V_t\left[r^{d,\$}_{t+1,\tau}\right] &= -Cov_t\left[m^{\$}_{t+1}, r^{d,\$}_{t+1,\tau}\right] \\
&= (e_{divm} + e_\pi + B^m_\tau)'\,\Sigma^{\frac{1}{2}}\Lambda_t
\end{aligned}
$$

The risky strips for REITs and infrastructure are defined analogously.

A.4.2 Strip Expected Holding Period Return over k-horizons

The expected nominal return on a dividend strip that pays the realized nominal dividend k quarters hence and that is held to maturity is:

$$
\begin{aligned}
\mathbb{E}_t[R_{t\to t+k}] &= \frac{\mathbb{E}_t\left[\frac{D^{\$}_{t+k}}{D^{\$}_t}\right]}{P^d_{t,k}} - 1 \\
&= \exp\left(-A^m_k - B^{m\prime}_k z_t + \mathbb{E}_t\left[\sum_{s=1}^{k} \Delta d_{t+s} + \pi_{t+s}\right] + \frac{1}{2} V_t\left[\sum_{s=1}^{k} \Delta d_{t+s} + \pi_{t+s}\right]\right) - 1
\end{aligned}
$$

$$
\begin{aligned}
&= \exp\Bigg(-A^m_k - B^{m\prime}_k z_t + k(\mu_m + \pi_0) + (e_{divm} + e_\pi)'\left[\sum_{s=1}^{k}\Psi^s\right] z_t \\
&\quad + \frac{k}{2}(e_{divm} + e_\pi)'\Sigma(e_{divm} + e_\pi)\Bigg) - 1
\end{aligned} \tag{A.12}
$$

These are the building blocks for computing the expected return on a PE investment.

A.4.3 Strip Forward Price and Return

The price of a dividend futures contract which delivers one quarter worth of nominal dividends at quarter $t + \tau$, divided by the current dividend, is equal to:

$$
\frac{F^d_{t,\tau}}{D^\$_t} = P^d_{t,\tau} \exp\left(\tau y^\$_{t,\tau}\right),
$$

where $P^d_{t,\tau}$ is the spot price-dividend ratio. Using the affine expressions for the strip price-dividend ratio and the nominal bond price, it can be written as:

$$
\frac{F^d_{t,\tau}}{D^\$_t} = \exp\left(A^m_\tau - A^\$_\tau + (B^m_\tau - B^\$_\tau)' z_t\right),
$$

The one-period holding period return on the dividend future of maturity τ is:

$$
R^{fut,d}_{t+1,\tau} = \frac{F^d_{t+1,\tau-1}}{F^d_{t,\tau}} - 1 = \frac{F^d_{t+1,\tau-1}/D^\$_{t+1}}{F^d_{t,\tau}/D^\$_t}\frac{D^\$_{t+1}}{D^\$_t} - 1
$$

It can be written as:

$$
\begin{aligned}
\log\left(1 + R^{fut,d}_{t+1,\tau}\right) &= A^m_{\tau-1} - A^\$_{\tau-1} - A^m_\tau + A^\$_\tau + \mu_m + \pi_0 \\
&\quad + (B^m_{\tau-1} - B^\$_{\tau-1} + e_{divm} + e_\pi)' z_{t+1} - (B^m_\tau - B^\$_\tau)' z_t
\end{aligned}
$$

The expected log return, which is already a risk premium on account of the fact that the dividend future already takes out the return on an equal-maturity nominal Treasury bond, equals:

$$
\begin{aligned}
\mathbb{E}_t\left[\log\left(1 + R^{fut,d}_{t+1,\tau}\right)\right] &= A^m_{\tau-1} - A^\$_{\tau-1} - A^m_\tau + A^\$_\tau + \mu_m + \pi_0 \\
&\quad + \left[(B^m_{\tau-1} - B^\$_{\tau-1} + e_{divm} + e_\pi)'\Psi - (B^m_\tau - B^\$_\tau)'\right] z_t
\end{aligned}
$$

Given that the state variable z_t is mean-zero, the first row denotes the unconditional dividend futures risk premium.

A.5 Capital Gain Strips

We also define capital gain strips. A capital gain strip is a strip that pays the realized ex-dividend stock price P^m_{t+k} at time $t+k$. For convenience, we scale this payout by the current stock price P^m_t. In other words, the claim pays off the realized cumulative capital gain between periods t and $t+k$, $\frac{P^m_{t+k}}{P^m_t}$.

By value additivity of the dividend strips, the time-t price of this claim is today's stock price minus the prices of the dividend strips of horizons $1, \cdots, k$:

$$\frac{P^m_t - \left(P^d_{t,1} + \cdots + P^d_{t,k}\right) D^m_t}{P^m_t} = 1 - \frac{P^d_{t,1} + \cdots + P_{t,k}}{P^m_t / D^m_t} = 1 - \frac{\sum_{\tau=1}^k \exp\{A^m_\tau + B^m_\tau{}' z_t\}}{\exp\{\overline{pd^m} + e_{pdm}{}' z_t\}}$$

The expected return on the capital gains strip is given by

$$\begin{aligned}
\frac{\mathbb{E}_t\left[P^m_{t+k}\right]}{P^m_t - \left(P^d_{t,1} + \cdots + P^d_{t,k}\right) D^m_t} &= \frac{\mathbb{E}_t\left[\frac{P^m_{t+k}}{P^m_t}\right]}{1 - \frac{\sum_{\tau=1}^k \exp\{A^m_\tau + B^m_\tau{}' z_t\}}{\exp\{\overline{pd^m} + e_{pdm}{}' z_t\}}} = \frac{\mathbb{E}_t\left[\frac{P^m_{t+k}/D^m_{t+k}}{P^m_t/D^m_t}\frac{D^m_{t+k}}{D^m_t}\right]}{1 - \frac{\sum_{\tau=1}^k \exp\{A^m_\tau + B^m_\tau{}' z_t\}}{\exp\{\overline{pd^m} + e'_{pdm} z_t\}}} \\
&= \frac{\mathbb{E}_t\left[\exp\{e'_{pdm}(z_{t+k} - z_t) + \Delta d^{\$}_{t+k} + \cdots + \Delta d^{\$}_{t+1}\}\right]}{1 - \frac{\sum_{\tau=1}^k \exp\{A^m_\tau + B^m_\tau{}' z_t\}}{\exp\{\overline{pd^m} + e'_{pdm} z_t\}}} \\
&= \frac{\mathbb{E}_t\left[\exp\{e'_{pdm}(z_{t+k} - z_t) + k(\mu_m + \pi_0) + \sum_{\tau=1}^k (e_{divm} + e_\pi)' z_{t+\tau}\}\right]}{1 - \frac{\sum_{\tau=1}^k \exp\{A^m_\tau + B^m_\tau{}' z_t\}}{\exp\{\overline{pd^m} + e'_{pdm} z_t\}}} \\
&= \frac{\exp\left\{\left[e'_{pdm}(\Psi^k - I) + (e_{divm} + e_\pi)' \sum_{\tau=1}^k \Psi^\tau\right] z_t + k(\mu_m + \pi_0) + \frac{1}{2}V\right\}}{1 - \frac{\sum_{\tau=1}^k \exp\{A^m_\tau + B^m_\tau{}' z_t\}}{\exp\{\overline{pd^m} + e'_{pdm} z_t\}}}
\end{aligned}$$

where

$$V = e'_{pdm}\left[\sum_{\tau=1}^k \Psi^{\tau-1}\Sigma(\Psi^{\tau-1})'\right] e_{pdm} + (e_{divm} + e_\pi)' \left[\sum_{\tau=1}^k \sum_{n=1}^\tau \Psi^{n-1}\Sigma\Psi^{n-1}\right](e_{divm} + e_\pi)$$

B Point Estimates Baseline Model

B.1 VAR Estimation

In the first stage we estimate the VAR companion matrix by OLS, equation by equation. We start from an initial VAR where all elements of Ψ are non-zero. We zero out the elements whose t-statistic is less than 1.96. We then re-estimate Ψ and zero out the elements whose t-statistic is less than 1.96. We continue this procedure until the Ψ matrix no longer changes and all remaining elements have t-statistic greater than 1.96. The resulting VAR companion matrix estimate, $\widehat{\Psi}$, is listed below.

0.90	0.00	0.00	0.00	0.00	0.00	0.00	0.00	0.00	0.00	0.00	0.00	0.00	0.00
0.00	0.21	0.00	0.00	0.02	0.00	0.01	0.00	-0.02	0.00	0.00	0.00	0.00	0.00
0.07	0.00	0.95	0.00	0.00	0.00	0.00	0.00	0.00	0.00	0.00	0.00	0.00	0.00
0.00	0.00	0.00	0.83	0.00	0.00	0.00	0.00	0.00	0.00	0.00	0.00	0.00	0.00
-4.77	0.00	0.00	0.00	0.96	0.00	-0.07	0.00	0.00	0.65	0.00	0.00	0.00	0.00
0.00	0.00	0.00	0.00	0.00	0.37	0.02	0.00	0.00	0.00	0.00	0.00	0.00	0.00
0.00	0.00	-3.66	0.00	0.00	0.00	0.89	0.00	0.00	0.00	0.00	0.00	0.00	0.00
0.00	0.00	1.97	0.00	0.07	0.00	0.09	0.00	-0.07	0.00	0.00	0.00	0.00	0.00
0.00	0.00	0.00	0.00	0.08	0.00	0.00	0.00	0.92	0.00	0.00	0.00	0.00	0.00
0.00	0.00	0.00	0.00	-0.05	0.00	0.00	0.00	0.05	0.00	0.00	0.00	0.00	0.00
-9.33	0.00	0.00	0.00	0.00	0.00	0.00	0.00	0.00	0.00	0.87	0.00	0.00	0.00
4.62	1.36	-1.72	-7.44	0.05	0.36	0.03	-0.07	-0.06	-0.32	0.04	0.00	0.00	0.00
-4.34	0.00	0.00	0.00	0.00	0.00	-0.05	0.00	0.00	0.65	0.00	0.00	0.93	0.00
-0.18	0.20	-1.89	-1.84	-0.04	0.12	0.02	-0.19	-0.05	-0.13	-0.01	0.01	0.09	0.11

The Cholesky decomposition of the residual variance-covariance matrix, $\Sigma^{\frac{1}{2}}$, multiplied by 100 for readability is given by:

0.25	0.00	0.00	0.00	0.00	0.00	0.00	0.00	0.00	0.00	0.00	0.00	0.00	0.00
0.04	0.67	0.00	0.00	0.00	0.00	0.00	0.00	0.00	0.00	0.00	0.00	0.00	0.00
0.03	0.06	0.17	0.00	0.00	0.00	0.00	0.00	0.00	0.00	0.00	0.00	0.00	0.00
-0.01	-0.01	-0.08	0.09	0.00	0.00	0.00	0.00	0.00	0.00	0.00	0.00	0.00	0.00
-1.42	1.11	-1.22	-0.61	8.08	0.00	0.00	0.00	0.00	0.00	0.00	0.00	0.00	0.00
-0.03	-0.07	0.11	-0.14	-0.17	2.13	0.00	0.00	0.00	0.00	0.00	0.00	0.00	0.00
-0.82	0.91	-1.17	-0.59	5.42	0.80	7.46	0.00	0.00	0.00	0.00	0.00	0.00	0.00
0.29	-0.06	0.04	-0.15	0.03	0.62	-1.51	3.21	0.00	0.00	0.00	0.00	0.00	0.00
-0.58	0.70	-0.93	-0.76	6.39	0.97	0.34	0.51	4.45	0.00	0.00	0.00	0.00	0.00
-0.08	0.09	0.07	-0.10	-0.42	0.52	-0.08	-0.07	-0.59	1.89	0.00	0.00	0.00	0.00
-2.31	1.64	-1.69	-0.10	10.10	-0.06	0.77	0.89	0.10	-0.07	8.57	0.00	0.00	0.00
0.33	-0.08	-0.02	0.09	-0.83	2.58	0.52	0.48	-0.69	0.69	-4.37	4.85	0.00	0.00
-1.69	1.37	-1.15	-1.13	8.18	-1.15	-1.53	-0.69	-1.16	0.64	0.20	-0.31	4.38	0.00
0.08	-0.20	-0.04	-0.13	-0.18	3.14	0.10	0.32	0.36	-0.39	-0.07	0.22	-2.55	2.40

The diagonal elements report the standard deviation of the VAR innovations, each one orthogonalized to the shocks that precede it in the VAR, expressed in percent per quarter.

B.2 Market Price of Risk Estimates

The market prices of risk are pinned down by the moments discussed in the main text. Here we report and discuss the point estimates. Note that the prices of risk are associated with the orthogonal VAR innovations $\varepsilon \sim \mathcal{N}(0, I)$. Therefore, their magnitudes can be interpreted as (quarterly) Sharpe ratios. The constant in the market price of risk estimate $\widehat{\Lambda_0}$ is:

$$\begin{bmatrix} -0.229 & 0.533 & -0.444 & -0.055 & -0.184 & 0.679 & 0.000 & 0.346 & 0.000 & 0.343 & 0.000 & -0.120 & 0.000 & 0.033 \end{bmatrix}'$$

The matrix that governs the time variation in the market price of risk is estimated to be $\widehat{\Lambda_1} =$:

61.07	0.00	0.00	0.00	0.00	0.00	0.00	0.00	0.00	0.00	0.00	0.00	0.00	0.00
0.00	10.97	0.00	0.00	0.00	0.00	0.00	0.00	0.00	0.00	0.00	0.00	0.00	0.00
0.00	0.00	-54.25	-249.73	0.00	0.00	0.00	0.00	0.00	0.00	0.00	0.00	0.00	0.00
54.26	-7.17	0.01	0.31	0.00	0.00	0.00	0.00	0.00	0.00	0.00	0.00	0.00	0.00
-5.97	3.95	5.91	9.18	-0.22	4.56	0.00	0.00	0.00	0.00	0.00	0.00	0.00	0.00
-104.12	-17.44	-89.11	-161.55	-0.95	-0.00	-1.89	0.00	0.00	7.75	0.00	0.00	0.00	0.00
0.00	0.00	0.00	0.00	0.00	0.00	0.00	0.00	0.00	0.00	0.00	0.00	0.00	0.00
100.79	-3.57	-70.55	-31.25	2.33	-7.53	-0.45	0.00	-1.78	-3.34	0.00	0.00	0.00	0.00
0.00	0.00	0.00	0.00	0.00	0.00	0.00	0.00	0.00	0.00	0.00	0.00	0.00	0.00
161.57	-5.96	-6.01	-6.97	1.60	-11.12	1.19	0.00	-1.49	-5.28	0.00	0.00	0.00	0.00
0.00	0.00	0.00	0.00	0.00	0.00	0.00	0.00	0.00	0.00	0.00	0.00	0.00	0.00
-37.65	29.48	-17.62	-139.50	1.04	-0.00	1.51	0.00	-0.44	-10.30	-2.01	0.37	0.00	0.00
0.00	0.00	0.00	0.00	0.00	0.00	0.00	0.00	0.00	0.00	0.00	0.00	0.00	0.00
17.10	11.92	-99.98	-105.52	-1.24	0.03	-0.00	-6.98	-1.39	0.99	-0.64	0.50	1.41	0.86

The first four elements of Λ_0 and the first four rows of Λ_1 govern the dynamics of bond yields and bond returns. The price of inflation risk is allowed to move with the inflation rate. The estimation shows that the price of inflation risk is negative on average ($\widehat{\Lambda_0}(1)$=-0.23), indicating that high inflation states are bad states of the world. The market price of inflation risk becomes larger (less negative) when inflation is higher than average ($\widehat{\Lambda_1}(1,1)$=61.07). The price of real GDP growth risk is positive ($\widehat{\Lambda_0}(2)$=0.53), indicating that high growth states are good states of the world. The price of growth risk increases when GDP growth is above average ($\widehat{\Lambda_1}(2,2)$=10.97). The price of level risk (the shock to short rates that is orthogonal to inflation and real GDP growth) is estimated to be negative ($\widehat{\Lambda_0}(3)$=-0.44), consistent with e.g., the Cox, Ingersoll, and Ross (1985) model. The price of level risk is allowed to change with both the level of interest rates, as in those simple term structure models, and also with the slope factor to capture the fact that bond excess returns are predictable by the slope of the yield curve (Campbell and Shiller, 1991). When interest rate levels are unusually high and the term structure steepens, the price of level risk becomes more negative ($\widehat{\Lambda_1}(3,3)$=-54.25and $\widehat{\Lambda_1}(3,4)$=-249.73), and expected future bond returns increase. The positive association between the slope and future bond returns is consistent with the bond return predictability evidence (Cochrane and Piazzesi, 2006). The price of (orthogonal) slope risk is estimated to be slightly negative on average ($\widehat{\Lambda_0}(4)$=-0.05). Since the spread between the five-year bond yield and the short rate is the fourth element of the state vector, and the short rate is the third element of the state vector, the five year bond yield can be written as:

$$y_{t,20}^{\$} = y_{0,20}^{\$} + (e_{yn} + e_{yspr})' z_t = -\frac{A_{20}^{\$}}{20} - \frac{B_{20}^{\$\prime}}{20} z_t$$

A necessary and sufficient condition to match the five-year bond yield dynamics is to allow for the first four elements of the fourth row of Λ_1 to be non-zero.

The last eight elements of Λ_0 and last eight rows of Λ_1 govern stock pricing. We assume that the market prices of risk associated with the price-dividend ratios are zero, since those variables only play a role as predictors. The only exception is the price-dividend ratio on the stock market. The evidence from dividend strip spot and futures prices and the evidence on strip future returns helps us identify the market prices of risk associated with the pd ratio (fifth element of Λ_t).

The risk prices in the 6th, 8th, 10th, 12th, and 14th rows of Λ_t are chosen to match the observed mean and dynamics of the equity risk premium in model, as shown in Appendix A, and data, as implied by the VAR. We only free up those elements of the 6th, 8th, 10th, 12th, and 14th rows of Λ_1 that are strictly necessary to allow the equity risk premia in the model to move with the same state variables as they do in the VAR. These rows of of Λ_t are also influenced by our insistence on matching the entire time series of the price-dividend ratio on the stock market, real estate, infrastructure, small, and growth stocks.

C Shock-exposure and Shock-price Elasticities

Borovička and Hansen (2014) provide a *dynamic value decomposition*, the asset pricing counterparts to impulse response functions, which let a researcher study how a shock to an asset's cash-flow today affects future cash-flow dynamics as well as the prices of risk that pertain to these future cash-flows. What results is a set of *shock-exposure elasticities* that measure the quantities of risk resulting from an initial impulse at various investment horizons, and a set of *shock-price elasticities* that measure how much the investor needs to be compensated currently for each unit of future risk exposure at those various investment horizons. We now apply their analysis to our VAR setting.

C.1 Derivation

Recall that the underlying state vector dynamics are described by:

$$z_{t+1} = \Psi z_t + \Sigma^{\frac{1}{2}} \varepsilon_{t+1}$$

The log cash-flow growth rates on stocks, REITs, and infrastructure stocks are described implicitly by the VAR since it contains both log returns and log price-dividend ratios for each of these assets. The log real dividend growth rate on an asset $i \in \{m, reit, infra\}$ is given by:

$$\log(D^i_{t+1}) - \log(D^i_t) = \Delta d^i_{t+1} = A^i_0 + A^i_1 z_t + A^i_2 \varepsilon_{t+1},$$

where $A^i_0 = \mu_m$, $A_1 = e'_{divi}\Psi$, and $A^i_2 = e'_{divi}\Sigma^{\frac{1}{2}}$.

Denote the cash-flow process $Y_t = D_t$. Its increments in logs can we written as:

$$y_{t+1} - y_t = \Gamma_0 + \Gamma_1 z_t + z'_t \Gamma_3 z_t + \Psi_0 \varepsilon_{t+1} + z'_t \Psi_1 \varepsilon_{t+1} \tag{A.13}$$

with coefficients $\Gamma_0 = A^i_0$, $\Gamma_1 = A^i_1$, $\Gamma_3 = 0$, $\Psi_0 = A^i_2$, and $\Psi_1 = 0$.

The one-period log real SDF, which is the log change in the real pricing kernel S_t, is a quadratic function of the state:

$$\log(S_{t+1}) - \log(S_t) = m_{t+1} = B_0 + B_1 z_t + B_2 \varepsilon_{t+1} + z'_t B_3 z_t + z'_t B_4 \varepsilon_{t+1}$$

where $B_0 = -y^{\$}_0(1) + \pi_0 - \frac{1}{2}\Lambda'_0\Lambda_0$, $B_1 = -e'_{yn} + e'_\pi \Psi - \Lambda'_0\Lambda_1$, $B_2 = -\Lambda'_0 + e'_\pi \Sigma^{\frac{1}{2}}$, $B_3 = -\frac{1}{2}\Lambda'_1\Lambda_1$, and $B_4 = -\Lambda'_1$.

We are interested in the product $Y_t = S_t D_t$. Its increments in logs can be written as in equation (**??**), with coefficients $\Gamma_0 = A^i_0 + B_0$, $\Gamma_1 = A^i_1 + B_1$, $\Gamma_3 = B_3$, $\Psi_0 = A^i_2 + B_2$, and $\Psi_1 = B_4$.

Starting from a state $z_0 = z$ at time 0, consider a shock at time 1 to a linear combination of state variables, $\alpha'_h \varepsilon_1$. The shock elasticity $\epsilon(z,t)$ quantifies the date-t impact:

$$\epsilon(z,t) = \alpha'_h \left(I - 2\tilde{\Psi}_{2,t}\right)^{-1} \left(\tilde{\Psi}'_{0,t} + \tilde{\Psi}'_{1,t} z\right)$$

where the $\tilde{\Psi}$ matrices solve the recursions

$$\begin{aligned} \tilde{\Psi}_{0,j+1} &= \hat{\Gamma}_{1,j}\Sigma^{1/2} + \Psi_0 \\ \tilde{\Psi}_{1,j+1} &= 2\Psi'\hat{\Gamma}_{3,j}\Sigma^{1/2} + \Psi_1 \end{aligned}$$

$$\tilde{\Psi}_{2,j+1} = \left(\Sigma^{1/2}\right)' \hat{\Gamma}_{3,j}\Sigma^{1/2}$$

The $\hat{\Gamma}$ and $\tilde{\Gamma}$ coefficients follow the recursions:

$$\begin{aligned}
\tilde{\Gamma}_{0,j+1} &= \hat{\Gamma}_{0,j} + \Gamma_0 \\
\tilde{\Gamma}_{1,j+1} &= \hat{\Gamma}_{1,j}\Psi + \Gamma_1 \\
\tilde{\Gamma}_{3,j+1} &= \Psi'\hat{\Gamma}_{3,j}\Psi + \Gamma_3 \\
\hat{\Gamma}_{0,j+1} &= \tilde{\Gamma}_{0,j+1} - \frac{1}{2}\log\left(\left|I - 2\tilde{\Psi}_{2,j+1}\right|\right) + \frac{1}{2}\tilde{\Psi}_{0,j+1}\left(I - 2\tilde{\Psi}_{2,j+1}\right)^{-1}\tilde{\Psi}'_{0,j+1} \\
\hat{\Gamma}_{1,j+1} &= \tilde{\Gamma}_{1,j+1} + \tilde{\Psi}_{0,j+1}\left(I - 2\tilde{\Psi}_{2,j+1}\right)^{-1}\tilde{\Psi}'_{1,j+1} \\
\hat{\Gamma}_{3,j+1} &= \tilde{\Gamma}_{3,j+1} + \frac{1}{2}\tilde{\Psi}_{1,j+1}\left(I - 2\tilde{\Psi}_{2,j+1}\right)^{-1}\tilde{\Psi}'_{1,j+1}
\end{aligned}$$

starting from $\hat{\Gamma}_{0,0} = 0$, $\hat{\Gamma}_{1,0} = 0_{1\times N}$, $\hat{\Gamma}_{2,0} = 0_{N\times N}$, and where I is the $N \times N$ identity matrix.

Let $\epsilon_g(z,t)$ be the shock-exposure elasticity (cash-flows $Y = D$) and $\epsilon_{sg}(z,t)$ the shock-value elasticity, then the shock-price elasticity $\epsilon_p(z,t)$ is given by

$$\epsilon_p(z,t) = \epsilon_g(z,t) - \epsilon_{sg}(z,t).$$

In an exponentially affine framework like ours, the shock price elasticity can also directly be derived by setting $Y_t = S_t^{-1}$ or $y_{t+1} - y_t = -m_{t+1}$, with coefficients in equation (**??**) equal to $\Gamma_0 = -B_0$, $\Gamma_1 = -B_1$, $\Gamma_3 = -B_3$, $\Psi_0 = -B_2$, and $\Psi_1 = -B_4$.

The shock-price elasticity quantifies implied market compensation for horizon-specific risk exposures. In our case, these risk compensations are extracted from a rich menu of observed asset prices matched by a reduced form model, rather than by constructing a structural asset pricing model. The horizon-dependent risk prices are the multi-period impulse responses for the cumulative stochastic discount factor process.

C.2 Results

Figure **??** plots the shock-exposure elasticities of the five dividend growth processes -on the market (blue), REITs (red), infrastructure (green), small (cyan), and growth stocks (magenta)- to a one-standard deviation shock to inflation (top left), real per capital GDP growth (top second), the short rate (top third), the slope factor (top fourth), , the price-dividend ratio on the market (top right), the dividend growth rate on the market (bottom left), the dividend growth rate on REITs (bottom middle), the dividend growth rate on infrastructure (bottom middle), the dividend growth rate on small stocks (bottom fourth), and the dividend growth rate on growth stocks (bottom right). The shock exposure elasticities are essentially impulse-responses to the original (i.e., non-orthogonalized) VAR innovations. They describe properties of the VAR, not of the asset pricing model. Since our private equity cash-flows are linear combinations of these dividends, the PE cash flow exposures to the VAR shocks will be linear combinations of the plotted shock exposure elasticities of these three dividend growth rates.

There is interesting heterogeneity in the cash flow exposures of the five risky assets to the VAR shocks. For example, the top left panel shows that infrastructure and to a lesser extent small stock cash flows increase in the wake of a positive inflation shock, while the dividend growth responses for the aggregate stock market and especially for REITs and growth stocks are negative. This points to the inflation hedging potential of infrastructure assets and the inflation risk exposure of REITs, growth stocks, and the market as a whole. The second panel shows that REIT and small stock dividend growth responds positively to a GDP growth shock, while cash flow growth on the market and on growth stocks (ironically) respond negatively. It is well known that the market portfolio as a whole is fairly growth-oriented. All cash flows respond negatively to an increase in interest rates in the long-run, but the response of REIT cash flows is positive for the first five years. REIT cash flows are rents which can be adjusted upwards when rates increase, which typically occurs in a strong economy (see the GDP panel). Small and growth stocks have a lot more interest rate level risk than the other asset classes. The market dividend growth shows a substantial positive response to a steepening yield curve. Slope exposure is even larger for growth stocks. The bottom panels show that the dividend growth shock on the market is nearly permanent, while the other four cash flow shocks are mean-reverting. A positive shock to infrastructure cash flows has strong and often long-lasting effects on the other four cash flow series (bottom middle panel). A positive innovation in REIT cash flows is associated with a decline in cash flows on growth firms. This makes sense given the value-like behavior of REITS (Van Nieuwerburgh, 2019).

Figure **??** plots the shock-price elasticities to a one-standard deviation shock to each of the same (non-orthogonalized) VAR innovations. Shock price elasticities are properties of the SDF process, and therefore depend on the estimated market price of risk parameters. They quantify the compensation investors demand for horizon-dependent risk ex-

Figure A.1: Shock Exposure Elasticities

The figure plots the shock-exposure elasticities of dividend growth on the market, dividend growth of REITs, dividend growth of infrastructure shocks, dividend growth on small stocks, and dividend growth on growth stocks to a one-standard deviation shock to inflation (top left), real GDP growth (top second), the short rate (top third), the slope factor (top right), the price-dividend ratio on the market (top right), dividend growth rate on the market (bottom left), the dividend growth rate on REITs (bottom second), the dividend growth rate on infrastructure (bottom third), the dividend growth rate on small stocks (bottom fourth), and dividend growth on growth stocks (bottom right).

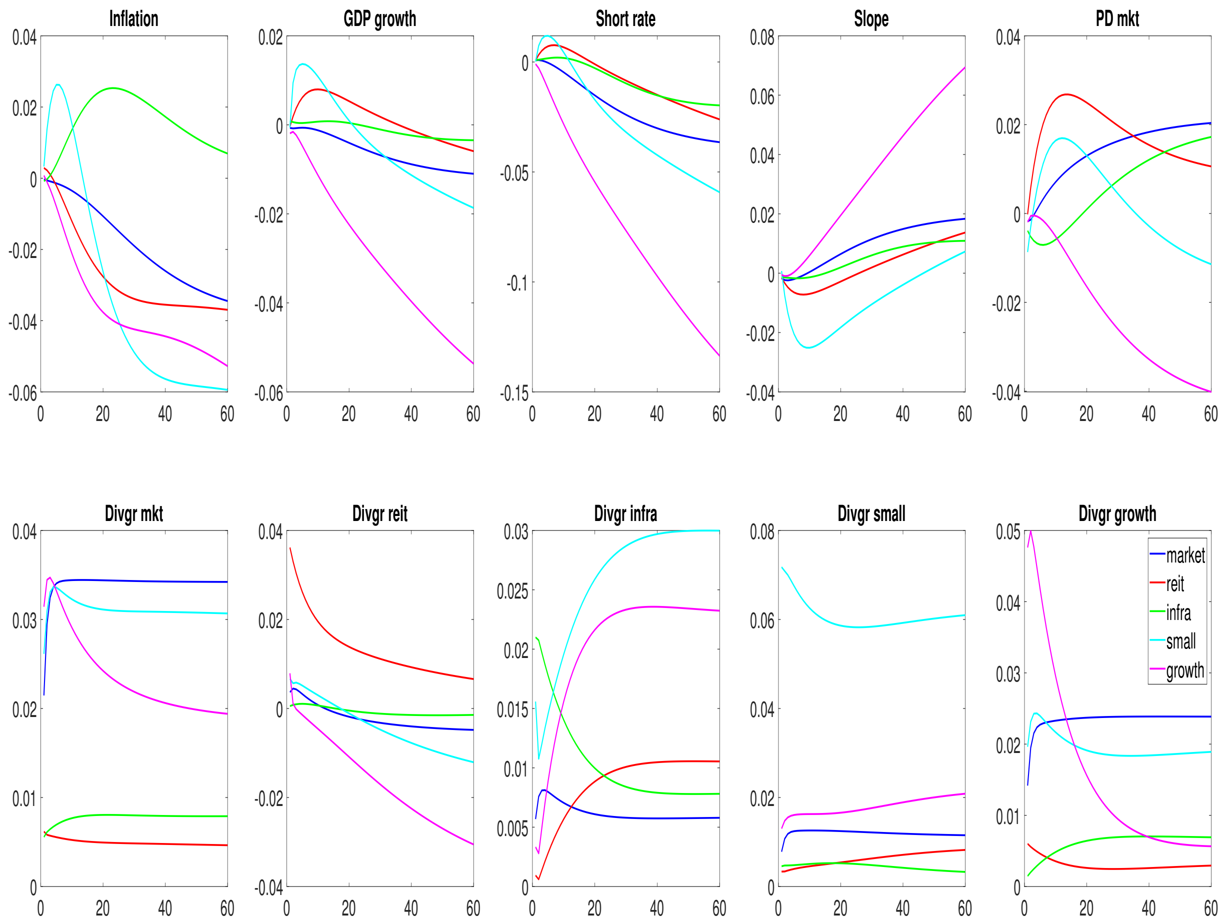

posures. The price of inflation risk is negative, consistent with increases in inflation being bad states of the world. GDP growth risk is naturally priced positively, and more so at longer horizons. Level risk is negatively priced, consistent with standard results in the term structure literature that consider high interest rate periods bad states of the world. The price of level risk becomes less negative at longer horizons. The price of slope risk is positive, consistent with the findings in (Koijen, Lustig, and Van Nieuwerburgh, 2017). All cash-flow shocks in the bottom five panels naturally have positive risk prices since increases in cash-flow growth are good shocks to the representative investor. The highest risk price is associated with shocks to the aggregate stock market, followed by infrastructure shocks, then growth shocks. Compensation for infrastructure and small stock risk increases with the horizon while it decreases for the other three dividend shocks.

Figure A.2: Shock Price Elasticities

The figure plots the shock-price elasticities to a one-standard deviation shock to the inflation factor (top left), real GDP growth (top second), short rate (top third), the slope factor (top right), the price-dividend ratio on the market (top right), the dividend growth rate on the market (bottom left), the dividend growth rate on REITs (bottom second), the dividend growth rate on infrastructure (bottom third), the dividend growth rate on small stocks (bottom fourth), and dividend growth on growth stocks (bottom right). The shocks whose risk prices are plotted are the (non-orthogonalized) VAR innovations $\Sigma^{\frac{1}{2}}\varepsilon$.

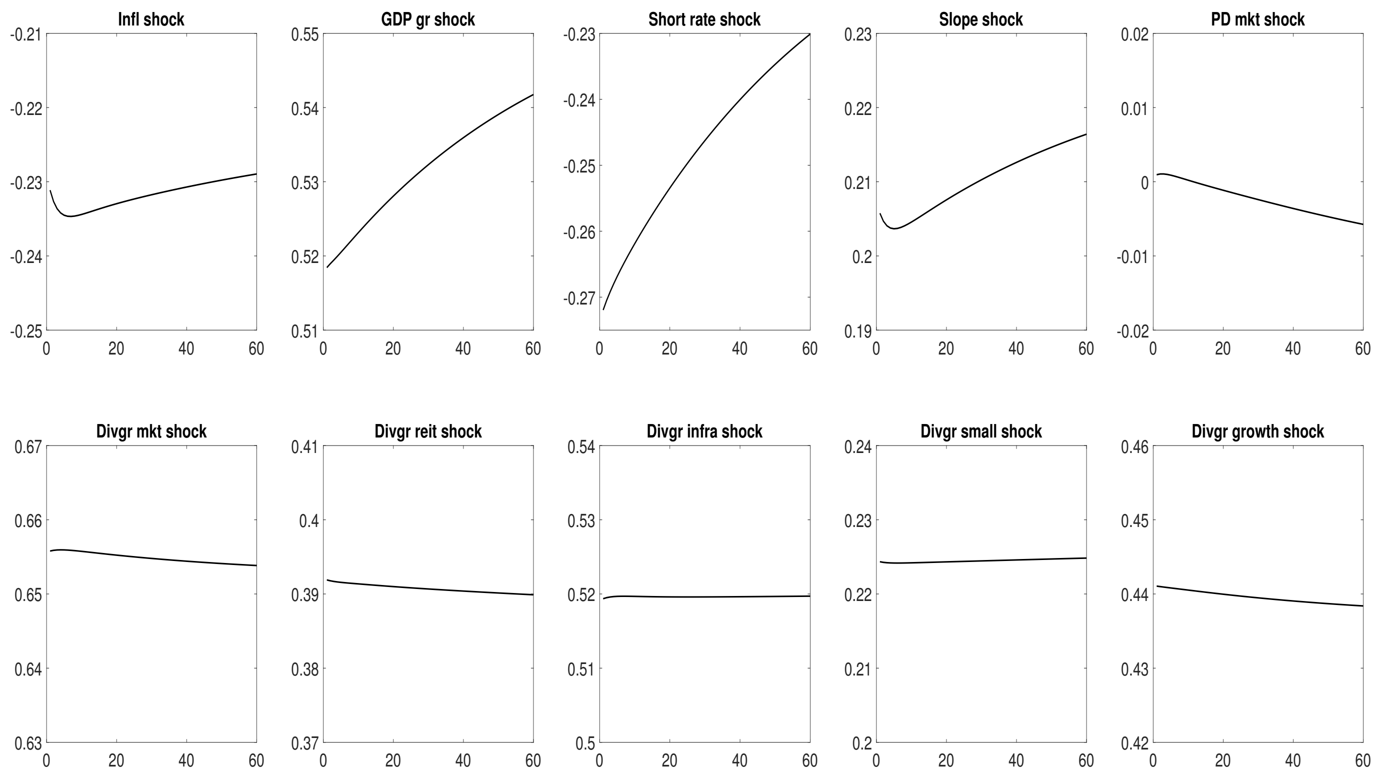

D Korteweg-Nagel Details

D.1 Connection between our approach, GPME, and PME

Korteweg and Nagel (2016) define their GPME measure for fund i as:

$$
\begin{aligned}
GPME_t^i - 1 &= \sum_{h=0}^{H} M_{t+h}^h X_{t+h}^i - 1 && \text{(A.14)} \\
&= \sum_{h=0}^{H} M_{t+h}^h \left\{ \boldsymbol{q}_{t,h}^i \boldsymbol{F}_{t+h} + v_{t+h}^i \right\} - 1 \\
&= RAP_t^i + \mathbb{E}_t \left[\sum_{h=0}^{H} M_{t+h}^h \boldsymbol{q}_{t,h}^i \boldsymbol{F}_{t+h} \right] - 1 + \sum_{h=0}^{H} M_{t+h}^h \boldsymbol{q}_{t,h}^i \boldsymbol{F}_{t+h} - \mathbb{E}_t \left[\sum_{h=0}^{H} M_{t+h}^h \boldsymbol{q}_{t,h}^i \boldsymbol{F}_{t+h} \right] \\
&= RAP_t^i + \sum_{h=0}^{H} \boldsymbol{q}_{t,h}^i \left(M_{t+h}^h \boldsymbol{F}_{t+h} - \mathbb{E}_t [M_{t+h}^h \boldsymbol{F}_{t+h}] \right) && \text{(A.15)}
\end{aligned}
$$

If the SDF model is correct, $\mathbb{E}_t[GPME^i] = 1$. The difficulty with computing (**??**) is that it contains the *realized* SDF which is highly volatile. In KN's implementation, the SDF is a function of only the market return: $M_{t+h}^h = \exp(0.088h - 2.65 \sum_{k=0}^{h} r_{t+k}^m)$. If the realized market return over a 10 year period is 100%, the realized SDF is 0.17. If the stock return is 30%, the SDF is 1.08. Because of the multiple sources of risk and the richer risk price dynamics, our SDF is substantially more volatile than one considered in KN; it has a higher maximum Sharpe ratio. The realizations of the SDF are on average much lower than in KN, so that the GPME approach leads to unrealistically low PE valuations. Our methodology solves this issue because it avoids using the realized SDF and instead relies on strip prices, which are *expectations* of SDFs, multiplied by cash-flows.

A second difference between the two approaches is that the realized GPME can be high (low) because the factor payoffs F_{t+h} are unexpectedly high (low). This is the second term in equation (**??**). Our measure does not credit the GP for this unexpected, systematic cash-flow component. RAP removes a “factor timing” component of performance that is due to taking risk factor exposure. Like our approach, the simple PME does not credit the GP with factor timing.

Third, our approach credits the GP for “investment timing” skill while the GPME approach does not. Because it assumes that the replicating portfolio deploys the entire capital right away, a manager who successfully waits a few periods to invests will have a positive RAP. If the GP harvests at a more opportune time than the replicating portfolio, whose harvesting timing is determined by the average PE fund in that vintage and category, this also contributes to the RAP. The GPME as well as the simple PME approach do not credit the manager for investment timing because they assume that the replicating portfolio follows the observed sequence of PE capital calls and distributions.

Fourth, our approach accommodates heterogeneity in systematic risk exposure across PE funds that differ by vintage and category. In the standard PME approach, the market beta of each fund is trivially the same and equal to 1. In the simplest implementation of the GPME approach, PE funds are allowed to have a market beta that differs from 1, but the beta is the same for all funds. We allow for multiple risk factors, and the exposures differ for each vintage and for each fund category. Because market prices of risk vary with the state of the economy, so does the RAP. The next section provides more detail on the KN approach and more discussion on the points of differentiation.

D.2 More Details

They propose:

$$m_{t+1} = a - br^m_{t+1},$$

whereby the coefficients a and b are chosen so that the Euler equation $1 = E[M_{t+1}R_{t+1}]$ holds for the public equity market portfolio and the risk-free asset return. More specifically, they estimate $a = 0.088$ and $b = 2.65$ using a GMM estimator:

$$\min_{a,b} \left(\frac{1}{N} \sum_i u_i(a,b) \right)' W \left(\frac{1}{N} \sum_i u_i(a,b) \right)$$

where

$$u_i(a,b) = \sum_{j=1}^{J} M_{t+h(j)}(a,b)[X_{if,t+h(j)}, X_{im,t+h(j)}],$$

N is the number of funds, and W is a 2×2 identity matrix. The T-bill benchmark fund cash-flow, X_{if}, and the market return benchmark cash-flow, X_{im}, are the cash-flows on a T-bill and stock market investment, respectively, that mimic the timing and magnitude of the private equity fund i's cash-flows. The $t + h(j)$ are the dates on which the private equity fund pays out cash-flow $j = 1, \cdots, J$. Date t is the date of the first cash-flow into the fund, so that $h(1) = 0$. For each of the two benchmark funds, the inflows are identical in size and magnitude as the inflows into the PE fund. If PE fund i makes a payout at $t + h(j)$, the benchmark funds also make a payout. That payout consists of two components. The first component is the return on the benchmark since the last cash-flow date. The second component is a return of principal, according to a preset formula which returns a fraction of the capital which is larger, the longer ago the previous cash-flow was.

A special case of this model is the public market equivalent of Kaplan and Schoar (2005), which sets $a = 0$ and $b = 1$. This is essentially the log utility model. The simple PME model is rejected by Korteweg and Nagel (2016), in favor of their generalized PME model.

There are several key differences between our method and that of Korteweg and Nagel (2016). First, we do not use SDF realizations to discount fund cash-flows. Rather, we use bond prices and dividend strip prices, which are conditional expectations. Realized SDFs are highly volatile. Second, the KN approach does not take into account heterogeneity in the amount of systematic risk of the funds. All private equity funds are assumed to have a 50-50 allocation to the stock and bond benchmark funds. Our model allows for different funds to have different stock and bond exposure. Third, the KN approach uses a preset capital return policy which is not tailored to the fund in question. For example, a fund may be making a modest distribution in year 5, say 10%, and a large distribution in year 10 (90%). Under the KN assumption, the public market equivalent fund would sell 50% in year 5 and the other 50% in year 10. There clearly is a mismatch between the risk exposure of the public market equivalent fund and that of the private equity fund. In other words, the KN approach does not take into the account the magnitude of the fund distributions, only their timing. Fourth, we use additional risk factors beyond those considered in KN.

To study just the importance of the last assumption, we can redo our calculations using a much simplified state vector that only contains the short rate, inflation, and the stock market return. This model has constant risk premia.

E Additional Results

Figure A.3: Cash-Flows by Vintage, Alternate Categories

(a) Fund of Funds

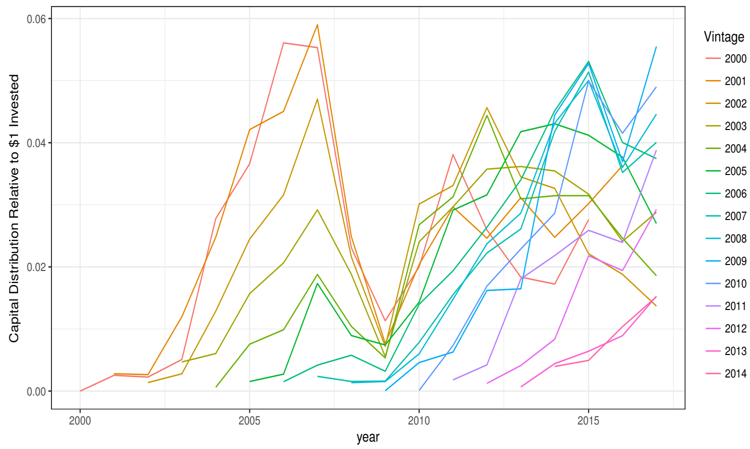

(b) Debt Funds

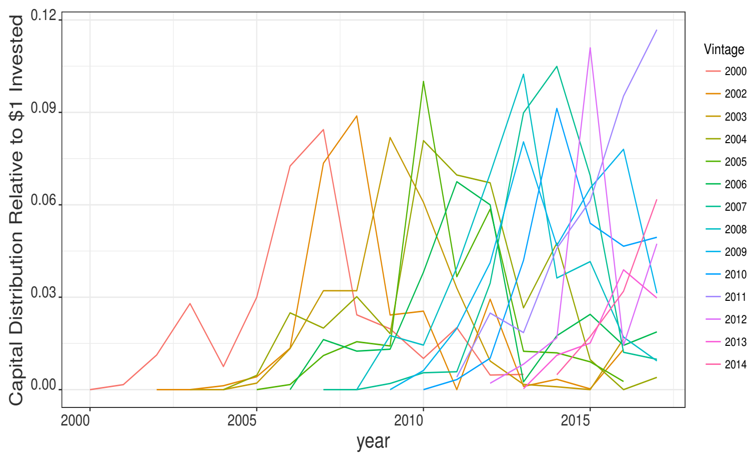

(c) Restructuring

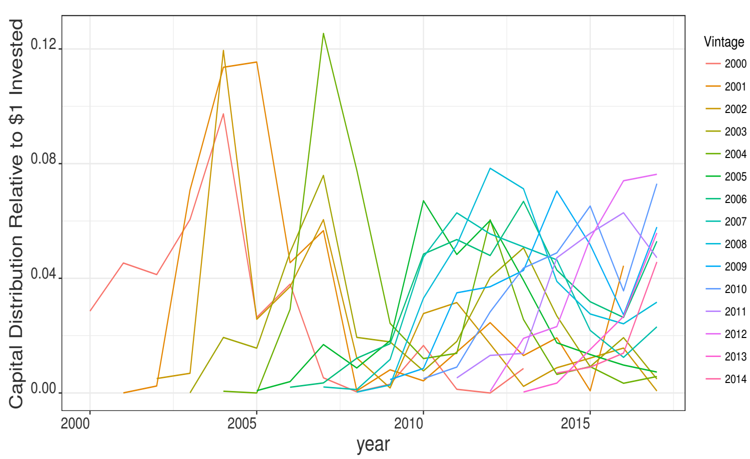

Figure A.4: OLS 3-Factor Model for other Categories

Panel A: Restructuring

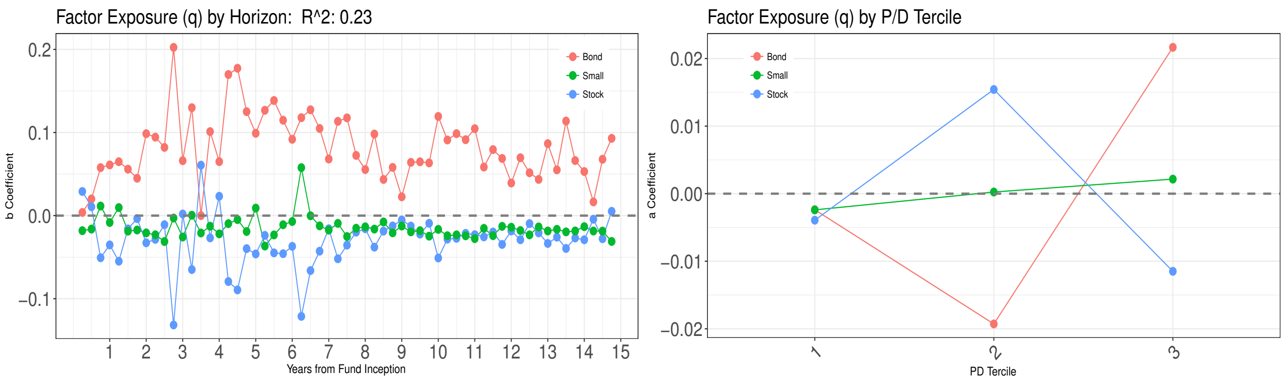

Panel B: Debt Fund

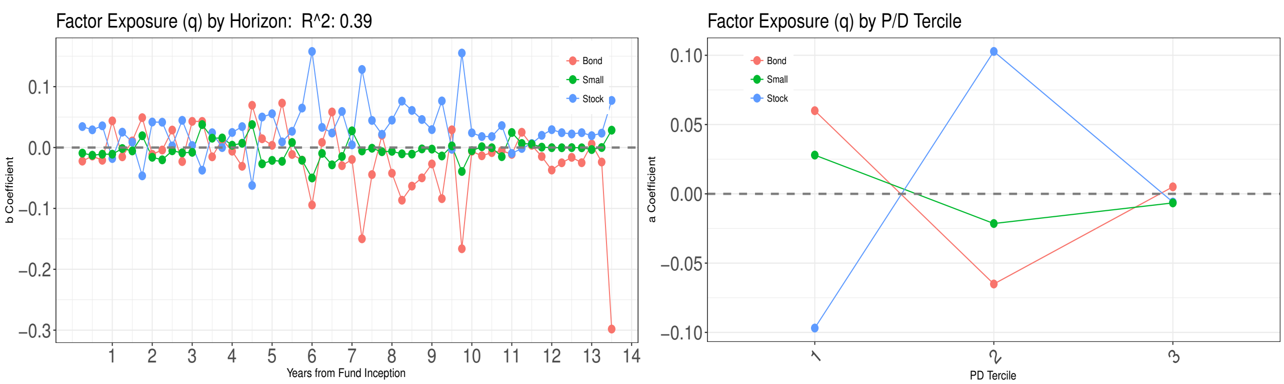

Panel C: Fund of Funds

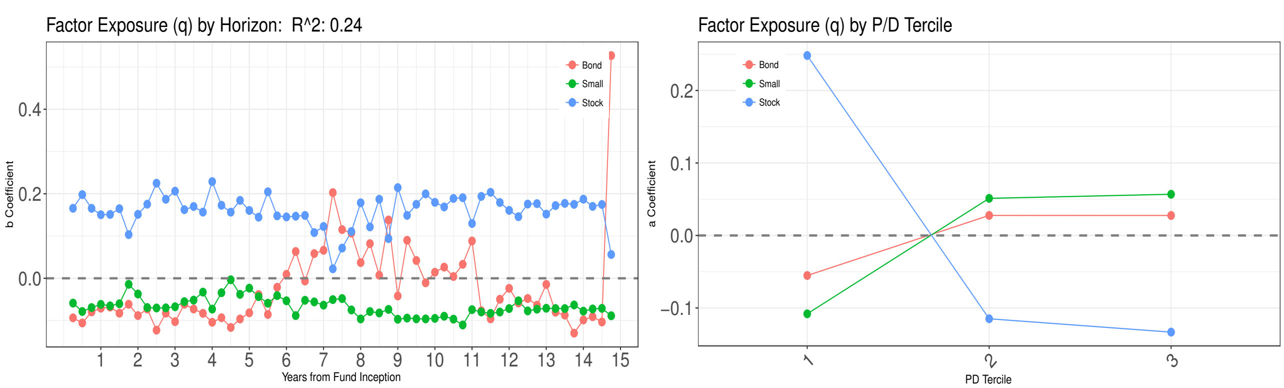

Figure A.5: OLS 3-Factor Model, Model Comparison

Panel A: Restructuring

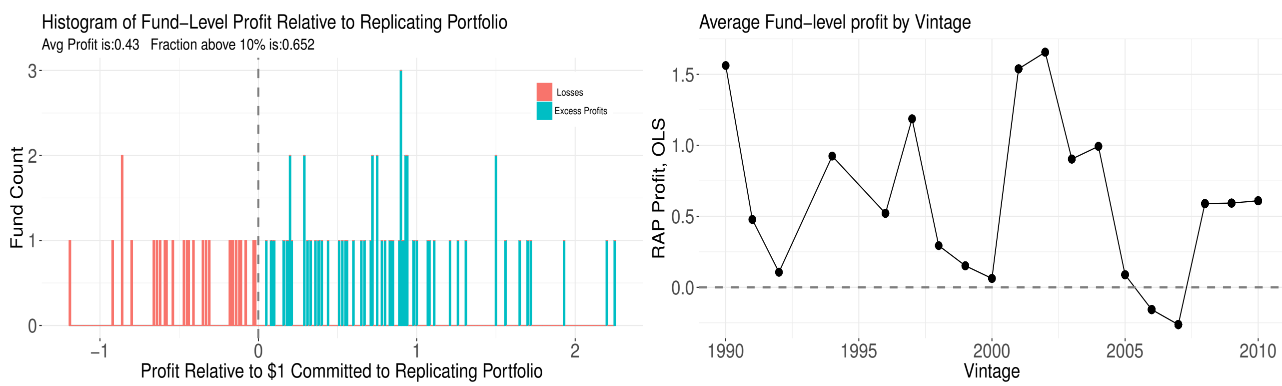

Panel B: Debt Fund

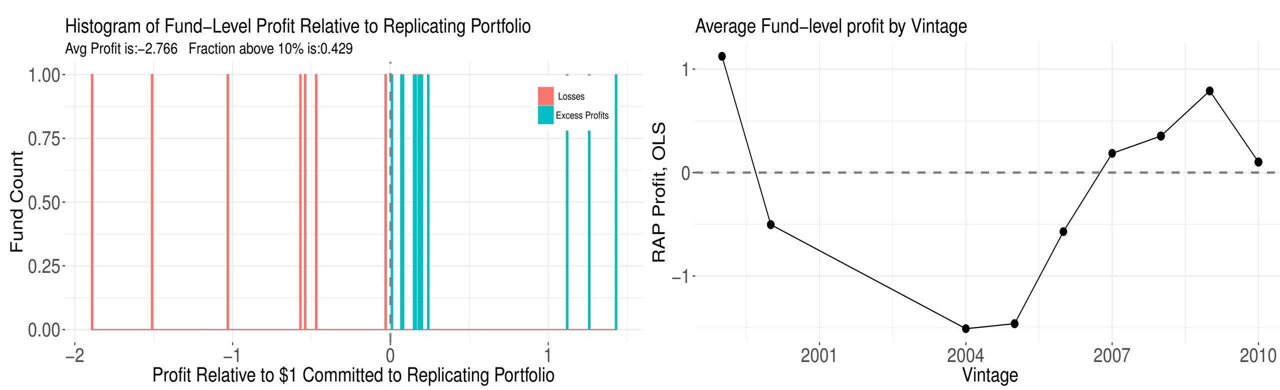

Panel C: Fund of Funds

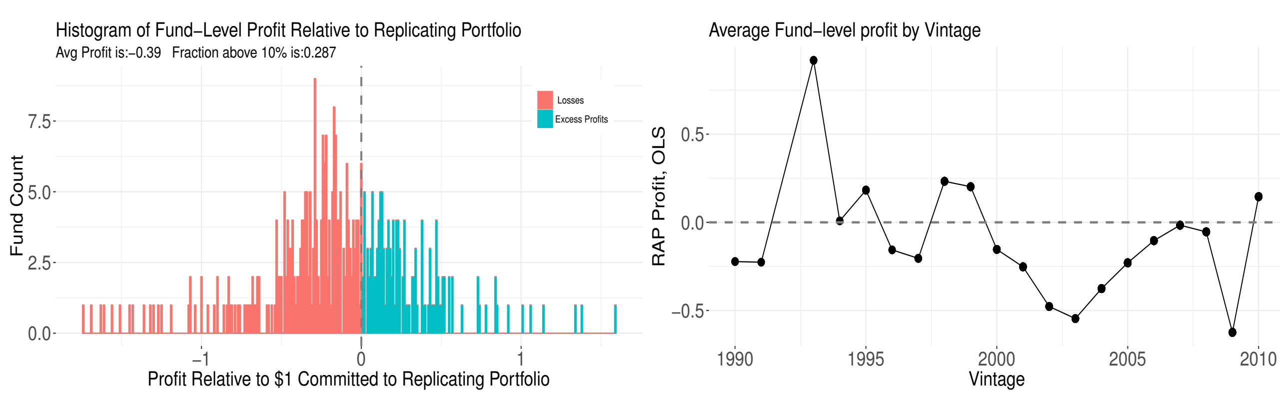

Figure A.6: OLS 3-Factor Model, Comparison—Other Categories

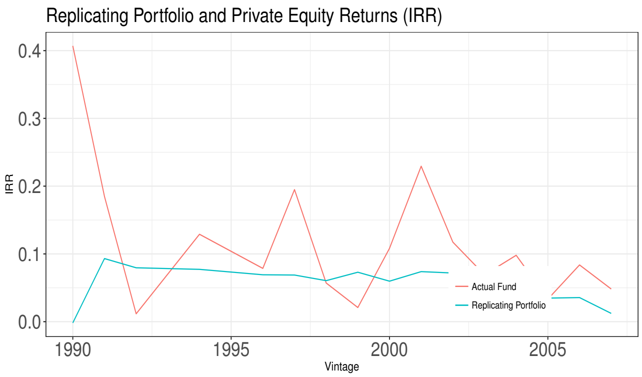

Panel A: Restructuring: Lasso Model

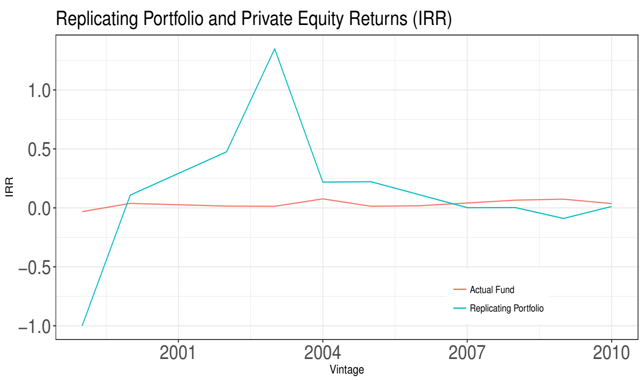

Panel B: Debt Fund: OLS Model

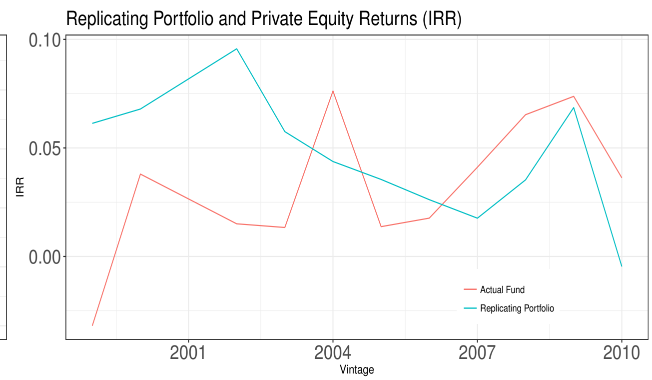

Panel C: Debt Fund: Lasso Model

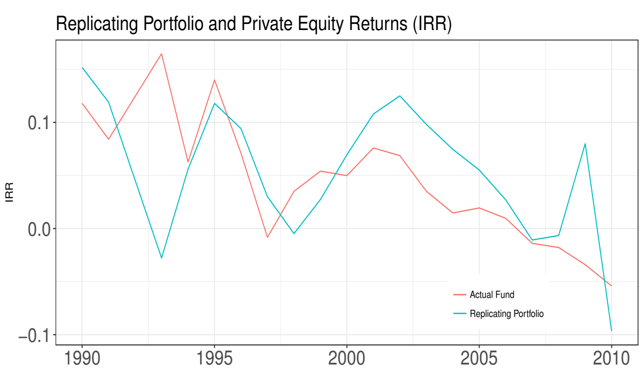

Panel D: Fund of Funds: OLS Model

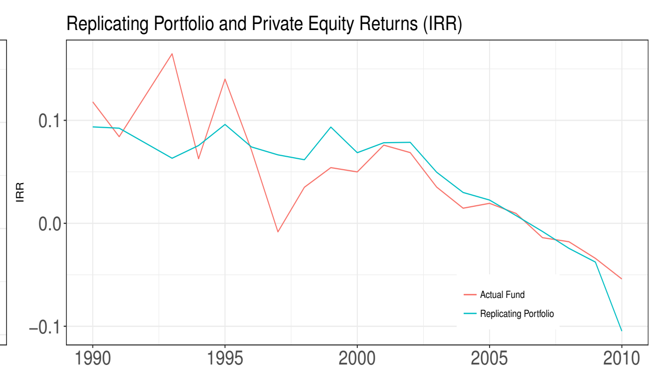

Panel E: Fund of Funds: Lasso Model

Figure A.7: Positive Coefficient 3-Factor Model

Panel A: Restructuring

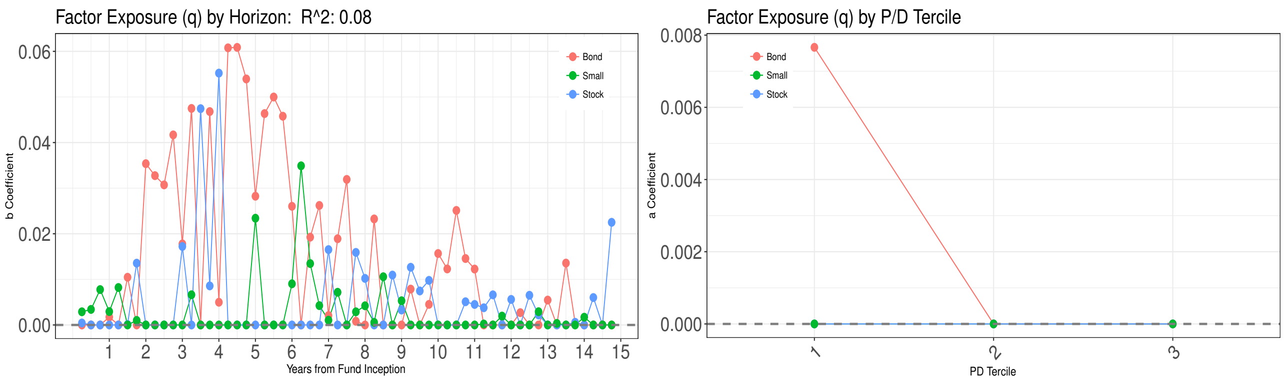

Panel B: Debt Fund

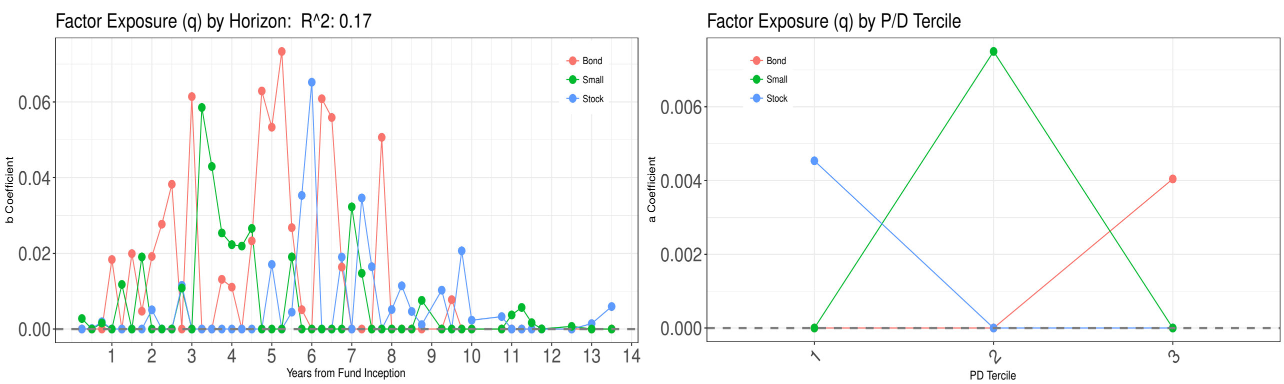

Panel C: Fund of Funds

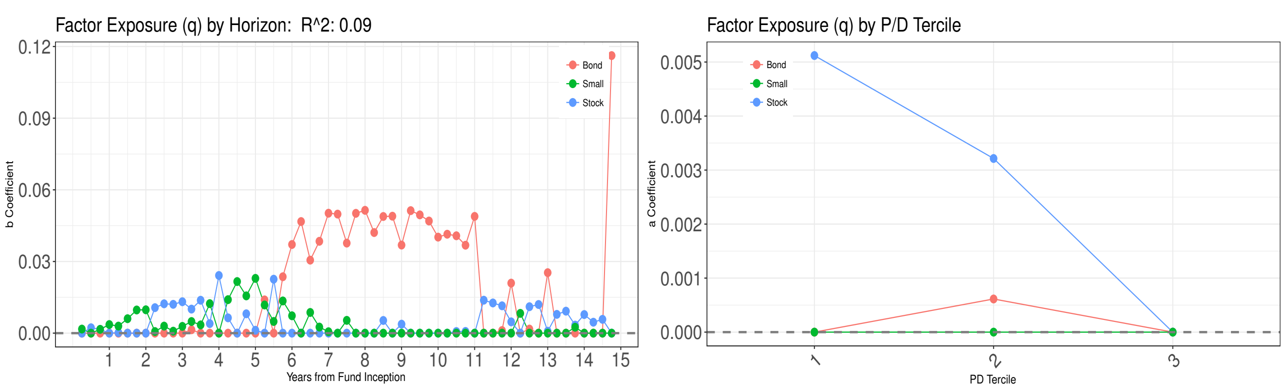

Figure A.8: Positive Coefficient 3-Factor Model, Model Comparison

Panel A: Restructuring

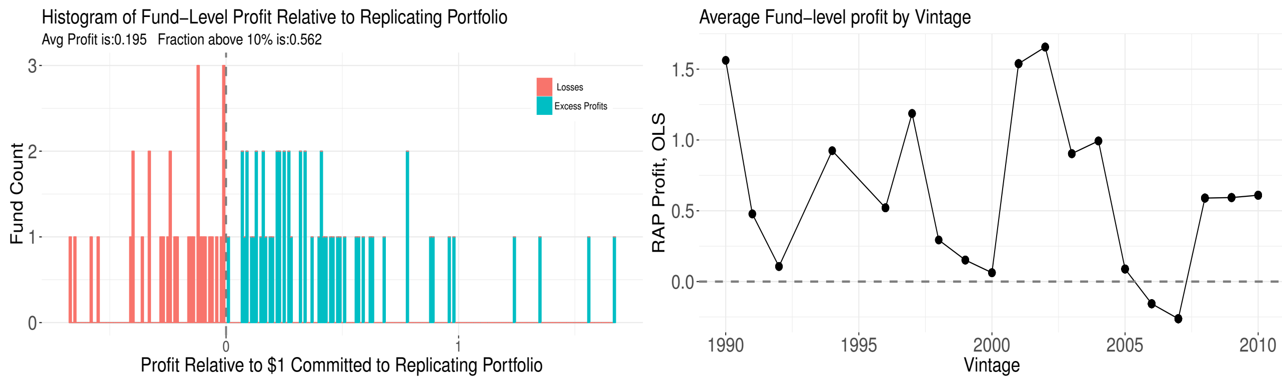

Panel B: Debt Fund

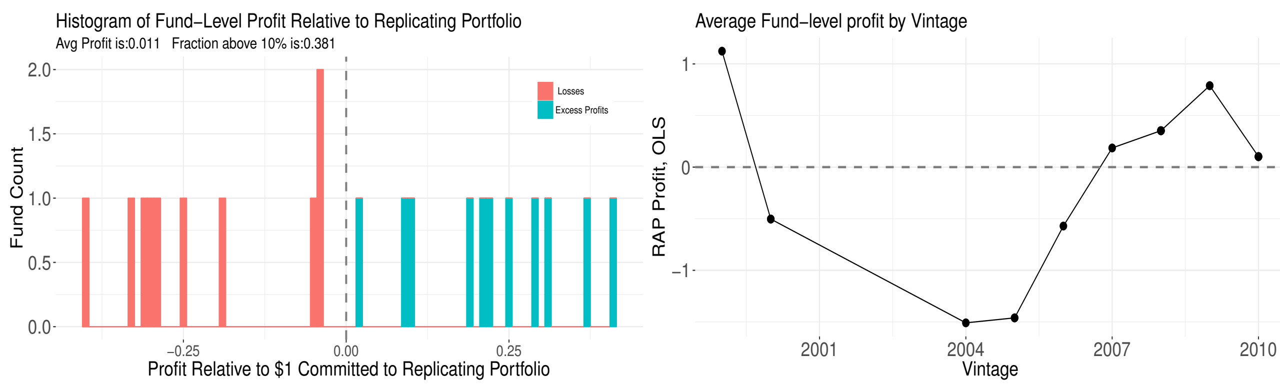

Panel C: Fund of Funds

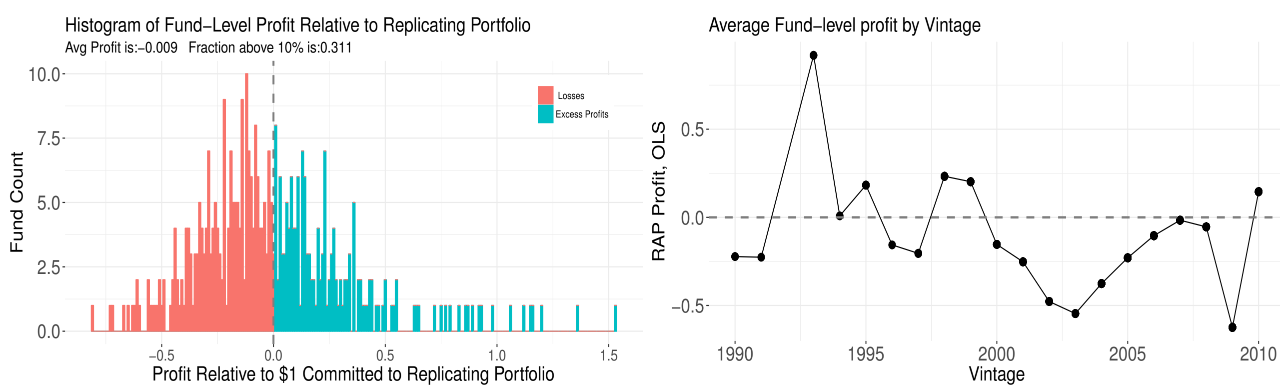

Figure A.9: Positive Coefficient Model — Expected Return

Panel A: Restructuring

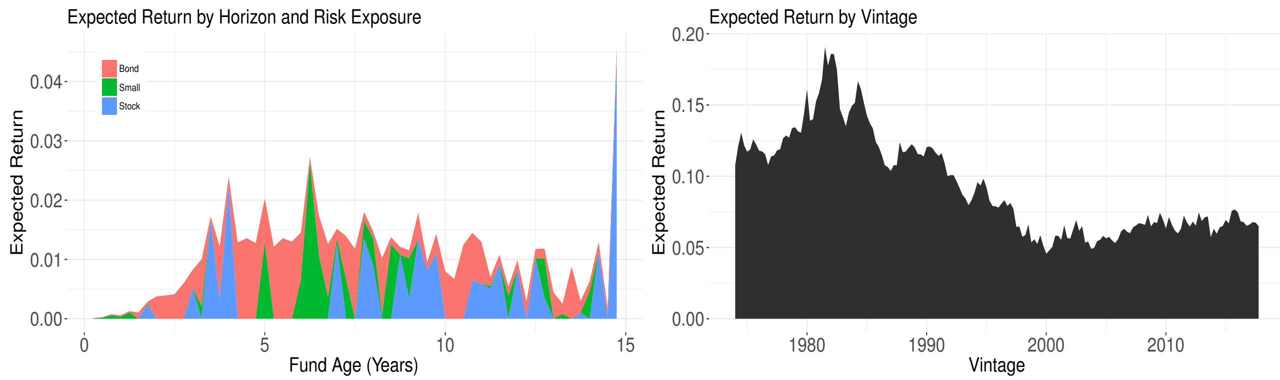

Panel B: Debt Fund

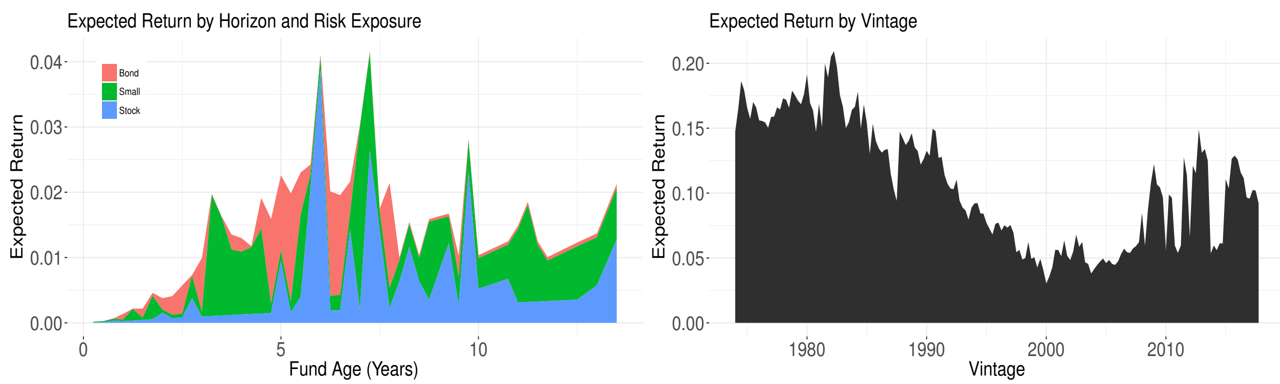

Panel C: Fund of Funds

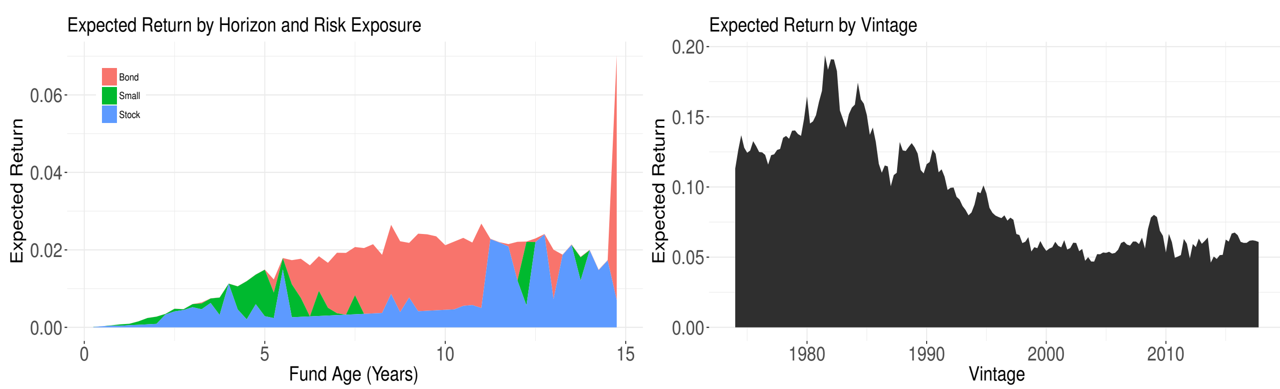

Figure A.10: Positive Coefficient Lasso Alternative Approach Comparison

Panel A: Buyout

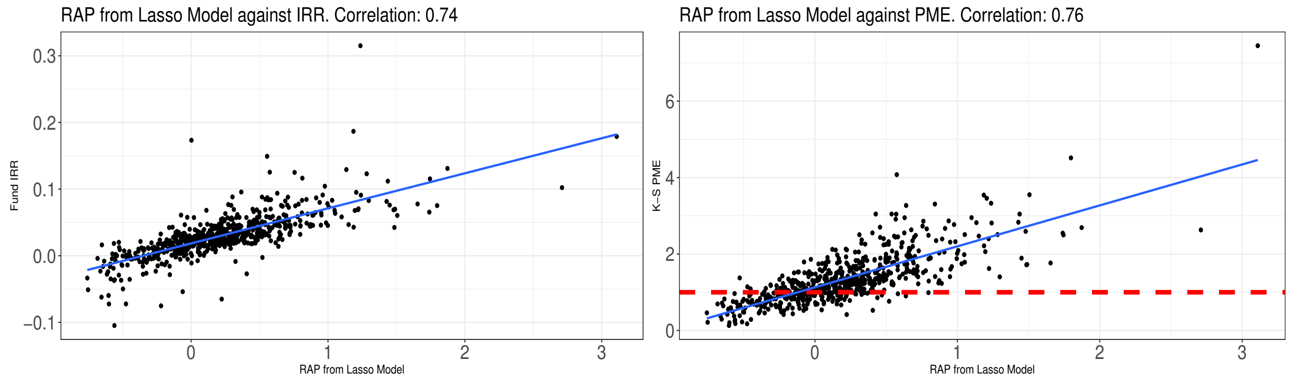

Panel B: Venture Capital

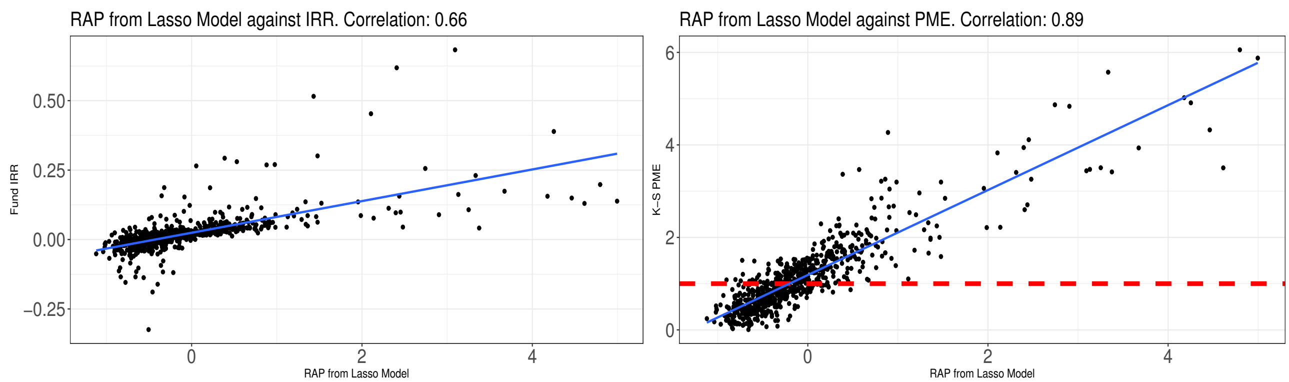

Panel C: Real Estate

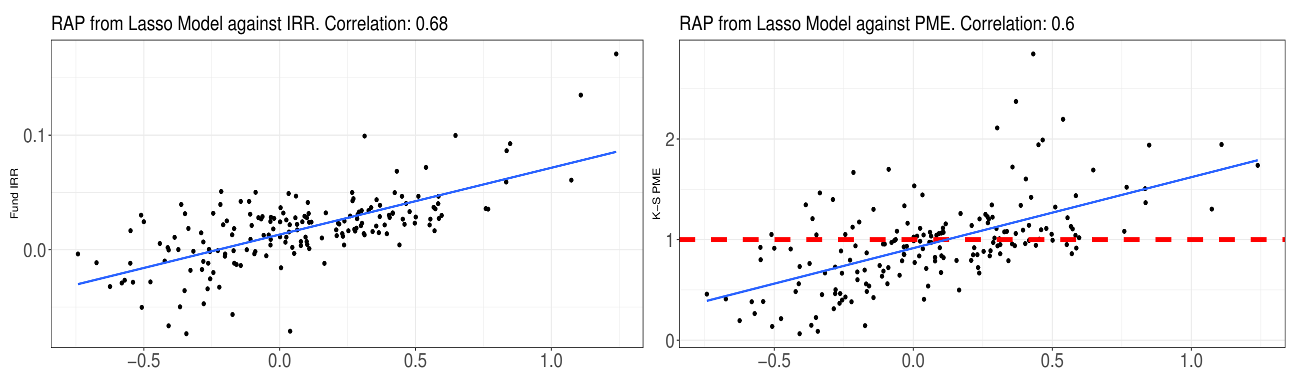

Panel D: Infrastructure

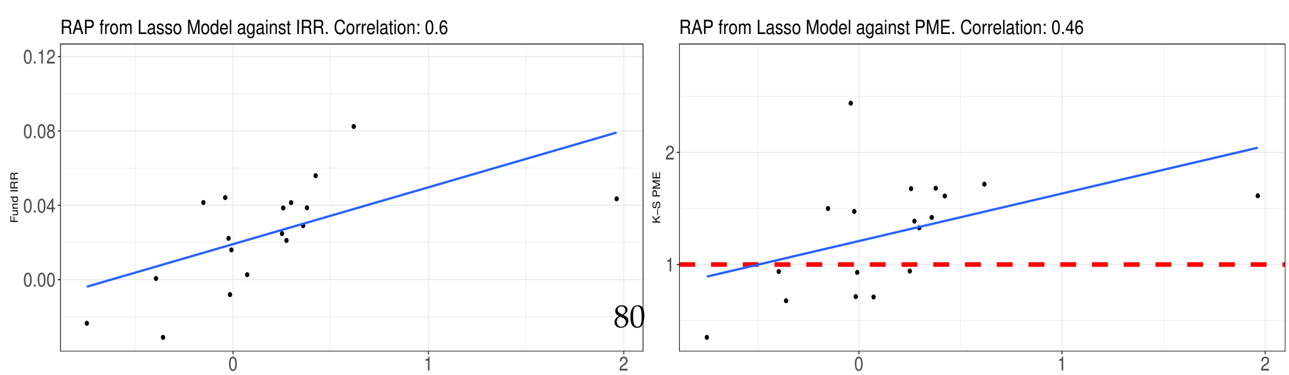

Figure A.11: Comparison with TVPI

Panel A: Buyout

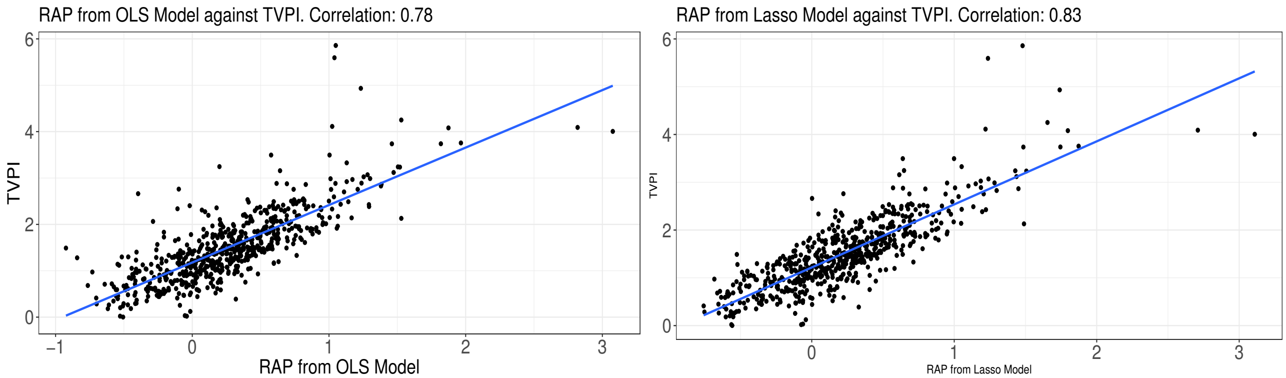

Panel B: Venture Capital

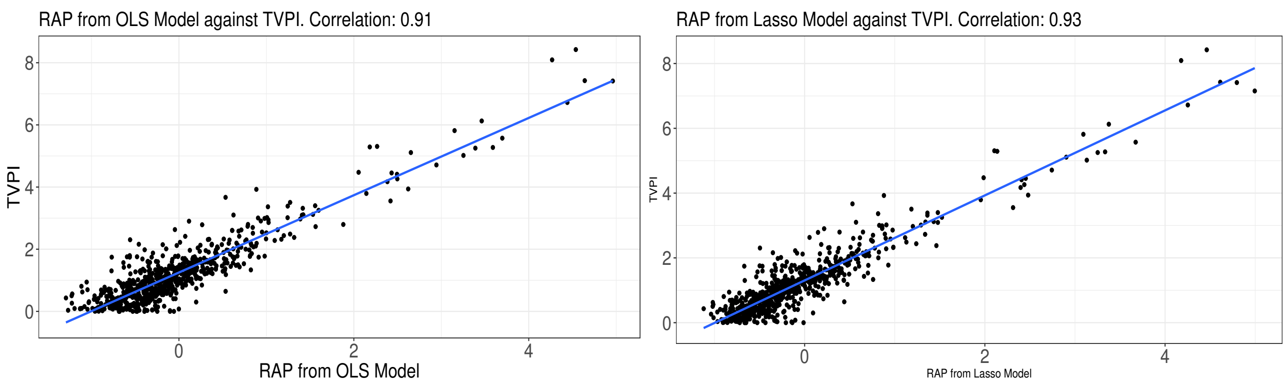

Panel C: Real Estate

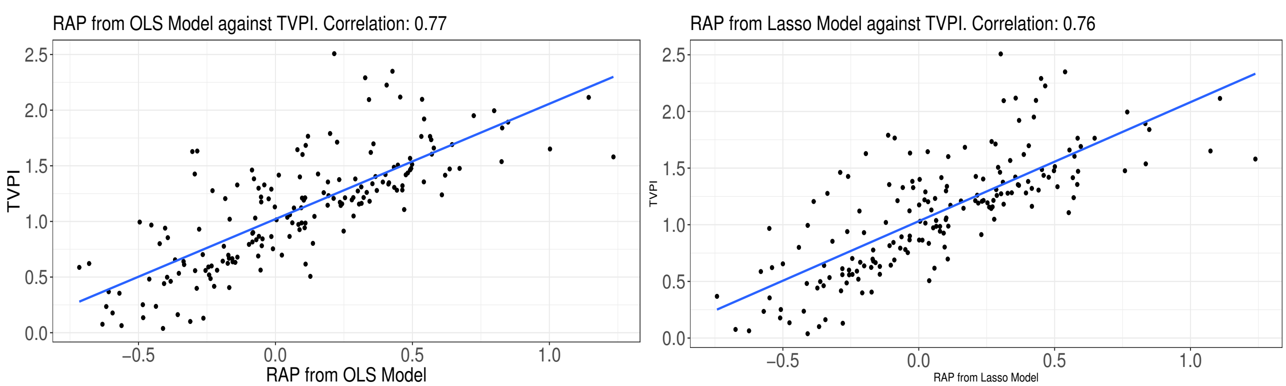

Panel D: Infrastructure